

University of Montana

ScholarWorks at University of Montana

Graduate Student Theses, Dissertations, &
Professional Papers

Graduate School

2011

Retracing the 1910 Carruthers Royal Geographical Society Expedition to the Torgen Mountains of Mongolia – Reconstruction of a Century of Glacial Change

Kevin Gregory McManigal
The University of Montana

Follow this and additional works at: <https://scholarworks.umt.edu/etd>

Let us know how access to this document benefits you.

Recommended Citation

McManigal, Kevin Gregory, "Retracing the 1910 Carruthers Royal Geographical Society Expedition to the Torgen Mountains of Mongolia – Reconstruction of a Century of Glacial Change" (2011). *Graduate Student Theses, Dissertations, & Professional Papers*. 838.
<https://scholarworks.umt.edu/etd/838>

This Thesis is brought to you for free and open access by the Graduate School at ScholarWorks at University of Montana. It has been accepted for inclusion in Graduate Student Theses, Dissertations, & Professional Papers by an authorized administrator of ScholarWorks at University of Montana. For more information, please contact scholarworks@mso.umt.edu.

RETRACING THE 1910 CARRUTHERS ROYAL GEOGRAPHICAL SOCIETY
EXPEDITION TO THE TURGEN MOUNTAINS OF MONGOLIA –
RECONSTRUCTION OF A CENTURY OF GLACIAL CHANGE

By

KEVIN GREGORY M^cMANIGAL

Bachelor of Arts in Geography, Humboldt State University, Arcata, California, 2006

Thesis

presented in partial fulfillment of the requirements
for the degree of

Master of Science
in Geography

The University of Montana
Missoula, MT

May 2011

Approved by:

Dr. Stephan Sprang, Associate Provost for Graduate Education
Graduate School

Dr. Ulrich Kamp, Chair
Department of Geography

Dr. Anna E. Klene
Department of Geography

Dr. Joel T. Harper
Department of Geosciences



*Do not tell all that you know,
Lest you tell more than you know.*

Persian proverb written on inside cover of
Douglas Carruthers' field book from 1910

McManigal, Kevin, M.S., May 2011
Geography

Retracing the 1910 Carruthers Royal Geographical Society Expedition to the Turgan
Mountains of Mongolia – Reconstruction of a Century of Glacial Change

Chairperson: Dr. Ulrich Kamp

The Turgan Mountains lie in northwestern Mongolia, roughly 80 kilometers south of the Russian border. The area was visited in 1910 by a Royal Geographical Society (RGS) expedition led by Douglas Carruthers. They undertook an extensive survey of the range and produced a detailed topographic map. They also documented the extent of the glaciers with photographs. This modern study consisted of three phases. The first step was to procure the historical documents from the RGS in London, including copies of the photos, journal entries, and the map. Field work in Mongolia entailed traveling to the remote study site and retracing portions the 1910 expedition. Camera locations were matched to the historical photographs and repeat images taken. In addition, the termini of the two main glacial lobes were surveyed by GPS. Finally, spatial analysis was conducted in the computer laboratory using a GIS to generate a ‘historic’ elevation model from the 1910 map and compare it to a modern DEM generated from SRTM data. Map analysis software was employed to evaluate cartometric accuracy of the 1910 map against modern Russian topographic sheets. The results of the DEM and map analysis were then validated using the field GPS data and remotely sensed imagery to quantitatively describe the changes in the glacial system. The repeat photography was analyzed using photogrammetric techniques to measure glacier changes. Also, a custom cartographic product was produced in the style of the 1910 Carruthers map. It displays the extent of the glaciers in 2010 and the locations of repeat photography stations for future expeditions. Placing the results of this study alongside previous work paints a clear picture of the Turgan glacial regime over the last century. The results suggest that while the snow and ice volume on the summits appears to be intact, lower elevation glaciers show significant ablation. This study successively demonstrates the utility of using historic expedition documents to extend the modern record of glacial change.

ACKNOWLEDGEMENTS

I would like thank my advisor, Dr. Ulrich Kamp for his patience and tutelage throughout the many stages of this project. I have come to know him as a fine scholar, mentor, gentleman, and friend.

I am indebted to the committee members Dr. Anna Klene and Dr. Joel Harper for their help with methods and background pertaining to glacial studies.

Many thanks go to Dr. Sarah Halvorson for her support in all things academic and her infectious enthusiasm.

Grateful appreciation goes to Dr. Dr. h.c. Michael Walther of the Mongolian Academy of Sciences at the National University of Mongolia for his logistical support in Mongolia, without which this study would have never materialized.

Deep respect is felt towards Avirmed Dashtseren (Dashka) of the Mongolian Institute for Geography Permafrost Laboratory, who was my partner on the rope and road, treating a perfect stranger like a brother, for which I can never express the true sincerity of my thanks.

The support of benefactors like the American Center for Mongolian Studies and the American Alpine Club funded the research, while the generous scholarships of The University of Montana help offset the costs of my higher education goals.

Mom, Dad, friends and family – thanks for all the support, pushing and consoling were appropriate.

And finally to my lovely wife, partner and best friend Anna Tina – I could not have done it without you – if not for all the coffee, massages and hugs, my body would have surely failed before I saw this through. It's all for you, you're the one. Thanks for believing. Eu at am!

CONTENTS

LIST OF FIGURES	vi
LIST OF TABLES	viii
LIST OF APPENDICES	ix

SECTIONS

1. INTRODUCTION	1
2. PURPOSE.....	2
3. RESEARCH SETTING	3
4. CONCEPTUAL FRAMEWORK	7
5. EXPEDITIONS.....	10
5.2 – 1910 ROYAL GEOGRAPHICAL SOCIETY EXPEDITION.....	10
5.3 – 2010 UNIVERSITY OF MONTANA EXPEDITION	14
6. CARTOGRAPHIC ANALYSIS	17
6.2 – DEM EVALUATION.....	27
6.3 – CARTOMETRIC EVALUATION.....	45
6.4 – CUSTOM CARTOGRAPHY.....	58
7. REPEAT PHOTOGRAPHY	67
7.2 – COMPARATIVE ANALYSIS	80
7.3 – PIXEL ANALYSIS.....	86
7.4 – MULTI-DATA INTEGRATIVE ANALYSIS	93
8. CONCLUSION.....	103
REFERENCES.....	110
APPENDICES	Supplemental Material

LIST OF FIGURES

1. Mongolia and study area.	4
2. Prismatic compass.....	19
3. Hypsometric apparatus	19
4. Plane table	19
5. Telescopic distance finding alidade.	20
6. Legend of original 1910 Carruthers map	23
7. Geodatabase structure.....	28
8. Digital mosaic of scanned 1910 Carruthers map	30
9. Hypsometric shaded relief map of the 2010 Torgen expedition	32
10. Affine transformation.....	33
11. Distortions in georeferencing transformations	34
12. Screenshot of rubber-sheet transformation of core study area	35
13. Clip of the 1910 map showing general agreement with SRTM DEM.....	37
14. Contour comparison between original and derived surfaces	39
15. Elevation error between 1910 and modern DEMs.....	40
16. Histogram showing distribution of elevation error	41
17. Plot of 1910 and CGIAR DEM comparison from validation statistic spreadsheet ..	43
18. Map depictions of monastery and settlement in 1910 and 1970	49
19. Map Analyst software with historic map, reference map, and coordinate pairs.	49
20. Scale variance in the 1910 map by Carruthers	53
21. Distortion and displacement in the 1910 map by Carruthers	54
22. Scale variance in the georeferenced clip of 1910 map by Carruthers	56

23. Distortion and displacement in the georeferenced clip of 1910 map by Carruthers .	57
24. Swiss hillshade model by ESRI	60
25. Identified Turgén glaciers in 2010 Landsat TM5	62
26. Comparison of typesets for 1910 and 2010 maps	65
27. Summit labels.....	66
28. Kodak A3 postcard camera.....	69
29. Newman & Guardia “Nydia” camera.....	69
30. Kodak panorama camera from 1910	70
31. Original page of Carruthers photo album.....	72
32. Original page of Carruthers photo album.....	73
33. Original Carruthers large format photograph of Turgén Peak	74
34. Original Carruthers large format panorama of Turgén Range	75
35. Aligning the historical photograph from 1910 to the modern landscape	76
36. Map of the Turgén study area	77
37. Panoramas ascending Duramyn Peak and of the Turgén Range from the summit ..	78
38. 1910 – 2010 blend mask to check alignment	80
39. Repeat 1910 and 2010 photo pair of Turgén Range from PS01	82
40. Repeat 1910 and 2010 photo pair of rock horn from PS05.....	83
41. Repeat 1910 and 2010 photo pair of nunatak from PS06	85
42. Bi-tonal classification.....	87
43. Pixcavator output screen	87
44. Repeat 1910 and 2010 photo pair of Turgén Peak from PS02.....	89
45. Repeat 1910 and 2010 photo pair of Turgén Peak from PS08.....	90

46. Repeat 1910 and 2010 photo pair of Turgen Peak from PS03.....	91
47. 1910 ice contour in red vs. 2010 ice contour in black from Pixcavator analysis	92
48. 3D model of nunatak in 2010.....	93
49. Rephotography blend with plotted terminus vector bisecting West Turgen Glacier.	95
50. Repeat 1910 and 2010 photo pair of nunatak from PS04	96
51. Photo pair from PS04 showing differences in height of nunatak above glacier	97
52. Repeat 1910 and 2010 photo pair of West Turgen Glacier from PS07.....	98
53. Map of West Turgen Glacier with glacier termini changes from 1910 to 2010	99

LIST OF TABLES

1. Digital data collected for project.....	26
2. Georeferencing coordinate pairs.....	34
3. Value differences between DEMs	41
4. Validation spreadsheet results.	42
5. Custom dataframe projection.....	46
6. Initial Helmert four parameter transformation results for full 1910 map	51
7. Hampel robust estimator transformation results for full 1910 map	51
8. Hampel robust estimator transformation results for study area clip.	51
9. Repeat photography stations	79
10. Results of Pixcavator analysis	88
11. Results of multi-data integrative analysis	100

APPENDICES

LARGE FORMAT

1. Print of 1910 Carruthers map at full resolution Cover pocket
2. Print of 2010 McManigal map at full resolution Cover pocket

DIGITAL MEDIA

3. 1910 geotagged expedition photographs Cover Pocket DVD
4. 2010 geotagged expedition photographs Cover Pocket DVD
5. 2010 geodatabase of all GIS layers Cover Pocket DVD

RETRACING THE 1910 CARRUTHERS ROYAL GEOGRAPHICAL SOCIETY EXPEDITION TO THE TURGEN MOUNTAINS OF MONGOLIA – RECONSTRUCTION OF A CENTURY OF GLACIAL CHANGE

INTRODUCTION

The Turgén Mountains lie in northwestern Mongolia, roughly 80 kilometers south of the Russian border. A Royal Geographical Society (RGS) expedition under Douglas Carruthers visited the area in 1910 and undertook an extensive survey of the range. The expedition produced a detailed topographic map and also documented glacier extents with photographs. It is assumed that the current global climatic shifts have had an effect on glaciers in the Turgén Range however, the extent of these changes are unclear. Relatively little work has been done on glaciers of Mongolia, but it is important to monitor them as they are the ‘water towers’ on which flora, fauna, and humans depend. It is vital to construct a body of research which can document previous changes and serve as a baseline to measure changes in the future. This research retraces portions of the 1910 expedition in order to reconstruct the last century of glacial variation.

The study has three parts. In the first step, historical documents were procured from the RGS in London, including copies of photos, maps, manuscripts, and diary entries. Then, during the Mongolian field campaign in the summer 2010, the Turgén Mountains survey by the 1910 RGS expedition was retraced. The historical photos were repeated and glacier termini were surveyed using GPS. Finally, spatial analyses was conducted using GIS to generate a ‘historic’ elevation model from the 1910 map and compare it to a modern digital elevation model (DEM) generated from SRTM satellite data. The cartometric accuracy of the 1910 map was also evaluated with specialized software developed for historical cartography. The repeat photography was assessed, along with comparing narratives of the two

expeditions, as a qualitative measure of glacier changes over the last 100 years.

Photogrammetric measurements were taken to establish estimates of glacial recession over the study period. This final report includes a new map of the Turgan Range, side by side repeat photographs, and statistics of changes in the glacial conditions.

The study represents a unique opportunity to monitor an isolated glacial system that has a detailed account in the historical record. The results are a valuable indicator of glacial responses to environmental change in Mongolia over the last century.

PURPOSE

In the warming of the current inter-glacial period, the glaciers of the world are experiencing pronounced wastage. Regardless of the anthropogenic contributions, the effects of the warming are observable and measurable. A global effort to assess the health of glaciers is underway. However, the majority of studies start with the satellite record of the sixties and seventies. By researching archives, it is possible to extend the baseline using expedition records from before the collection of modern satellite data.

The purpose of this project is to quantify glacial change over an extended centennial time span by integrating historical data with modern remotely sensed imagery. The scope of the research utilizes proven field techniques to merge the archival record with the technology of satellite and GIS derived spatial statistics. It is a conglomeration of both qualitative and quantitative techniques to produce a more comprehensive measure of the glacial regime over time. In this way, a complete assessment can be accomplished that reveals glacier characteristics prior to the monitoring techniques of the modern age.

The work will answer these three research questions:

1. Are the historical archives of mountain expeditions a valid resource for extending the modern record of glacial change?
2. How has the glacial system of the Turgan Mountains changed over the last century?
3. What is an effective methodology for integrating historical and modern data in order to increase our comprehension of long term glacial dynamics?

The study addresses these questions by integrating analysis of cartometric evaluation, repeat photography, and remote sensing using both standard and hybrid methods.

RESEARCH SETTING

The research was conducted in the Turgan Mountains in northwestern Mongolia (Figure 1). The range is heavily glaciated in northern aspects, feeding several rivers which flow northeast towards the regional capital of Ulaangom, and into the UNESCO World Heritage-designated Lake Uvs Nuur Basin. Turgan and its sister range, Kharkhiraa, lie within the Uvs Nuur Strictly Protected Area, part of the Mongolian national system of environmental conservation. The remote mountain range contains all the prerequisites required to address the focus of the study:

- A variety of glaciers and periglacial landforms to measure in the field and compare to both historic and modern data.
- A well-documented historic expedition to the range that produced a detailed survey and photographs of the glacial system exactly one century ago.
- A modern satellite record that has already been evaluated by previous research on which this study can build.

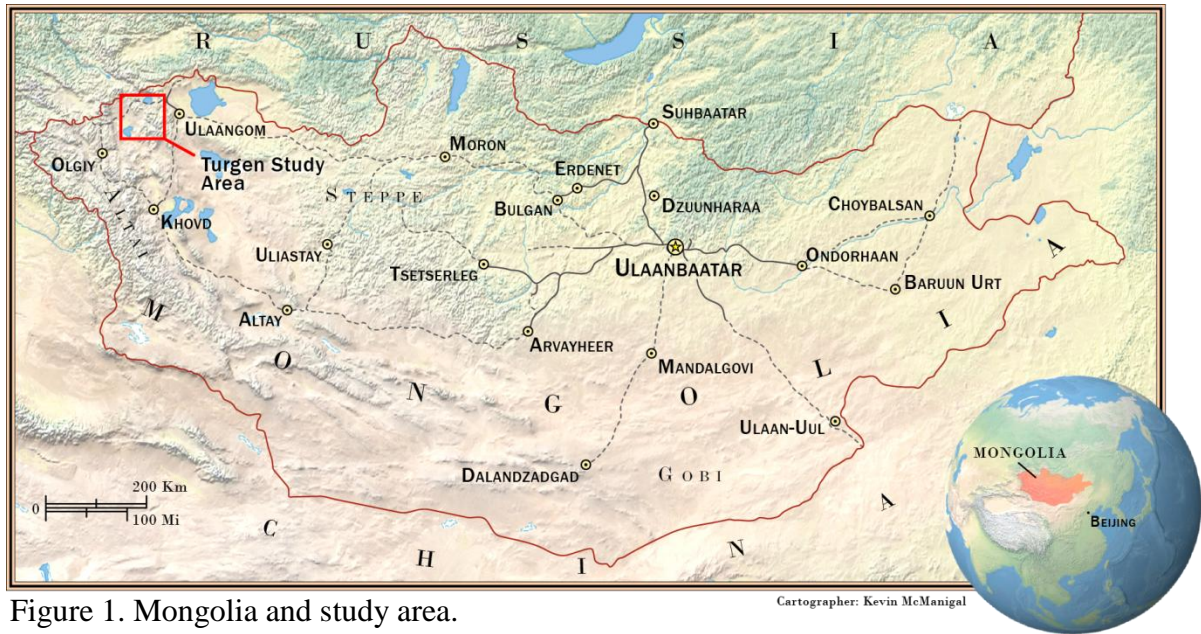


Figure 1. Mongolia and study area.

The mountains are an isolated rampart surrounded by foothills forming lush valleys that are the headwaters for multiple rivers. These summer pastures are rich in vegetation and have been used for centuries by Nomads grazing their herds. As an island in the Steppe, the ranges are also home to several endangered species, including snow leopards, Asian ibex and agali sheep, as well as being a haven for migratory birds. Carruthers (1914a, 276–277) described the range as they approached it from the north one hundred years ago:

With superb grandeur the snow pinnacles rise above the forested valleys and grassy plateaux. From every point of the compass, for many days' journey away, one can see the principal peak, a cone of ice, which rises to over 13,000 ft. in altitude. [...] As a snow-capped mountain of alpine character, the Turgun stands solitary, rising sharply above the steppes and the desert-ranges which surround it on all sides.

These words speak to the beauty and unique setting of this remote range, and add historical context to the research.

While isolated, the Turgen and Kharkhiraa ranges are generally accepted to be related to the Altai Mountains. They are not directly connected however; rising alone over the three lake basins of Uvs Nuur, Uureg Nuur, and Achit Nuur which make up the Mongolian Great Lakes Basin. The mountains are formed predominately by the strong tectonic uplift of the Altai Mountains, while the forces of glacial erosion have carved large U-shaped valleys bordered by cirques and evidence of previous hanging glaciers (Khrutsky and Golubeva 2008). In the modern epoch, the glaciers have retreated to the highest basins and continue to recede (Lehmkuhl 1998). However, recent research has suggested that the rate of ablation has stabilized around the end of the 20th century (Kadota and Davaa 2007).

This solitary range is known for persistent cloud cover, possibly due to orographic lifting (Khrutsky and Golubeva 2008). Even Carruthers (1914b, 383) a century ago remarked how the summer veil of clouds was responsible for the preservation of the large snowpack. Carruthers took sporadic temperature readings in his notes, but no complete weather data for 1910 was found. He does mention that the bad weather during July and August of 1910 hampered their work (Carruthers 1914a, 284). There may be climate records from this period in Russian archives, but they are inaccessible at this time. During the 2010 expedition, the weather in July was mostly stable and clear. However, recent studies have estimated that up to 70% of the annual precipitation falls in the summer months from June to August (Kadota and Davaa 2007). Much of that would fall as snow in the high elevations of the range, where summits can reach to above 4000 meters. The winters are cold and dry, with the Mongolian anti-cyclone dominating the regime, perhaps even ablating some summer snow (Khrutsky and Golubeva 2008).

For Ulaangom (939 m; 49°55'N, 92°03'E) located in a basin northeast of Turgen-Kharkhiraa Mountains and the closest urban center to the range with weather data, the measured mean annual temperature is -4°C , and the mean monthly temperature ranges between -32°C in January and 19°C in July (Jansen 2010). The measured mean annual precipitation is 136 mm with a 'rainy season' from June to September (Jansen 2010). Snow contributes less than 20 percent to the annual total precipitation (Batima et al. 2005), with the maximum snow depth occurring in January, and the main ablation period in March (Shinoda et al. 2001; Morinaga et al. 2003). Without the presence of weather stations within the Turgan Range, Khrutsky and Golubeva (2008) estimated that above 2,500 meters, mean annual precipitation is 400-500 mm, while Böhner (2006) interpolated mean temperature in the region of the summits to be -8°C , both substantially wetter and colder than Ulaangom. Looking at the time period of 1940–2003 Batima (2006) documented a temperature rise of 1.8°C , with clear warming from the beginning of the 1970's intensifying towards the end of the 1980's. This general trend of temperature increase in Mongolia is slightly above the general trend in the Northern Hemisphere (Jacoby et al. 1999). Both authors detected a slight increase in precipitation during the second half of the 20th century, however, the changes were statistically insignificant and within the range of long term variations (Batima et al. 2005; Jacoby et al. 1999). Finally, Batima and others (2004) estimated short term temperature increases of 2°C , with long term increases of up to 7°C when comparing studies that applied standard climate models to Mongolia and the Mongolian Great Lakes Basin.

CONCEPTUAL FRAMEWORK

Since the end of the Little Ice, approximately 12,000 years ago, the terrestrial alpine glacial regime has been in recession. Towards the end of the 20th century, scientists began to document increasing temperatures, especially in high latitude and mountain environments. These changes are most evident in the glaciers of the world's mountains (McCarthy et al. 2001). Mountain ranges on every continent, from the Alps to the Rockies, the Sierra Nevada to the Himalaya, and even the isolated super volcanoes such as Kilimanjaro, are seeing pronounced ablation in their glaciers. These glaciers are an important indicator of global climate changes, and perhaps more germane, are vital resources for human cultures and natural ecosystems. They need to be studied and monitored to evaluate the degree of these changes and develop adaptation strategies to address the environmental challenges already being felt (Bury et al. 2010).

Glaciers are the natural reservoirs of the hydrologic system on which innumerable downstream communities depend. They store water by converting winter snows to ice, which is then metered out during the hottest of the summer months, acting as a buffer to the seasonal variations in water supply (Knight 2009). This water supply is crucial not only to late season irrigation of agriculture, but also carries flora and fauna through dry periods and counter-acts episodic droughts. These seasonal fluctuations can literally be felt thousands of miles downstream, highlighting the dependence on glaciers of billions of people and entire ecosystems, covering large swaths of the planet (Oerlemans 1994).

Besides the dependence on glaciers as the stewards of water reliability, society is increasingly dependent on an even supply of water for the generation of hydroelectric power. Developing nations are investing heavily in hydroelectric infrastructure as a sustainable

source of electricity to fuel economic growth. For example, Mongolia has evaluated and started construction of small scale hydroelectric power generation as part of a national strategy to increase renewable energy production (Enebish 2004). Without the consistent contribution of glacial melt water, these investments could cease to produce power part or all of the year. Therefore, assessment of glaciers is essential both in the planning stages of proposed hydroelectric development and in management of existing installations.

Another threat in need of evaluation, opposite of reduced water reliability, is too much water all at once. As glaciers retreat, many of them form lakes behind a dam of terminal moraine debris. These notoriously weak dams of unconsolidated till, regularly fail causing glacial lake outburst floods (GLOFs). This sudden release of water can destroy entire villages causing incalculable tragedies in lost human lives, not to mention the monetary loss of investments in downstream infrastructure. With proper measurement and evaluation of GLOF potential, many of the risks can be reduced, or eliminated altogether. Programs are already underway to drain high risk lakes throughout the Himalayan region (Mool 2001). Mongolia experienced large jökulhlaups on par with the Glacial Lake Missoula events in the Pleistocene (Herget 2005). The potential for future flooding certainly exists, however the risk has yet to be accessed.

For all of the reasons mentioned above, national governments and international organizations have undertaken a broad program to measure and document changes in alpine glaciers throughout the world. Due to the vast numbers of glaciers, with their broad distribution, the limited and expensive access, and the urgency of establishing a global baseline in the midst of rapid change, remote sensing techniques are being employed to catalogue the world's terrestrial glaciations. Programs such as the Global Land Ice

Measurement from Space (GLIMS) and World Glacier Inventory (WGI) are analyzing satellite data and compiling the results in regional centers such as the National Snow and Ice Data Center in Boulder Colorado (Raup et al. 2001). The programs continue to refine data and techniques to quantitatively assess the health of global glacial systems. Part of this process is the ground-truthing of results; however, it is only being performed on a limited scope.

While remote sensing techniques are improving every year, the most accurate way to evaluate the state of a glacial system is with long-term, annual mass balance measurements. This process requires fieldwork to measure ablation rates with highly accurate GPS surveys and the assessment of accumulation by digging mass balance pits on the glacier. It is also important to establish the Equilibrium Line Altitude (ELA) on the last day of summer for each year (Hubbard and Glasser 2005). When annual fieldwork data of longer temporal scales is compared, a very clear picture of glacial balance emerges. The accurate assessments of proxy glaciers can in turn be used to correct remotely sensed data, making global estimates more valid (Bamber and Rivera, 2007).

The Torgen-Kharkhiraa range has seen several remote sensing studies with various results. Using aerial photo generated topographic maps and satellite data, Lehmkuhl (1998) concluded that the Torgen glaciers had retreated between 200-500 meters from 1948 to 1991. Employing only remote sensing techniques, Kadota and Gombo (2004; 2007) reported that while the Torgen glacier had lost 19% of its surface area, the loss had occurred between 1970 and 1990, remaining stationary afterwards. Interestingly, another study by Khurtshy and Golubeva (2008) found that the glaciers had lost 35% of their area in a similar time span. The inconsistencies in these reports speak to the problems that arise when comparing only

slightly different methodologies. Another discrepancy may stem from limited to no fieldwork being used to validate the results of remote sensing analysis.

Finally, all three studies look only to the beginning of the satellite record basically starting in the 1960's. Only Lehmkuhl (1998) attempted to extend the glacier record with maps. Recent studies by Racoviteanu et al. (2007) in the Peruvian Andes have taken modern topographic maps and used them to create DEMs for comparative glacial analysis. Schmidt and Nüsser (2009) combined remotely sensed imagery with rephotography in the Nanga Parbat region Pakistan, successfully demonstrating the multi-temporal, integrative data approach. Those methods are expanded here to incorporate Carruthers' data and peer back into the records at the beginning the century.

EXPEDITIONS

1910 ROYAL GEOGRAPHICAL SOCIETY EXPEDITION

The 1910 RGS expedition to the Turgan Mountains was only one small part of the longer journey lead by Douglas Alexander Carruthers. Along with his colleagues, Morgan Phillips Price and John Humphrey Miller, Caruthers traveled from London on the Siberian Express to Krasnoyarsk, then south through the Upper Yenisei River basin, over the divide onto the Mongolian Steppe, east over the Altai Mountains, and eventually south again through Kashmir and into India. Traveling mostly on horseback and foot, the voyage took over two years to complete, with the team not returning to Great Britain until the fall of 1912. The expedition was one on the last classic Victorian explorations, epitomizing the style of English Geographers that were 'masters of all they surveyed' (Burnett 2000). By this, it is meant that the party truly 'explored' the landscapes that they moved through, collecting

samples of everything that they encountered, and documenting every waking moment. The expedition returned to England with over 300 unique flora and fauna samples, hundreds of photographs, and several detailed maps. The account of the journey filled two volumes of the book titled *Unknown Mongolia*, and provided content for at least half a dozen articles in the *Geographical Journal*.

Douglas Carruthers, the expedition leader, was born in 1882, and by his early twenties was a respected Geographer that had become an expert taxidermist and an accomplished cartographer. By the time he began the 1910 voyage, he had already participated in research trips to the Congo and the Syrian Desert where he collected specimens that still bear his name in the British Natural History Museum (RGS Biography 2008). He was famous for his work ethic, spending entire days surveying, and then preparing skins by candle light until dawn, documenting everything in his journals, only to begin again after a few hours sleep (Lattimore 1978, 210). He wrote that “if you give a man more work than he can do, he will do it” (Carruthers 1914a, 289). However, he was also somewhat humble, asking the RGS in telegraphs to ensure that the trip not be labeled as “his show” in newspaper reports, insisting on credit for the contributions of Price and Miller (RGS Archives 2010). Upon his return, Carruthers was awarded the Gold Medal for Exploration by the RGS, and served as secretary of the Society from 1916 to 1921 (RGS Biography 2008). He worked as a cartographer for the British War Office during WWI, being recognized as an expert on the Middle East and Central Asia, writing in correspondence that the war effort was overwhelming his responsibilities to produce maps for the *Geographical Journal* (RGS Archives 2010). Later, he continued to work for the RGS, giving lectures and writing on various topics until his death in 1962.

The period of the journey, in context with the overall geopolitical situation, can offer insight into the nature of the Carruthers expedition. At the time, 1910, Outer Mongolia was controlled by the Manchus of China, but was about to declare independence in 1912. The Chinese had a system of governors that ruled the Mongolian Steppe, while Russian traders freely traveled the area. Interestingly, there was very little knowledge of Central Asia in the English speaking western world. The Russian Empire had explored much of the area, but those records were increasingly withheld as the nation plunged into the Revolution of the Proletariat. Great Britain was in the last moves of the Great Game, holding on to the colony of India, even as The Great War loomed just around the corner. From this stage, England was trying to fill in the last blanks on its maps, and as it had done in the past, geographical exploration was used to establish some entitlement. As discussed by Burnett (2000), these expeditions, while scientific in nature, provided the British Crown with invaluable information on natural resources and routes of passage though the landscapes.

In *The Power of Maps*, Wood (1992, 42-47) relays how the race to chart an area often leads to assertions of control, sometimes using the accuracy of the latest map to trump the claims of previous explorers. Carruthers repeatedly mentions the need to “correct the wildly erroneous Russian maps,” and while not overt with any feelings of ownership, he does assert that he “knows” the landscape better than any who have come before him (RGS Archives 2010). Carruthers does not seem to ever treat the expedition as a reconnaissance for colonization, but he could not have helped being a product of his society. He is judgmental of the cultures he visits, taking careful stock of class status as if to note which “breeds” could be trusted for trading or soldiering (Carruthers 1912, 533). There is contemplation in one passage over the plight of the Mongolian Nomads. Carruthers wondered if Buddhism was not

just another form of serf enslavement, and predicts the permanence of the Mongol Empire if only they had adopted Islam (Carruthers 1912, 532-533). He also freely participates in the common practice of inventorying resources such as timber, wildlife, and minerals. At one point he remarks that the lamasery at the foot of the Turgun Valley would likely be full of “treasure.” (Carruthers 1914a, 271). He is not an unkind man however, treating even the poorest people with respect and even packing toys for the children along the way (RGS Archives 2010).

It is interesting then that the expedition spent so much time with the detailed survey of the Turgun Range. Beyond the scientific purposes of the journey, the writings make clear that the men were also intrigued by the adventure of the endeavor. The Victorian gentlemen of the period were most enamored with the sport of mountaineering. Trips to the Alps were considered vital training for all trekkers, and the love of mountains runs through many explorers’ narratives of the time (Gilbert 2004). Carruthers (1914a, 266) claimed that the “first sight of those eternal snows stirred us to a pitch of enthusiasm” that they changed their proposed route to visit the range.

They entered the Turgun Valley on August 13th, 1910, and after sending gifts to the local Khan, who was ill, they proceeded to head towards the peaks conducting a plane table survey. On the 15th, they camped on the bench above the Turgun River “within striking distance of the high peaks” (RGS Archives 2010). In bad weather, they made it to the divide of the East Turgun Glacier at around 11, 300 ft. on the 17th, after climbing “great amounts of snow” (RGS Archives 2010). Carruthers (1912, 534; 1914a, 283) writes that old moraines were present one mile from the snouts of the glaciers, with the East Turgun Glacier calving in seracs at the terminus, and “in all cases, were in a state of retreat.” They also attempted to

climb Turgen Peak, but found it too difficult (Carruthers 1914a, 282). After a deluge of rain on the 19th, the party headed down valley to the village near the lamasery and traded brandy for silks and a saddle with the Khan (RGS Archives 2010). They continued to the west, and then south, returning east up the Yamachu River valley. On the 21st, they encountered snow at 7,500 ft., which forced them to stay in a cave (RGS Archives 2010). They attempted Turgen from the south, but found the glacier too steep, so crossed the pass onto the Yamachu Plateau, headed west again, and finally proceeded down into the Achit Nur Basin on the 25th (Carruthers 1914a, 287). They finished the Turgen portion of the expedition with a swim in the lake, writing that they had “good fun” (RGS Archives 2010).

In an article by Price (1968) after the death of Carruthers, he remarked how they were possibly the last great geographical expedition undertaken in the ‘old way,’ before the revolution of transportation. The style of travel completely changed in the ensuing decades, and Carruthers, in his last days, agreed that one could no longer be immersed in the world from behind the wheel of a motor vehicle (Price 1968). Theirs was truly an end of an era.

2010 UNIVERSITY OF MONTANA EXPEDITION

Before leaving Montana, considerable time was spent developing a logistics plan for the field research. Contacts were continued from the previous summer’s fieldwork and the groundwork was laid for the season’s expedition. Preliminary work was done on the 1910 map, including georeferencing and digitalization the routes and campsites of the original Carruthers expedition, which then were imported into GPS units for fieldwork.

Gear was organized and packed based on the weight limitations of international air travel. Unfortunately, restrictions made larger, more accurate GPS base-station systems

prohibitive. Both the research equipment and personal gear was condensed to fit into a single large expedition backpack. The logistics required self-contained mobility through many forms of transportation; including flights, vehicles, horses, and on foot.

The first leg of the journey in early June led to the Royal Geographical Society in London. The archive librarians had multiple items on reserve for the PI, and during the course of a three day visit, complete access to the records of the Carruthers' expedition was granted. Thorough notes were taken from the original journals and high resolution scans of the 1910 glacier photographs arranged. The original map and the notes concerning its construction were explored. The visit concluded with a members-only invitation to a showcase on arctic exploration. Incredibly, the PI was able to interact with artifacts including Shackelton's bible and Scott's monocular. The society's archives are truly an international treasure and it was a privilege to have access to them.

The team arrived in Ulaan Baatar the first week of July and only had a few days in the city to prepare. Visa extensions, permits, and visits to benefactors were carried out. The team shopped for provisions and made final plans for the field work, packing SUV trucks for the excursion. On the 7th of July, the expedition began in earnest, starting the drive of over 1200 km to the regional capital of Ulaangom, which took five days.

Arriving in the village on a Sunday, July 11th, a meeting with the superintendent of the Turgen Strictly Protected Area was arranged. Due to official letters and prearranged agreements made by Dr. Walther, the research permits were secured at a reduced cost. Resupplies were procured before heading over Ulan Dava Pass into the park. From the shores of Uureg Nuur Lake, the team drove south into the Turgen Range and contacted the ranger, Baatar Chou, who agreed to guide the party into the mountains and provide horses for the

gear. The next day, Dr. Kamp, Baatar Chou, Dashka and the PI packed four houses and followed the track of the 1910 expedition up-valley towards Turgen Peak. Dr. Walther remained in base camp with a colleague, repeating explorations of side valleys and peaks depicted on the Carruthers map.

Over the next seven days, the team ascended several mountains and repeated photos from the original stations occupied a century before by Carruthers. The climbs required technical glacier skills, and combined with long alpine days, proved to be very challenging. Camp was moved successively further into the range until an advanced base camp was established at the head of the valley below Turgen Peak. Based on GPS coordinates, the camp was likely within 30 meters of the 1910 Carruthers camp. Using horse support, the research team trekked up to and beyond the alpine meadows of the East Turgen Glacier, where Dashka and the PI climbed to the col and retook several photos of the unnamed glaciers further to the east. Both East and West Turgen Glacier were surveyed with GPS while repeating photographs within the moraine system. After all the 1910 photographs had been repeated and the glacier termini satisfactorily reconnoitered, the team returned to base camp over the course of two days.

The entire expedition party then returned to Ulaangom and spent several days re-supplying. Dr. Kamp and Dr. Walther left the team, while Dashka and the PI, along with the cook, drove to the southern reaches of the Turgen Range. There, horses were hired again and ridden over 80 km into the Yamachu Plateau, where the Carruthers route was rejoined. Several days were spent exploring the southern reaches of the Turgen Range and repeating photographs from the original expedition. However, the weather had turned, and lightning

storms forced a retreat from the mountains. After riding out of the highlands, a few days were spent living with nomads until the long drive back to Ulaan Baatar was finally made.

CARTOGRAPHIC ANALYSIS

BACKGROUND

Historical Mapping:

In the introduction to *Unknown Mongolia*, Carruthers (1914a, 278) states that not only was his expedition undertaken to be the first British explorers of the Yenisei River, North West Mongolia, and Dzungaria, but also to fill large empty quarters on the maps of Russian explorers that preceded him. To this end, Carruthers mapped vast regions along the track of the expedition by extensive plane table surveys in the field. In many cases, he used astronomically fixed points from previous Russian work, citing map sheets Nos. V and XIII of the *Southern Frontier Regions of Asiatic Russia*, published by the Topographical Section of the Russian General staff in 1891 and 1887 (Carruthers 1913). Where he found errors in the Russian work or unmapped terrain, his expedition fixed their own locations using a sextant, astronomical compass, and marine chronometer to derive latitude and longitude from the angle of the sun or stars, and the difference from Greenwich Meantime at high noon (Carruthers 1913). These locations were in turn used as the benchmarks for plane table stations along the transect of their survey.

For the Turgan Range, Carruthers (1914a) consulted the work of the Russian explorer Potanin, who mapped the eastern slopes from 1876-1879. However, Carruthers (1913) was unable to join the previous survey with his own work and simply let the eastern contours trail off, with only rough shading to depict the general lie of the terrain. Carruthers also differed from Potanin in the naming conventions of Turgan Peak. At the entrance of the Turgan

Valley, the river that runs north past the lamasery was called Kundelun by the locals in 1910. Carruthers (1914a, 266) bestowed the mountain at the headwater of this valley Kundelun Peak, while moving ‘Turgun’ (Carruthers spelling) to the east. He expressed difficulty with determining place names as they often had a Turkic, Mongolia, Chinese and Russian version simultaneously (Carruthers 1913, 346). His solution was to use the Russian transliteration were available, as is commonly done today. Modern Russian topographic maps from 1970 and the 2005 Mongolian Road Atlas by Tserennyam have reverted back to Turgen as the name of both the peak and the river, with all references to Kundelun being absent. Therefore, this study consistently uses Turgen to refer to the main peak (while not the highest), even when speaking of the Carruthers expedition and map.

The 1910 expedition carried extensive gear for the purposes of conducting a topographical survey as they traversed their route. Much of this gear was loaned to the party by the Royal Geographical Society (RGS) in London. The following list comes from the personal diaries of Carruthers viewed at the RGS archives in the summer of 2010:

- Two Mark V prismatic compasses with bronzed cases and luminous pearl dials in leather carrying cases (Figure 2).
- Two hypsometric apparatus with boiling point thermometers; one made by Cary and the other by Negretti & Zambra (Figure 3).
- Plane table and wooden tripod with a Johnson Head inferred from photos (Figure 4).
- Reeves folding distance finder telescopic alidade with a clinometer made by C.F. Casella & Co. Ltd (Figure 5).
- Reeves astronomical (starfinder) compass made by Stanford.
- Aneroid barometer reading to 20,000 ft.

- Two pedometers.



Figures 2, 3, 4. Prismatic compass, hypsometric apparatus, plane table (Harvard, RGS).

No record of returning the gear is documented other than to note the hypsometric thermometers were recalibrated at the Kew Observatory upon returning to London, and that they measured the same as at the onset (Carruthers 1914b, 385). With this kit, the expedition carried more than adequate instrumentation for producing detailed maps.

In the Carruthers records, there is little information describing how the gear was used, however the procedures of a general plane table survey are well documented by the *Textbook of Topographical Surveying* from the Carruthers period (Cheetham 1905). In fact, the art of plane tabling was developed well before Carruthers by the likes of Gillespie (1855) and continued to be refined into the modern era (Low 1952). Of the many considerations at the time of Carruthers was the issue of paper warping due to moisture, which can cause considerable error. This was alleviated by complicated preparation of the map sheets being laminated on wet linen and stretched onto the table, but it is unlikely Carruthers went to these lengths on the extended journey (Cheetham 1905). A more practical solution discussed by



Figure 5. Telescopic distance finding alidade (Harvard).

Mather (1938) suggests the use of laminated paper with opposing grains to counteract paper shear. Notes by Carruthers hint at this with the inclusion of “prepared survey sheets” in the gear list (RGS Archive 2010).

From research into the techniques, and clues from the writings of Carruthers, the plane table procedure may have progressed thus: Once the location of a control station was fixed as discussed previously, the altitude would have been established by measuring the boiling temperature of water with the hypsometric apparatus. Carruthers (1913, 349) mentions the use of the *Climatological Atlas of the Russian Empire*, St. Petersburg 1910, as the source of his elevation corrections. It appears that the aneroid barometer was only used as a back-up instrument. Next, the table would have been leveled and oriented to north. From the fixed station pin placed on the table board, rays are drawn out with the ruler edge of the telescopic alidade to prominent features on the landscape. The ray azimuths shot from the prismatic compass are recorded directly onto the sheet, along with the distance to features read from

the focal stadia in the alidade. Simultaneously, the elevations of the points are recorded from the clinometer on the instrument. Once a representative number of points were mapped, the station was moved to one of the points shot along the transect, and the prior station back-sighted to reorient the table. Finally, the previous points are re-shot, creating a triangulated network of rays that are used to confirm distances and angles. Index contours are drawn in the field, as well as labeling as many features as possible. In this way, a detailed map of the topography can be drawn as one moves through the landscape (Pugh 1975).

In his diaries, Carruthers writes of “moving slowly through the terrain” and “performing careful surveys of the varied relief” (RGS Archive 2010). He describes spending long hours at the plane table while his partners, Price and Miller, collected samples and photographed the scenery (Carruthers 1914a, 288-289). He and his partners were enamored with the Turgan Range, saying “the remarkable beauty of this almost isolated highland, its Alpine valleys, forests of pine and larch, and high pastures, tenanted by the herds of yaks, leading up to glaciers and snowfields, attracted us more than anything else we saw in Mongolia” (Carruthers 1912, 533). The final product of his survey is a beautiful map of the Turgan Range that represents the landscape with surprising precision. So accurate in fact, that it was used to navigate while trekking through the region during the 2010 expedition.

However, for the purposes of evaluating the changes in the glacial regime over the last century, the locations and elevation of those features on the Carruthers map must be quantified. This is the goal of the forthcoming analysis.

Analysis Phases:

The map data were processed and analyzed in two distinct phases, with a third phase consisting of a custom cartographic product being prepared. Preliminary work on the DEM evaluation phase was done prior to the expedition in the summer of 2010, and continued upon return. The tiles of the original map were mosaicked and georeferenced so that the camps and route of the 1910 expedition could be digitized. The data was then imported into GPS units for the fieldwork. The process produced a rough estimate of accuracy for the original 1910 map and revealed irregularities compared with the actual landscape. Once back in the computer lab, refinements to this first phase were conducted to analyze the accuracy of elevations in the 1910 map.

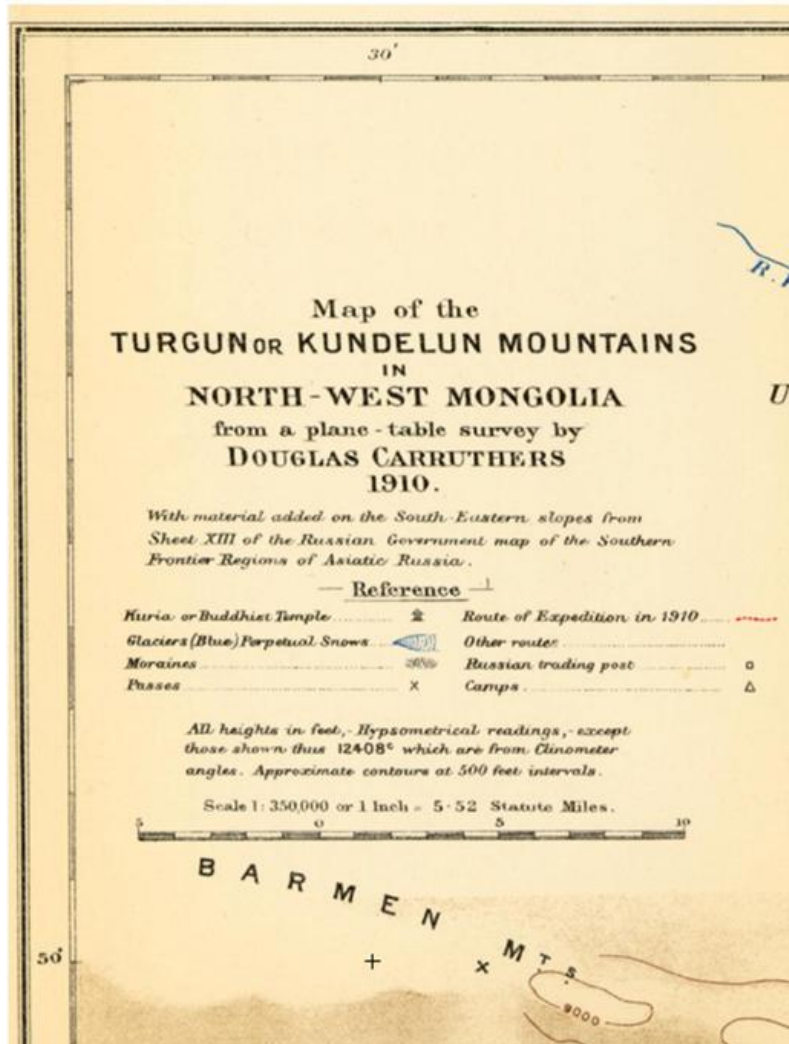
The second phase of cartometric analysis was a more detailed evaluation of the 1910 map using specialized software to quantify positional error compared to modern Russian topographic maps. This phase consisted of extensive computer processing and data manipulation, with some tasks requiring overnight computation. Utilizing advanced techniques of historical map evaluation, the analysis attempts to demonstrate the usefulness of expedition maps in the monitoring of landscape evolution, specifically, glacial change.

Third phase methods consisted of constructing a highly stylized cartographic product. Image classification was also conducted during this phase to extract glacial extents and small lakes from the landscape. Specialized techniques and custom software were employed to produce a map which attempts to emulate the cartographic style of the original 1910 sheet. The final 2010 map incorporates historic cartographic techniques imitated within a modern digital workflow.

DATA

Maps:

The 1910 map was originally published in the RGS *Geographical Journal* (Carruthers 1912). An archived copy was viewed in London, however, the fold-out that is



bound inside the back cover of the magazine was too fragile to be scanned on a large format drum. A high resolution scan was found in an online pdf of the Carruthers' (1914b) article *Further Information on the Turgun or Kundelun Mountains of North-Western Mongolia, and Notes on a New Map of this Region*. The map was located in an appendix of the scanned

document and covered six pages of the pdf. The legend of the 1910 map calls out 500 foot contour intervals and a 1:350,000 scale. It also details natural features including glaciers, moraines and passes. In addition, it shows specific cultural sites such as temples, trading posts, as well as the route and camps of the original expedition (Figure 6). The margins contain latitude and longitude

ticks at two second intervals. The extent of the map is 49° 17' N to 50° 21' N, by 90° 19' E to 92° E. No map projection was provided.

Russian 1:100,000 topographic maps were downloaded from the Mapstor web portal. The ground surveys for the Russian maps were originally conducted in 1942, and then updated in 1949. The area around the Turgén Range was updated with aerial photography in 1970 and the map of Turgén Peak sites this date as the latest revision on the collar. Twenty map tiles were obtained to cover an extent somewhat larger than the 1910 map.

Imagery:

Landsat 5 TM scenes were downloaded from the Earth Explorer data portal. They are of 30 meter horizontal resolution and were imaged between August 29th and September 10, 2010. Ideally, late summer scenes with little to no snow cover should be used, however, this period is also the rainy season over the study area. There was difficulty in finding cloud-free scenes, though the August 29th scene is very clear and covers 90% of the 1910 map extent. There are a few smoke streaks from fires and some low clouds, but the entire Turgén Range is cloud and smoke-free. Unfortunately, the matching path from August that covers the southern 10% of the study area was obscured by clouds, so a corresponding path image from September was substituted. The colormaps do not match perfectly, but this is of no consequence for the glacier analysis. The geotiff files measure 8281 x 7521 pixels at 96 dpi and have the standard terrain correction (Level 1T) applied.

A Landsat MSS scene was downloaded from the Global Land Cover Facility (GLCF) data portal. It has a 60 meter horizontal resolution and was imaged on June 25, 1992. It was only used as a visual aid for georeferencing in the first phase of analysis.

DEMs:

A set of ASTER gDEM tiles were downloaded from the WIST data portal. They have an estimated resolution of 20 m vertically, and of 30 m horizontally. The tiles are composed of a number of ASTER scenes and also have numerous pixels filled by SRTM data that can be viewed in the accompanying ‘Quality Assessment’ files downloaded with the gDEM. Because so many scenes are used to generate the gDEM, no single date could be confirmed that the surface represents. This is an issue when trying to measure glacial change.

A set of SRTM DEM tiles were downloaded from the Earth Explorer data portal. The finished grade DEMs with a 3 arc-second horizontal resolution (90 meter) were obtained for an area extending past the extent of the 1910 map. The DEMs, which were collected in 2002 and last updated in 2010, were received in a bil format. In addition, SRTM DEM coverage of the study area was also downloaded from the CGIAR data portal. It is also a 90 meter horizontal resolution dataset, but has been corrected and filled to provide 16 meters of resolution in elevation. This set of filled DEMs was used to compliment and patch holes in the data from Earth Explorer. The process is discussed in the methods.

Vector Data:

The Geo Community data portal provided vector layers covering all of Mongolia. These include roads, rivers, lakes, villages and *soums* (districts). While in Mongolia, a set of nationwide 1:500,000 scale road shapfiles were also procured from the Mongolia Academy of Sciences, but were only useful as a reference.

GPS Data:

Various point and line data were collected in the field including photo station waypoints and tracks around the glacial margins. A consumer grade Garmin 60CSx was used. The more robust Trimble Recon GPS unit failed in the mountains because of software boot issues. Accuracy information for the Garmin unit was noted in field books with the average error being 9-12 meters. This error falls within the resolution of both the satellite and DEM data. The time stamped active GPS track files were used to geotag the photographs taken during the trek into the Turgan Range, while the glacial extents were saved as individual track records. Table 1 shows all of the raw data collected in the various resolutions and formats.

Table 1. Digital data collected for project.

Name	Format	Date	Resolution	Source
Map of the Turgan Mountains, Carruthers	Paper Topographic, Digital Mosaic of pdf Scans	1912	1:350,000	RGS
Russian Topographic Maps	Digital Scans of Paper Sheets	Updated 1970, from 1968 Aerial Photos	1:100,000	Mapstor
Landsat L5 TM	Digital Satellite Imagery	8/29/2010 and 9/27/2010	30 m	Earth Explorer
Landsat MSS	Digital Satellite Imagery	6/25/1992	60 m	GLCF
ASTER	gDEM	Various	30 m, 20 m Z	WIST
SRTM	DEM	2002	90 m	Earth Explorer
CGIAR SRTM	DEM	2002, Updated 2010	90 m, 16 m Z	CGIAR
Mongolian Roads Rivers, Lakes, Villages	GIS Shapefile	Various	Various	Geo Community
GPS Field Data	GPX	July 2010	9-12 m	PI

DEM EVALUATION

BACKGROUND

The science of DEM evaluation for the detection of glacial change has been in use for over two decades (Rentsch et al. 1990). Pellikka (2010) gives a thorough treatment of modern techniques for mapping glaciers, including the monitoring of ice loss by comparing multi-temporal DEMs. The combination of satellite imagery and DEMs to map glaciers is covered by Bolch and Kamp (2006), while Chaplot et al. (2006) evaluated the various interpolation methods for DEMs used in landscape analysis. Kamp et al. (2003) went further in describing the generation of high resolution DEMs from ASTER satellite data, which was then applied to geomorphometric analysis of glacial features. The use of cartographic data as a source for the measurement of geomorphic and glacial change is justified by Lawniczak (2008) citing previous work by Bartkowski (1974), who considered maps as valid field surveys of the terrain. The work of Brown et al. (1998) further established the use of DEMs derived from cartographic products as a means of classifying glacial landscapes. Pearson et al. (2009) used laser scans of 18th century plaster terrain models of the Swiss Alps to create historic DEMs which were then compared to modern SwissTopo elevation data similar to the methods used here. The methodology of Racoviteanu et al. (2007) was helpful, as they also digitized historic Peruvian topographic maps to create DEMs, and then used raster calculations to compare them to multiple elevation datasets on a cell by cell basis. However, the maps in that study were from 1952 and did not have the georeferencing challenges present in the Carruthers map from 1910. The extended technique here then was to reference the hand-drawn map and create a model of the 1910 terrain for comparison to satellite derived elevation data.

METHODS

Geodatabase Construction:

A number of intermediate geodatabases (GDB) were constructed to facilitate the various GIS operations leading up to a “clean” dataset for analysis. For example, a working

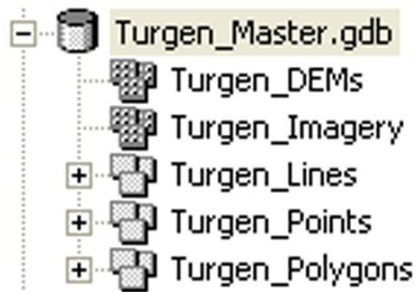


Figure 7. Geodatabase structure.

raster GDB was created to hold mosaic, composite, resample and georeference operations on the raster data before it was clipped and imported into a master GDB.

A working vector GDB was also created to hold the intermediate processing steps of the point, line and

polygon data such as GPS, roads and lakes features. The Master Turgen file GDB was structured in a way as to organize data along their respective classes (Figure 7). A point, line, and polygon feature dataset format were employed to organize each feature class element of the data. The feature datasets were all assigned WGS 84 as a geographic coordinate system throughout. As the final feature classes were imported into the feature datasets, they inherited this projection. Raster catalogs were also constructed within the GDB to accept the clipped rasters and standardize those projections to WGS 84. However, because of the tendency for raster data to hold projection information, each image was re-projected before import into the catalog. The structure of the Master Turgen GDB was built along the best practices outlined by Zeiler (1999).

Map Image Preparation:

The six pdf scans of the 1910 map were converted to hi-resolution tiff files using Adobe Photoshop (PS). Each was saved at 4200 x 6000 pixels with a dpi of 600. The six

converted tiffs were then mosaicked using the Photomerge tool in PS (Adobe, 2010). The default settings produced very good results; aligning the six tiles into a virtually seamless reconstruction of the original work. The large map file was flattened, cropped, and resized in accordance with the measurements derived from the original scale bar. Guides were set up in PS and small crosshair tick marks drawn at six internal points of latitude and longitude based off the coordinate grid in the neat line of the original map. The final map file was down-sampled to 360 dpi and saved as a 5120 x 5120 pixel tiff that measures 14.2 x 14.2 inches. As a visual check, the map was printed on two tiled 11 x 17 inch sheets and the graphic scale measured by hand. The reconstructed image matched with the paper map, corresponding exactly to the 1:350,000 scale at 1 mile to 5.52 inches. The final 1910 map was then imported unprojected into the working raster geodatabase (GDB). See Figure 8 for an example of the entire 1910 map.

DEM Processing:

A blank target raster dataset was created within the working raster GDB and assigned a geographic coordinate system of WGS 84. The Import Raster Dataset (Mosaic) tool was used in Arc Catalog to stitch the six ASTER gDEM tiles together as they were loaded into the target raster. The resulting data set was a seamless gDEM that extend beyond the extent of the original 1910 map. This process was also used to mosaic the SRTM data from both Earth Explorer (EE) and CGIAR. The EE metadata revealed that NoData pixels had been assigned the value of 32,769. This value was reclassified as NoData in the mosaic tool. To fill the NoData pixels in the EE DEM, a Mosaic To New Raster routine was run using the

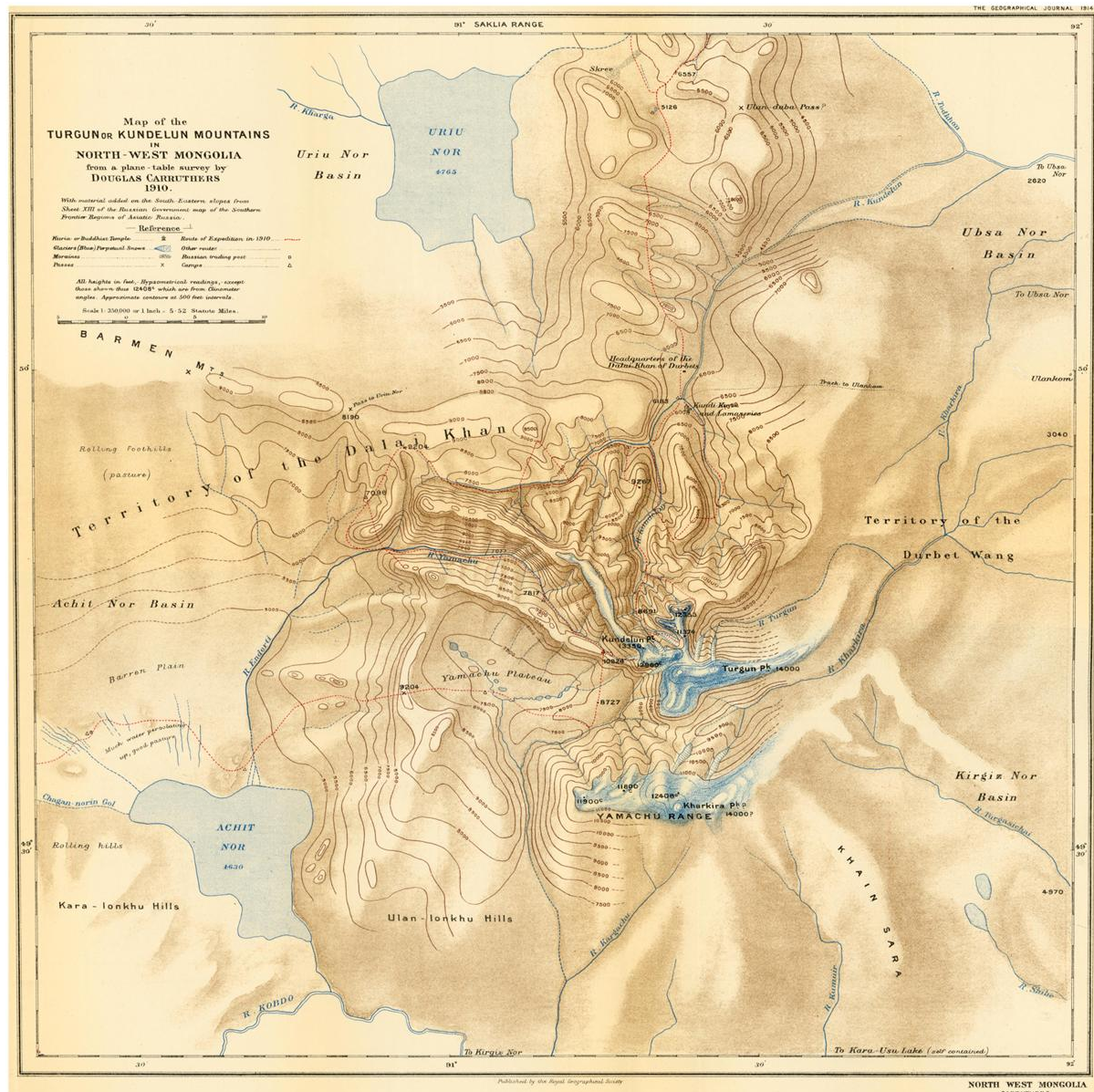


Figure 8. Digital mosaic of scanned 1910 Carruthers map (1912).

CGIAR DEM as the patch. As these results were unsatisfactory, another method was employed to fill the NoData holes in the EE DEM. The conditional statement:

```
new_DEM_name = con(isnull(old_DEM_name), focalmean(old_DEM_name, rectangle(4,4), old_DEM_name))
```

was employed where each pixel is checked with 'isnull', and if true, is then filled with a focal mean of the four pixels around it (Easson, 2001). The process was run several times to fill the largest holes, instead of increasing the sample grid and running the

risk of filling voids with erroneous values. After comparing all of the processed DEMs, it was determined that the CGIAR DEM was of the best quality and should be used throughout. The reasoning behind this decision is addressed in the discussion section. From this point forward, all references to the modern DEM refer to the data from CGIAR.

A Turgen GeoRef ArcMap document was created and the mosaicked DEM added as a layer. A hillshade was then generated from the DEM using a z-factor of 0.00003. This z-factor is needed to compensate for the fact that the DEM data is in mixed units. The x and y are in decimal degrees, while the z units are in meters. The conversion factor corrects for the discrepancy and allows a 'smoother' hillshade to be created, removing overly dark shadows and 'warming' the plastic texture found in many hillshades (ESRI 2007). The hillshade was then re-sampled during display to bilinear interpolation, and draped with a semi-transparent version of the original DEM that has a stretched color ramp applied. This process created a hypsometric tinted shaded relief that aided in visual recognition of terrain features for the georeferencing procedure (Figure 9).

Georeferencing:

The 1910 map image was added to the Turgen GeoRef document and the Fit To Display command used in the Georeferencing toolbar to pre-align the map. The map was then ready to be georeferenced. Georeferencing is the process of assigning geographic coordinates to unreferenced data, so that it can be aligned spatially (Hill 2006). The process requires that points on the unreferenced data be matched to coordinates within a GIS. This can be done either graphically by clicking concomitant locations with crosshairs, or by entering known coordinates for given points. A polynomial affine transformation is then

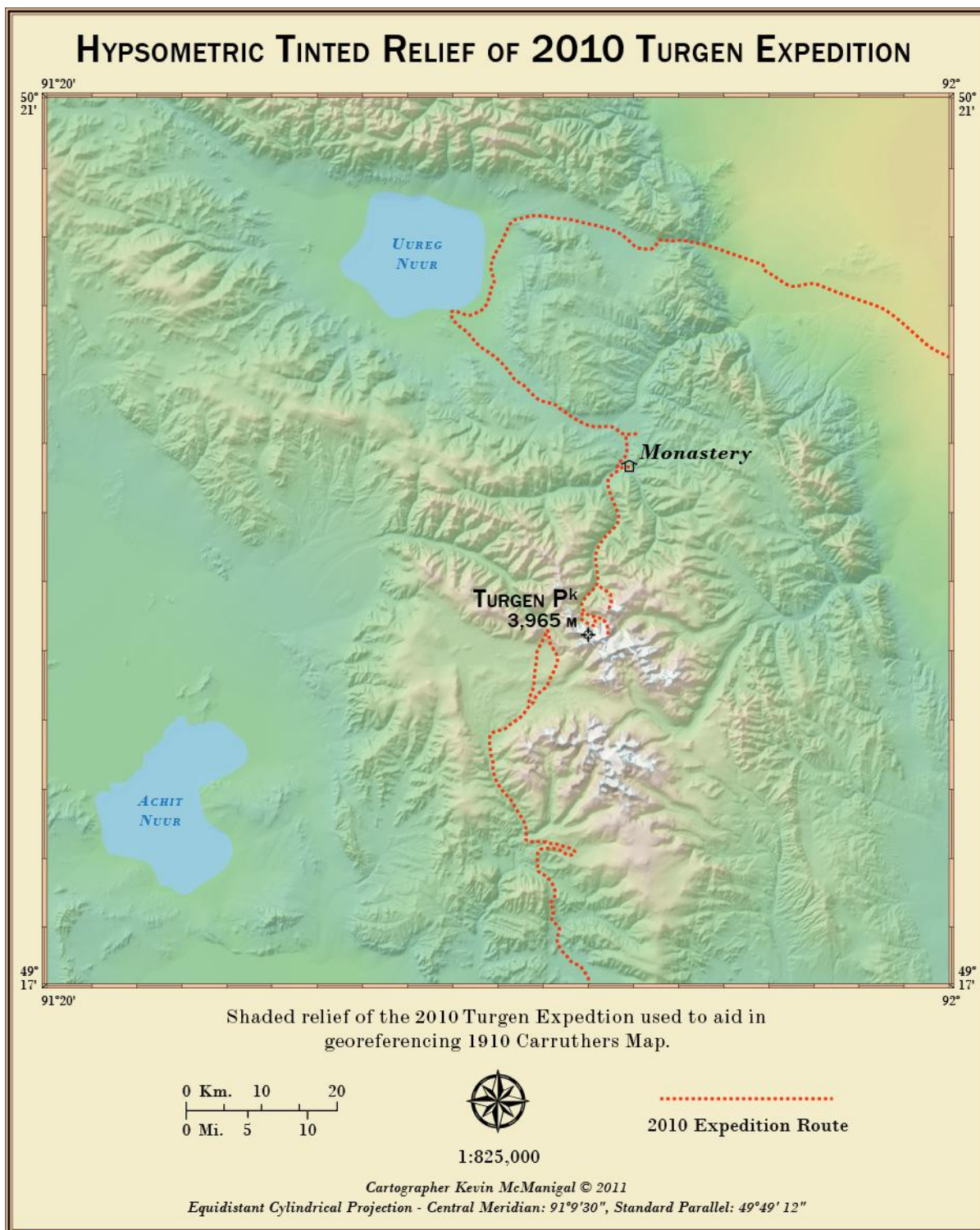
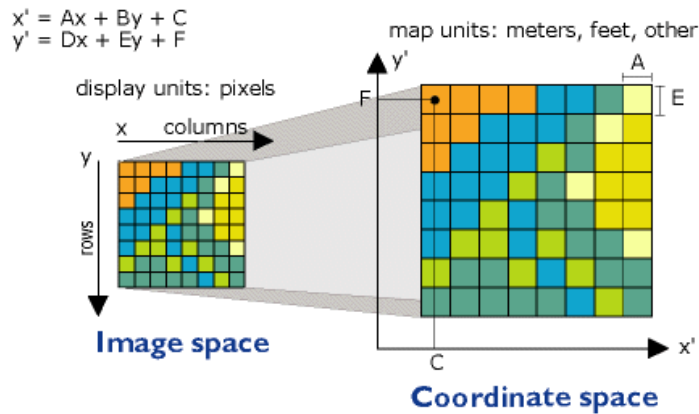


Figure 9. Hypsometric shaded relief map of the 2010 Turgun expedition.

applied with a least squares fitting algorithm (ESRI 2009). The first order transformation is shown in Figure 10.

First, the six tick marks in the body of the map were assigned coordinate pairs using the Add Control Points tool and the Enter Coordinates DMS field accessed when right-



x is column count in image space.
y is row count in image space.
x' is horizontal value in coordinate space.
y' is vertical value in coordinate space.
A is width of cell in map units.
B is a rotation term.
C is the x' value of the center of upper-right cell.
D is a rotation term.
E is negative of height of cell in map units.
F is the y' value of the center of upper-right cell.

Figure 10. Affine transformation (ESRI).

clicking the crosshairs. A First Order Polynomial (Affine) transformation was done and the map visually checked. The map features did not line up with the landscape, so fourteen additional coordinate pairs were added to the grid in the map margins. The points were ordered in clockwise fashion starting with the four pairs around the Turgen Range,

and radiating out from the center (Table 2).

Using the twenty coordinate pairs that correspond to known latitude and longitude, 1st, 2nd, and 3rd Order Polynomial transformations were performed. The RMS values were lowest for the 3rd order transformation, however, this transformation causes the most distortion (Figure 11). A straight Spline transformation, where the points are snapped directly to the coordinates specified, produced a georeference of the 1910 map that was true to the coordinate grid in the neatline.

Table 2. Georeferencing coordinate pairs.

Point Number	Latitude	Longitude
1 (Study Clip Corner)	50° N	91° E
2 (Study Clip Corner)	50° N	91° 30' E
3 (Study Clip Corner)	49° 30' N	91° 30' E
4 (Study Clip Corner)	49° 30' N	91° E
5 (Internal Coordinate)	49° 30' N	90° 30' E
6 (Internal Coordinate)	50° N	90° 30' E
7 (1910 Extent Corner)	50° 21' N	90° 20' E
8 (Internal Coordinate)	50° 21' N	90° 30' E
9 (Internal Coordinate)	50° 21' N	91° E
10 (Internal Coordinate)	50° 21' N	91° 30' E
11 (1910 Extent Corner)	50° 21' N	92° E
12 (Internal Coordinate)	50° N	92° E
13 (Internal Coordinate)	49° 30' N	92° E
14 (1910 Extent Corner)	49° 17' N	92° E
15 (Internal Coordinate)	49° 17' N	91° 30' E
16 (Internal Coordinate)	49° 17' N	91° E
17 (Internal Coordinate)	49° 17' N	90° 30' E
18 (1910 Extent Corner)	49° 17' N	90° 20' E
19 (Internal Coordinate)	49° 30' N	90° 20' E
20 (Internal Coordinate)	50° N	90° 19' E

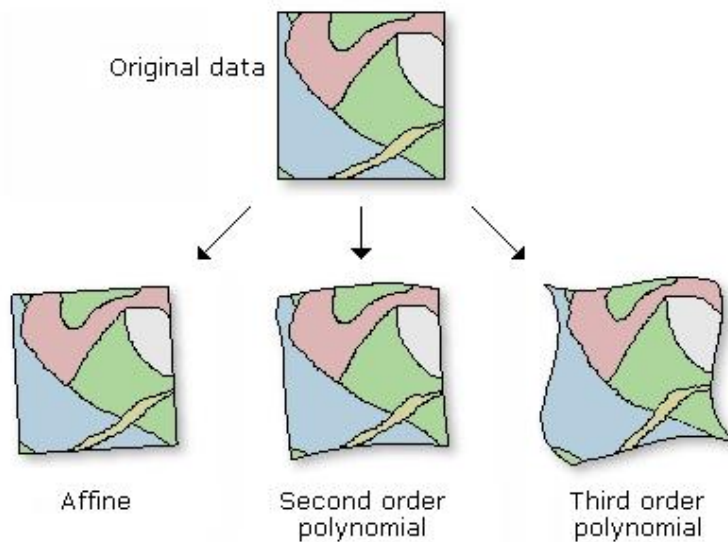


Figure 11. Distortions in georeferencing transformations (ESRI 2010).

In order to perform a true ‘Rubber Sheet’ transformation, the Landsat MSS image was pan-sharpened by the hypsometric relief and control points added to geomorphologic structures. Stable features were chosen such as large river confluences, summits, and glacier terminus moraines (Figure 12). Fifty control points were added mostly within the core study area of the Turgun Valley and south towards Turgun Peak. A Spline transformation was applied and each control point snapped to the exact location specified. The results showed acceptable agreement, especially in the core study area around Turgun Peak.

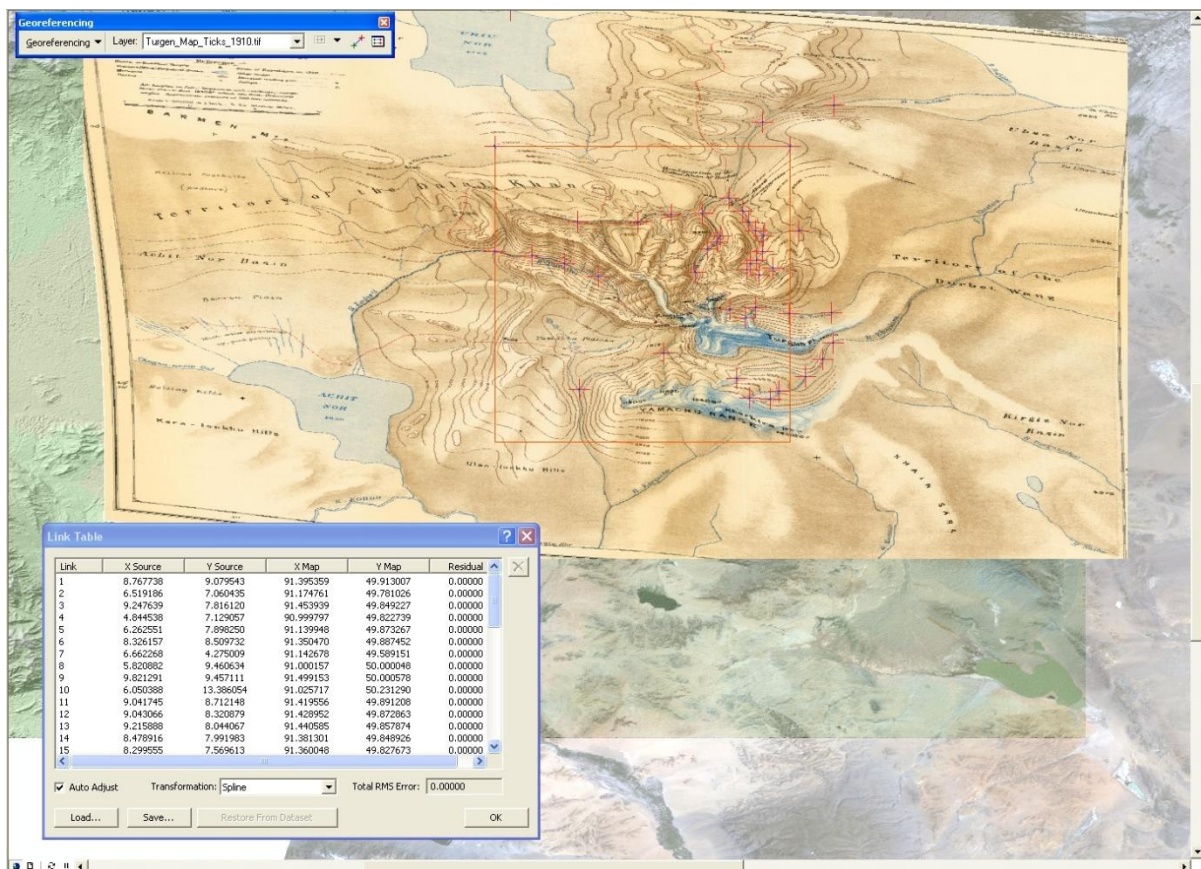


Figure 12. Screenshot of rubber-sheet transformation of core study area.

Significant portions in the north western and south eastern sections of the 1910 map were missing contours, so a clipping polygon was sized to avoid most of these areas, while still encompassing the core study area. A rectangular area based on four of the original

coordinate pairs used to georeference was the best compromise and a polygon feature class was digitized to this extent (Table 2, Study Clip Corners). The rubber-sheeted 1910 map was then clipped to the study area in preparation for digitizing the contours. The CGIAR DEM, and Landsat images were clipped as well. As a visual check, the study area clip of the 1910 map was draped over the modern hillshade, showing general agreement with the true landscape (Figure 13). It must be noted here that the 1910 study area clip was severely distorted from the historic map and does not represent the original Carruthers' survey.

Contour Generation:

A new Feature Class was created within the GDB with fields for the contour elevations in both meters and feet. Each of the 500 ft. contours was digitized manually and the corresponding elevation values entered into the CONTOUR_FEET field of the attribute table. Contours that were missing in the NW and SE corners of the study area were interpolated using 500 ft. contours generated from CGIAR DEM as a visual aid. The CONTOUR_METER attribute column was then populated with the Field Calculator, multiplying the CONTOUR_FEET field by 0.3048. The finished contour class was finally simplified using the Bend Simplify method with a tolerance of one third the CGIAR DEM resolution, or 30 meters. This was done to remove the sharp corners that creep in due to the limitations of the digitizing tools in ArcMap.

The contours were then processed into a 1910 DEM using the Topo To Raster tool. The tool utilizes the Inverse Distance Weighted (IDW) Interpolation method based on the ANUDEM program developed by Hutchinson (1993). As recommended by Hutchinson (1988, 1989), the output was evaluated by producing contours from the constructed surface at

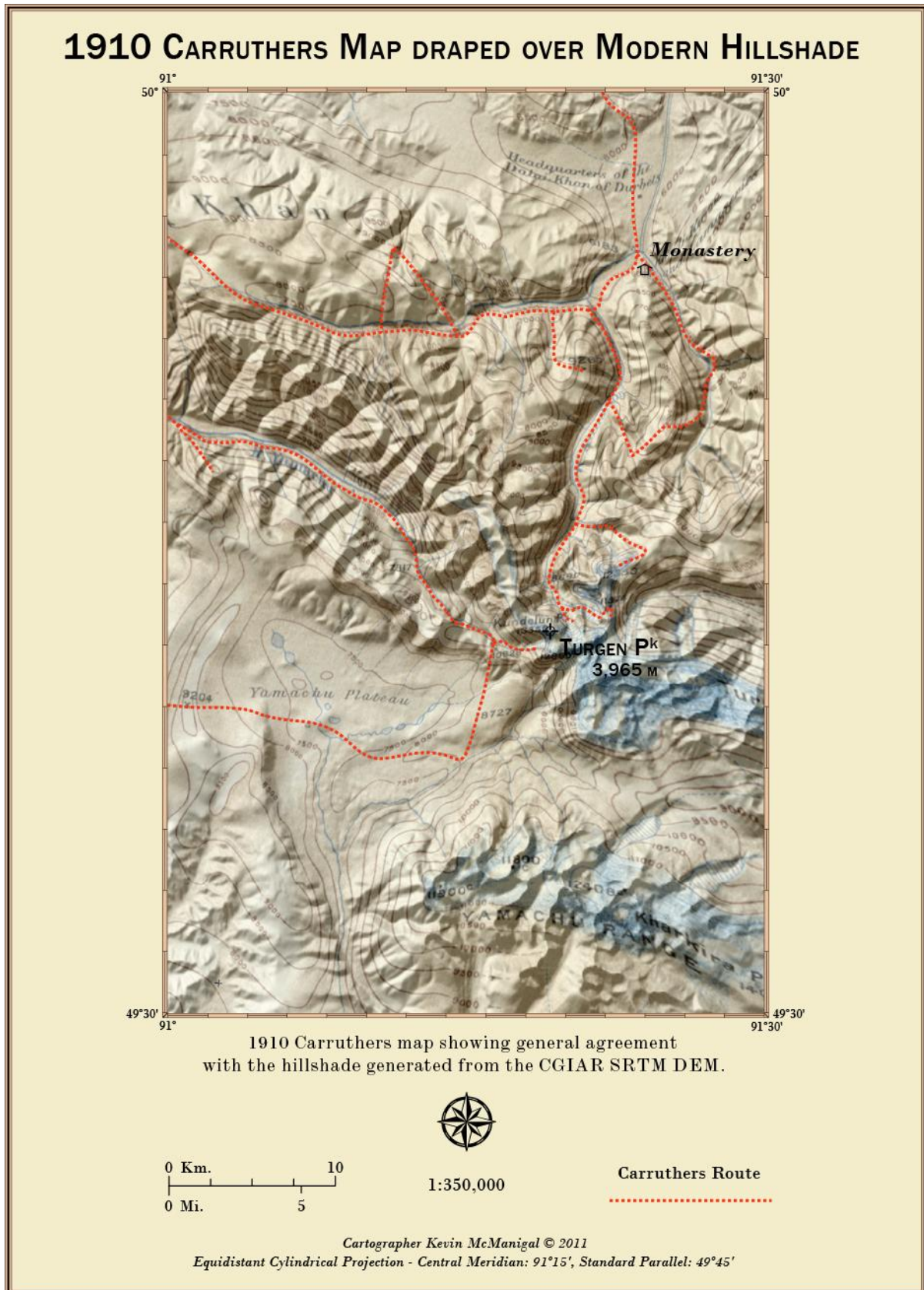


Figure 13. Clip of the 1910 map showing general agreement with SRTM DEM.

half the original contour interval and displaying both sets together. The 1910 DEM was used to make a hillshade, draped with the original map, and then displayed with both sets of contours for visual evaluation of the terrain generalization (Figure 14).

Finally, to evaluate the elevation accuracy, the 1910 DEM of the study area was divided by the clipped CGIAR DEM using the Raster Calculator. The resulting division calculation (DV) shows the range of elevation differences between the DEMs by computing an error factor where 1 is equality. Also, the contours from the 1910 map were converted to raster and then to points, with the values for both DEMs being extracted at those points. The resulting table of 17,710 rows of paired values was pasted into the Validation Statistics spreadsheet in Excel to evaluate the elevation accuracy of the 1910 DEM.

RESULTS

The resulting division calculation reveals that the elevation error in the 1910 clip DEM varies across the study area. The regions in the NW and SE corners show high error values, where the contours were interpolated. Conversely, the areas of low elevation error are variable; sometimes in valleys and other times located on ridges. The error factor ranges from 0.59 to 1.41, with 1 representing equality between the DEMs displayed as the division between yellow and blue in Figure 15. Blue to green represents low values, while yellow to red represents high values in the 1910 DEM. The mean error factor for the Division Calculation is 0.99, while the standard deviation is ± 0.12 . As can be seen in Figure 16, the majority of values fall within one standard deviation with the distribution being weighted towards errors of low elevation.

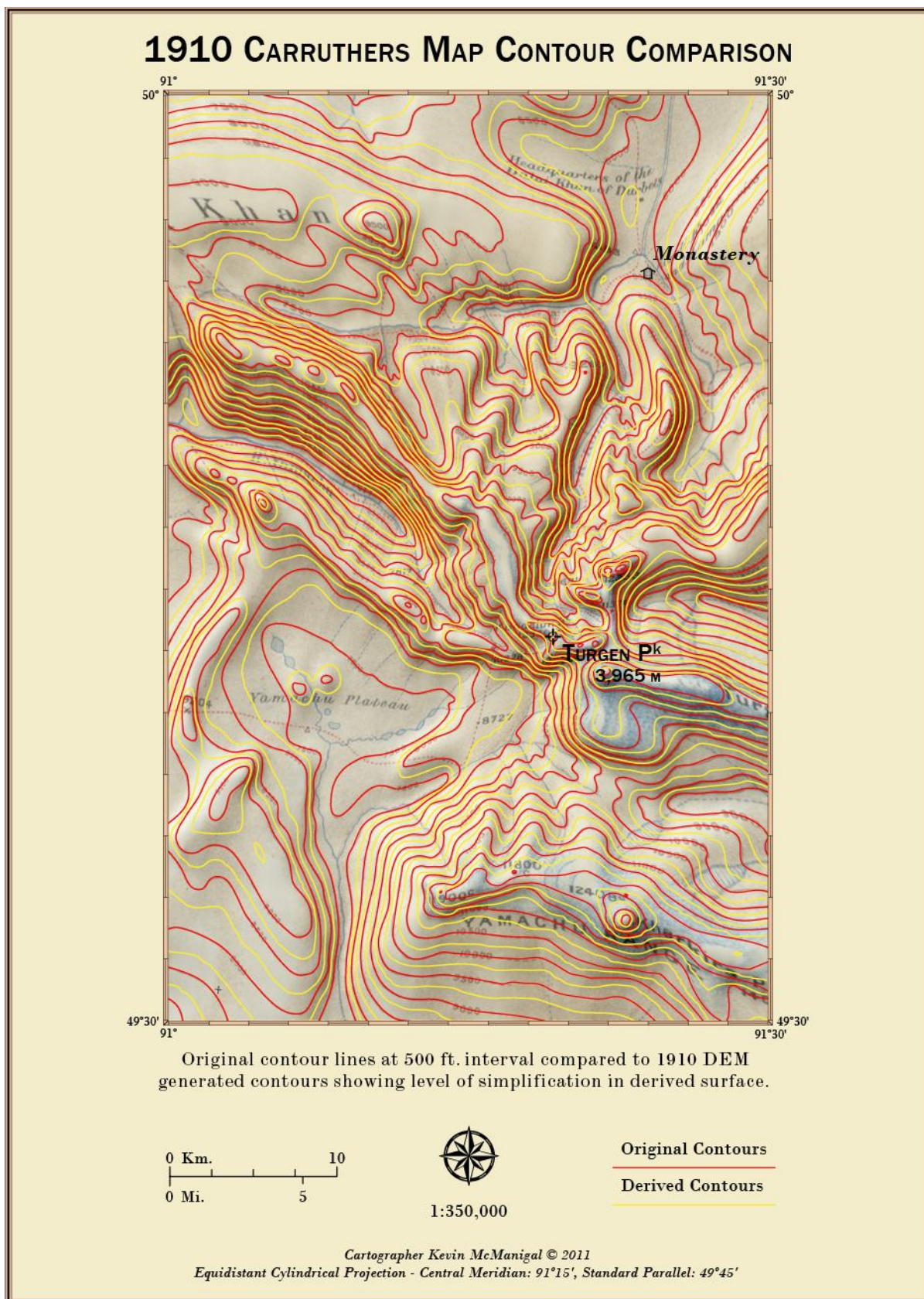


Figure 14. Contour comparison between original and derived surfaces.

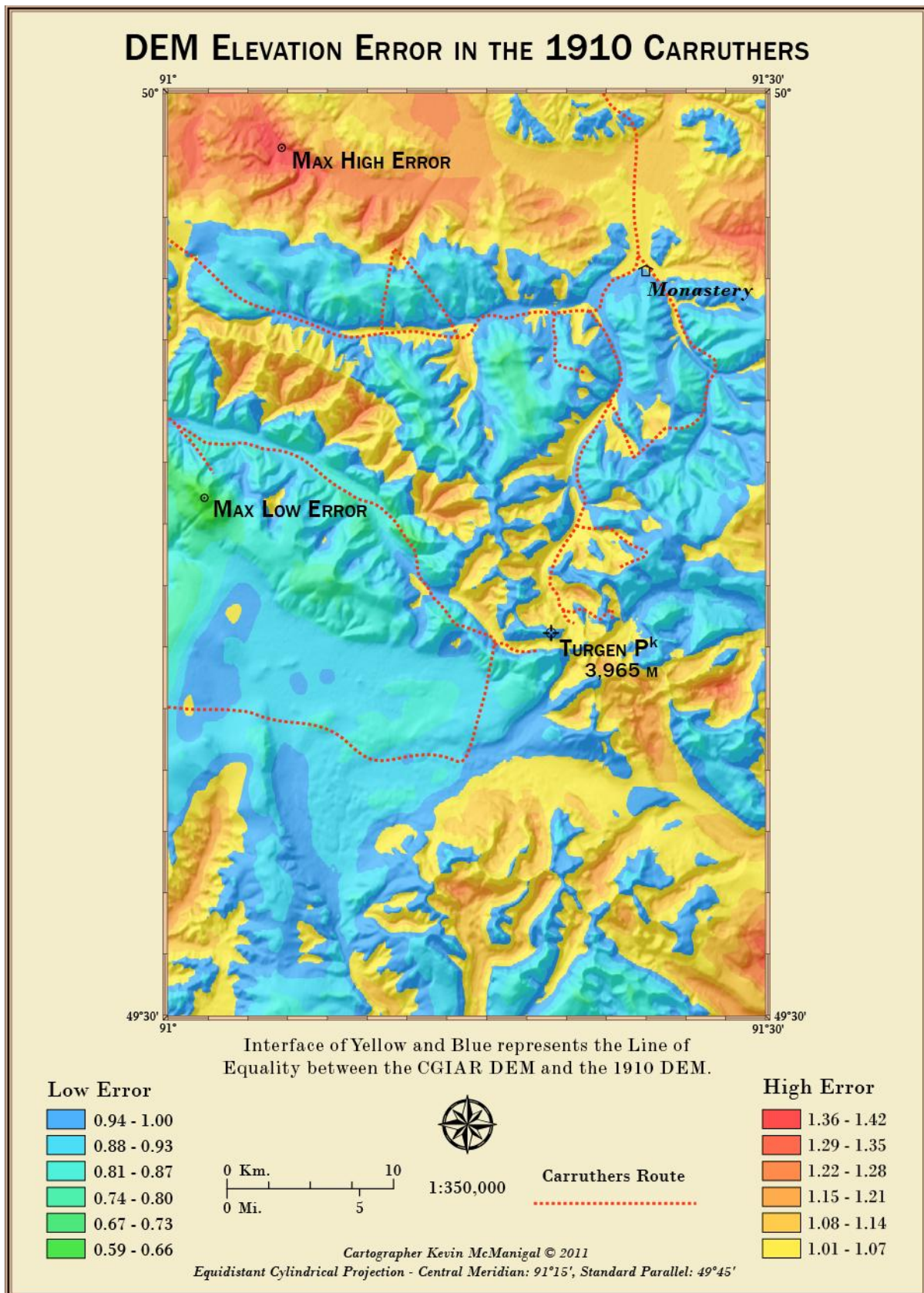


Figure 15. Elevation error between 1910 and modern DEMs.

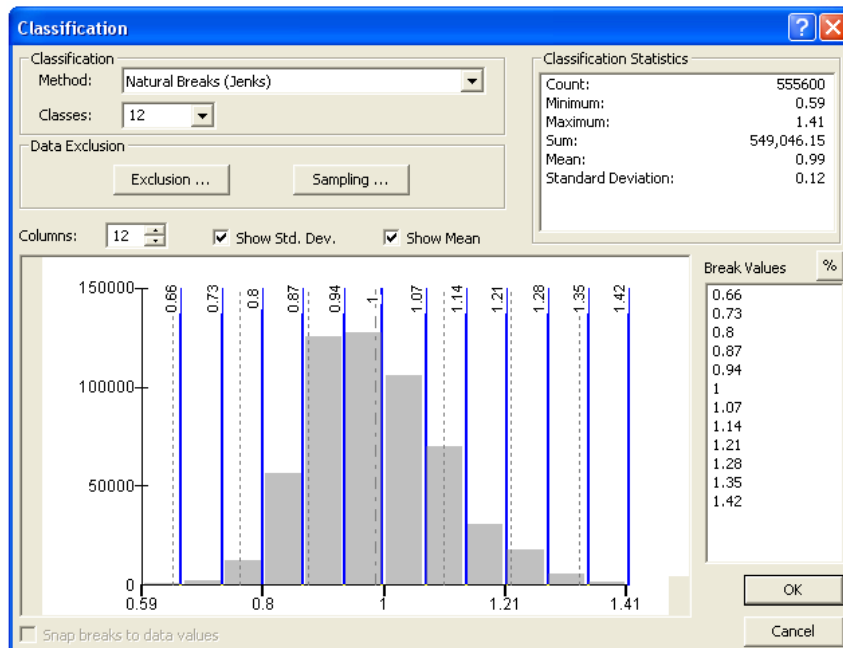


Figure 16. Histogram showing distribution of elevation error.

Table 3 compares the minimum, maximum, and selected point values for the respective DEMs, along with the differences. While both the minimum and maximum elevation of the 1910 DEM have a positive error factor of 1.14 and 1.02 respectively, there is a greater overall error in various regions. In the area with the lowest error factor of 0.59, the 1910 DEM is 1362 meters lower than the CGIAR DEM. In the area with the highest error factor of 1.42, the 1910 DEM is 759 meters higher than the CGIAR DEM.

Table 3. Value differences between DEMs.

	Min m	Max m	Turgen Peak m	Lowest Error m	Highest Error m
Turgen 1910 DEM	1811	4133	3843	1985	2592
CGIAR DEM	1589	4039	3898	3347	1833
Difference	+ 222	+ 94	- 55	- 1362	+ 759
Error Factor	1.1397	1.0232	0.9858	0.5930	1.42
% Error 1910 DEM	114%	102%	99%	59%	142%

The validation statistics (VS) spreadsheet results represent sampled data of both DEMs along the lines of the digitized 1910 contours. Table 4 shows the difference between the means of the observed and predicted samples as -58.4 meters. The Mean Absolute Error (MAE) is 240 m and the standard deviation is ± 294 m. The plot of the data in Figure 17 shows a generally good fit. The red line represents the mean, while the white line is the regression of the data with a 0.88 Indices of Agreement and an even distribution of data around the mean.

DISCUSSION

The elevation error in the geo-referenced clip of the 1910 map varies across the sheet, with less inaccuracy along the route of the expedition, where more careful surveying would have been conducted. The interface of equality line tends to correspond with the Carruthers track, especially in the Torgen Valley proper. However, there are some of the lowest error factors along the expedition track on the southern side of the range. This may be due to the

Table 4. Validation spreadsheet results.

Overall General Stats:			
	Observed	Predicted	Delta
mean	2776.2	2717.8	-58.4
min	1610.0	1819.2	-1370.4
max	4011.0	4125.8	910.5
stdev	438.8	472.5	293.8
count:	17,710	17,710	17,710
Model Performance Stats:			
MBE=	-58.4 m		
MAE=	239.5 m		
RMSE=	299.6 m		
Ind. Agreement, d=	0.88		
R Squared	0.63		

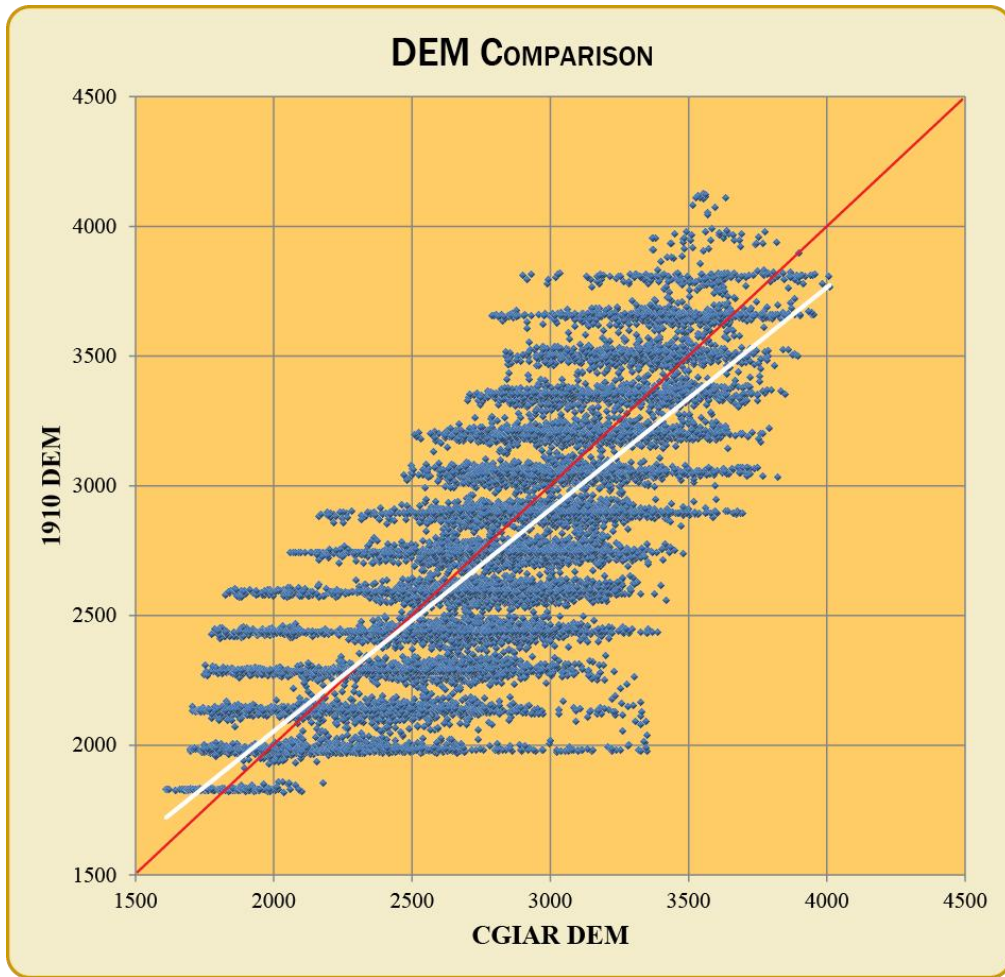


Figure 17. Plot of 1910 and CGIAR DEM comparison from validation statistic spreadsheet.

storms encountered in the Yamachu Valley affecting barometric readings (RGS Archives 2010). It may also be caused by misaligned georeferencing, however the track of the 1910 expedition does generally follow the valley floor on the CGIAR DEM. Regardless, the overall mean error factor of 0.99 and the standard deviation of only ± 0.12 communicate the relative elevation accuracy of the 1910 map. This accuracy also speaks to the close fit of the georeferencing.

Validation statistics (VS) seem to show more error, however, they represent a smaller sample that was only taken along the contour lines. Because of the interpolation methods used to create the 1910 DEM from the contours, some of the error would necessarily have

been ‘smoothed’ out in the generalization of the terrain. This appears to have occurred more on the mountain tops than the valleys, as demonstrated by the maximum high difference in the VS being 151 meters more than in the division calculation (DC). The maximum low difference was only 8 meters lower. The VS is consistent with the DC in that the standard deviation of ± 294 meters is roughly the standard deviation of the error factor ± 0.12 multiplied by the range of elevation values from the modern CGIAR DEM.

The combined statistics support the statement that the elevations represented on the clip of the 1910 map are low, with the average elevation being 0.99 of the true height. Of all sampled locations, 68% will have an error factor of 0.99 ± 0.12 , while 95% will fall within an error factor of 0.99 ± 0.24 . However, the range of error extends from 0.59 to 1.14 and can be substantial in some areas as shown in the DC. The DC can be used to extract the error factor for any given point in the study area clip; so, depending on the positional error, it may be possible to evaluate elevation accuracy of specific locations mapped by Carruthers, including glacier termini. The MAE of 240 meters shown in the VS representing the variance between the two DEMs is most likely larger than the amount of vertical ice ablation in the last century. However, the uniform distribution of the error speaks to the tendency Carruthers’ survey techniques to self-correct and cluster around the true elevations in the landscape. While the elevation errors may be too great to quantify overall changes in glacial volume, the 1910 map certainly was an effective generalization that depicts the landscape well, considering the techniques of the period.

CARTOMETRIC EVALUATION

BACKGROUND

The analysis of historic maps is a traditional tool for geographers to evaluate cultural changes in the landscape (Jenny and Hurni 2011). Rumsey and Williams (2002) convincingly demonstrated how the science of georeferencing historical maps in a GIS was sparking a technological revolution in historical geography. In the field of glaciology, SAR and Lidar data, along with high resolution spectral imagery, make it possible to take detailed measurements of current ice coverage, but baseline data of past states is harder to find (Bamber 2009). Recent advances in technology and the availability of geospatial data have increased accuracy in ways that now facilitate monitoring of changes in the global glacier regime (Raup et al. 2007). In particular, new programs have been developed that allow for detailed measurements of historic maps that can help recreate past glacial extents (Jenny et al. 2007).

To conduct a detailed analysis of the 1910 Carruthers map, a program developed by Jenny (2006) was employed. The Java-based tool, MapAnalyst (MA), requires the inputs of both a historic and modern map that have been matched in pixel size and extent. The modern map also requires a world file (.tfw) that contains the geographic reference for the image. In order to perform an effective analysis, the original projection of the historic map needs to be duplicated and applied to the modern reference map.

The original map was plotted by Carruthers with the top northwest corner being one minute longer in longitude than the southwest corner, $90^{\circ} 19' E$ vs. $90^{\circ} 20' E$. It is believed that this was done to compensate for the meridian convergence at the high latitude allowing the map extent to be drawn square, and supports the assumption that the 1910 map is in

straight longitude and latitude, essentially unprojected. The georeferencing was carried out with the shared coordinate of 90° 20' E, considering that the one minute of extra longitude depicted in the 1910 map was behind the title legend marque, and contained no information critical to the analysis.

Based on discussions with cartographic professionals (Strebe 2011) and experimentation suggested in Tobler (1966), an equidistant cylindrical projection was chosen. After designing a custom display projection with a local central meridian and standard parallel positioned in the middle of the 1910 map extent, the minutes of longitude measured correctly for their corresponding latitude (Table 5).

Table 5. Custom dataframe projection.

Name	Turgen Equidistant Cylindrical
Central Meridian	91° 9' 30" E
Standard Parallel 1	49° 49' 12" N
Datum	WGS 1984

Once the projected reference map and the historic map of matching dpi have been imported, the program is ready for analysis. Controls points are set in both maps at coordinates of know location. The program then computes the difference between known x, y location on the modern map, and the corresponding locations on the historic map. As outlined in Fortsner and Oehrli (1998), the Helmert affine least squares transformation is the accepted starting point for the analysis. Coordinates of the historic map (X , Y) are evaluated against the same locations on the reference map (x , y) as:

$$X = x0 + ax - by \text{ and } Y = y0 + bx + ay$$

Where: $a = M * \cos(\text{map rotation})$ and $b = M * \sin(\text{map rotation})$

And: $x0 = \text{Horizontal Translation}$, $y0 = \text{Vertical Translation}$ and $M = \text{Scale Factor}$

The transformation computes a mean positional error of the historic locations, a standard deviation from the mean and a table of residuals for each point. The generated report also identifies those points that are $\geq 3 \sigma$. The program produces a number of visualizations that can help in describing the differences between the maps. These include distortion grids, displacement vectors, neighbor proximity circles, and scale isolines. From this suite of statistics and graphics, one can quantify planar accuracy of the historic map.

Considerations must be taken to establish as many points as possible; however, this proves difficult in mountainous regions with few anthropogenic features (Jenny and Hurni 2011). This is the case on the 1910 Turgen map. It is also important to note that the visualizations can be misleading as more distortions will be observed around clusters of points when there is an uneven distribution. On the Turgen map, there were far more identifiable points along the route of the expedition and few matches near the margins. These two factors lead to the use of a Hampel Robust Estimator to modify the affine transformation by limiting the influence of the most egregious outliers (Andrews 1974).

METHODS

Map Image Preparation:

The twenty individual Russian topographic maps were collected for comparison to the 1910 map. Each 4722 x 5200 pixel tiff was cropped in PS to remove the collars and then all twenty images were mosaicked by hand. The Photomerge tool in PS was not satisfactory due to the lack of contrast between the maps and the variable rotation of each map tile. Therefore, each cropped map was aligned on the vertical edge with the neighboring tile into five rows of four maps each. Then the rows were rotated so they could be aligned along the

horizontal edges. The large map file was flattened, cropped, resized and re-sampled to 360 dpi. The final composite of the Russian maps was saved as a 21,074 x 26,897 pixel tif. The final Russian map was then imported into the working raster GDB for georeferencing in the manner outlined above. Each Russian map sheet contains an internal crosshair of coordinates, totaling twenty points in the final composite. After the Russian map was georeferenced, it was clipped to the extent of the 1910 map. It was finally exported as a 360 dpi tif in the custom Turgen Equidistant Cylindrical projection for use in Map Analyst.

Map Analysis:

The projected Russian topographic map of the entire study extent was imported into MapAnalyst. Then the unprojected 1910 map was imported and given its 360 dpi setting within the program. The process of cartometric analysis requires multiple iterations; preliminary results are evaluated and then parameters are adjusted to fine-tune the program. For the initial analysis, the four corner points from the coordinate grid of the 1910 map and the nine internal crosshairs added in Photoshop were input. First run results of the Helmert affine transformation with 4, 5, and 6 parameters did not indicate shrinkage or shear of the paper map as there were not large differences between the transformation means and standard deviations (Jenny and Hurni 2011). Additional matching points were then added to the maps for identifiable features. Only two permanent cultural entities could be located: the monastery, which is in ruins today, and the settlement of Delgermoron (abandoned), which was labeled as the HQ of the Dalai Khan on the 1910 map (Figure 18). Further matching points were chosen from stable physical features in the landscape such as peaks, passes, rock out crops, and major river confluences in canyons. A total of 31 points were identified and

matched between the maps (Figure 19). With each iteration of the analysis the displacement vectors, distortion grid and statistics report were evaluated, which supported decisions about parameter adjustment.



Figure 18. Map depictions of monastery and settlement in 1910 and 1970.

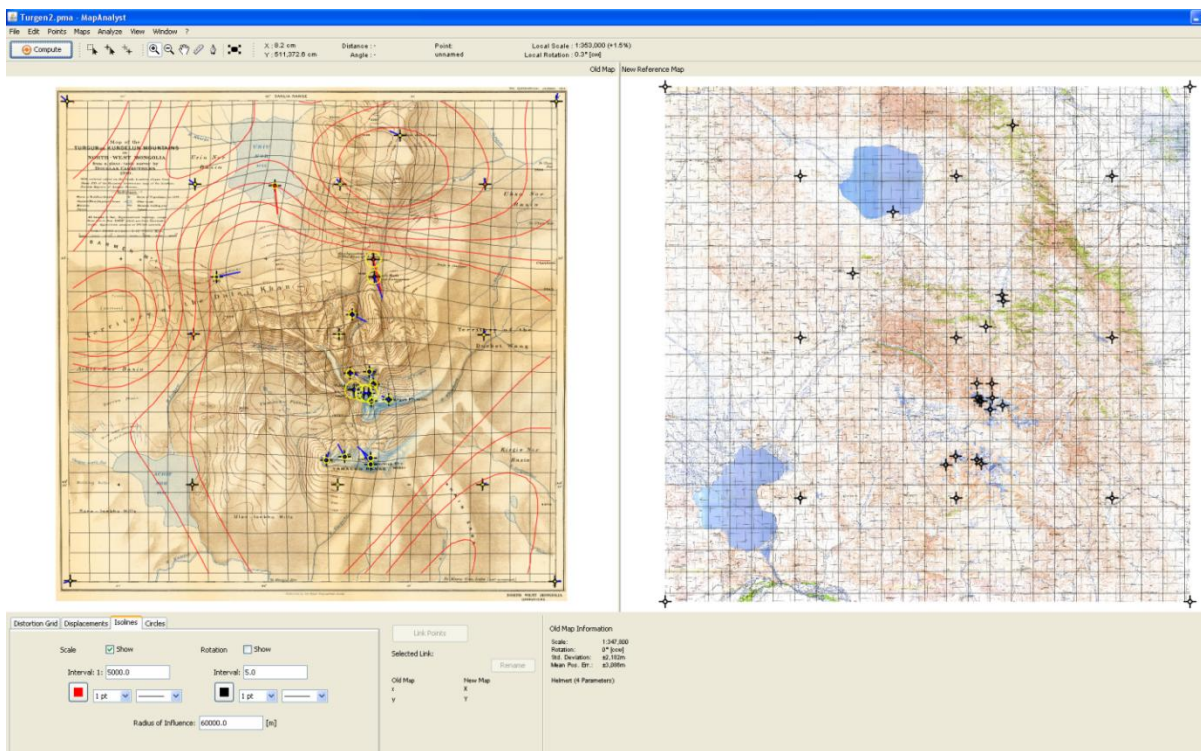


Figure 19. Map Analyst software with historic map, reference map, and coordinate pairs.

Experimentation with Robust Estimators of Huber, Hampel, and V after Hardy (1971) helped narrow the estimate of planar accuracy in the 1910 Carruthers map. The Robust Hampel Estimator was deemed the best and used to set cut-off values to reduce influence of

points more than three standard deviations from the mean (Andrews 1974). The lower the k parameter is set, the less weight is given to the outliers. However, care must be taken as setting k too low pushes more points past the σ_3 threshold. With the Hampel, this threshold can be further refined by setting b to a midpoint that allows semi-contaminated points partial influence. The least valid points are then capped by the value c , which discards those above the acceptable limit for the analysis. There is no empirical formula for setting the thresholds, other than to start with the lowest and highest k and c , respectively, and then work towards the middle in successive iterations (Jenny 2005). This was done with caution not to induce $\geq \sigma_3$ displacement vectors in the core area around Turgan Peak, while at the same time not allowing more than one third of the points to be discarded. The process resulted in an approximation of overall cartometric error, which is addressed in the results section.

Additionally, an entirely separate analysis was done on the georeferenced study area clip of the 1910 map. The goal was to evaluate the georeferencing in the core study area around the Turgan glaciers. The cartometric analysis workflow was applied to this clip and a localized error factor computed to facilitate comparison of the historic and modern glacial extents.

RESULTS

As mentioned, the analysis was an iterative process that produced many intermediate statistics. The default and best fit results will be reported here. The initial report of the Helmert least squares four parameter affine transformation are shown in Table 6. The mean positional error for matched locations was ≈ 3.1 kilometers with a standard deviation of ≈ 2.1 kilometers. Using the 31 matched locations, the mean computed scale ratio was 1:347,813.

To reduce the influence of outlier points, the Hampel Robust Estimator with the values of $k = 1.2$, $b = 4.9$, and $c = 7.0$ was used. The results of the Hampel Estimator on the entire unreferenced Carruthers map are shown in Table 7. The mean positional error for matched locations using the Hampel Estimator was ≈ 1.0 kilometer with a standard deviation of ≈ 0.7 kilometers and a calculated scale of 1:350,782. The Hampel Robust Estimator applied to the georeferenced clip of the 1910 map utilized 21 matched points. The RMSE of positions on the referenced historic map are 338 meters with a standard deviation of ± 239 meters and a calculated scale of 1:350,607 (Table 8). The analysis also produced a number of graphics that are evaluated in the discussion.

Table 6. Initial Helmert four parameter transformation results for full 1910 map.

x0 Translation Horizontal	0.3143 m	± 0.00113
y0 Translation Vertical	5101.94 m	± 0.00113
Mean Scale Factor:	1:347,813	± 3248.22
Alpha Rotation deg. ccw.	0.31346	± 0.53508
Root Mean Square Position Error in Historic Map: 3,086.39 m		
Standard Deviation in Historic Map: $\pm 2,182.41$ m		

Table 7. Hampel robust estimator transformation results for full 1910 map.

x0 Translation Horizontal	0.2635 m	± 0.68802
y0 Translation Vertical	5102.04 m	± 0.68802
Mean Scale Factor:	1: 350,782	± 0.00496
Alpha Rotation deg. ccw.	0.06822	± 0.0
Root Mean Square Position Error in Historic Map: 1038.42 m		
Standard Deviation in Historic Map: 734.27 m		

Table 8. Hampel robust estimator transformation results for study area clip.

x0 Translation Horizontal	0.1984 m	± 2.43499
y0 Translation Vertical	-16.3022 m	± 2.43499
Mean Scale Factor:	1: 350,607	± 0.00902
Alpha Rotation deg. ccw.	0.19274	± 0.0
Root Mean Square Position Error in Historic Map: 338.24 m		
Standard Deviation in Historic Map: 239.17 m		

DISCUSSION

The default Helmert transformation produced a fairly large mean positional error. However, this was to be expected considering the non-uniform distribution of sample points and the mountainous nature of the terrain being mapped. When the analysis was weighted using the Hampel robust estimator transformation, the mean positional error was dropped considerably. This is justified for the purpose of this study as the main area of concern is the Turgen Valley and specifically, the glaciers north of Turgen Peak. Since Carruthers' survey would have been more accurate along the route of the expedition where the plane table stations were located, reducing point weight further from the survey is valid with this analysis (Jenny and Hurni 2011).

Using the Hampel transformation, the computed scale on the original map endorses the theory of increased accuracy along the expedition route. Figure 20 displays the scale variation with isolines at a 5,000 unit interval. The average computed scale of 1:350,782 is somewhat greater than the original of 1:350,000. However, as seen on the map, the area around Turgen Peak remains consistently lower than the original stated scale and then increases rapidly away from the study area. A test done with a 1,000 unit interval did not produce additional isolines below 1:350,000.

In Figure 21 the distortion of the original map is shown using a grid of 5,000 m. The general trend of the map is a considerable distortion to the north, and slightly to the west. The displacement vectors shown in red are $\geq 3\sigma$ from the mean. Interestingly, the only identifiable anthropogenic locations, i.e. the settlement and the monastery, are points with high error. The settlement could have been moved owing to the nomadic nature of the Mongolians, but the location of the monastery ruins were firmly established by GPS in the

SCALE VARIANCE WITHIN THE 1910 CARRUTHERS MAP

Isoline representation of scale variation on the 1910 Carruthers Map using the Hampel Robust Estimator Transformation.

Original Scale 1:350,000
Computed Average Scale 1:350,782

Scale Isoline Interval is 5,000 Units

Original Projection - Possibly Unprojected Latitude and Longitude
Cartographer Kevin McManigal © 2011

53

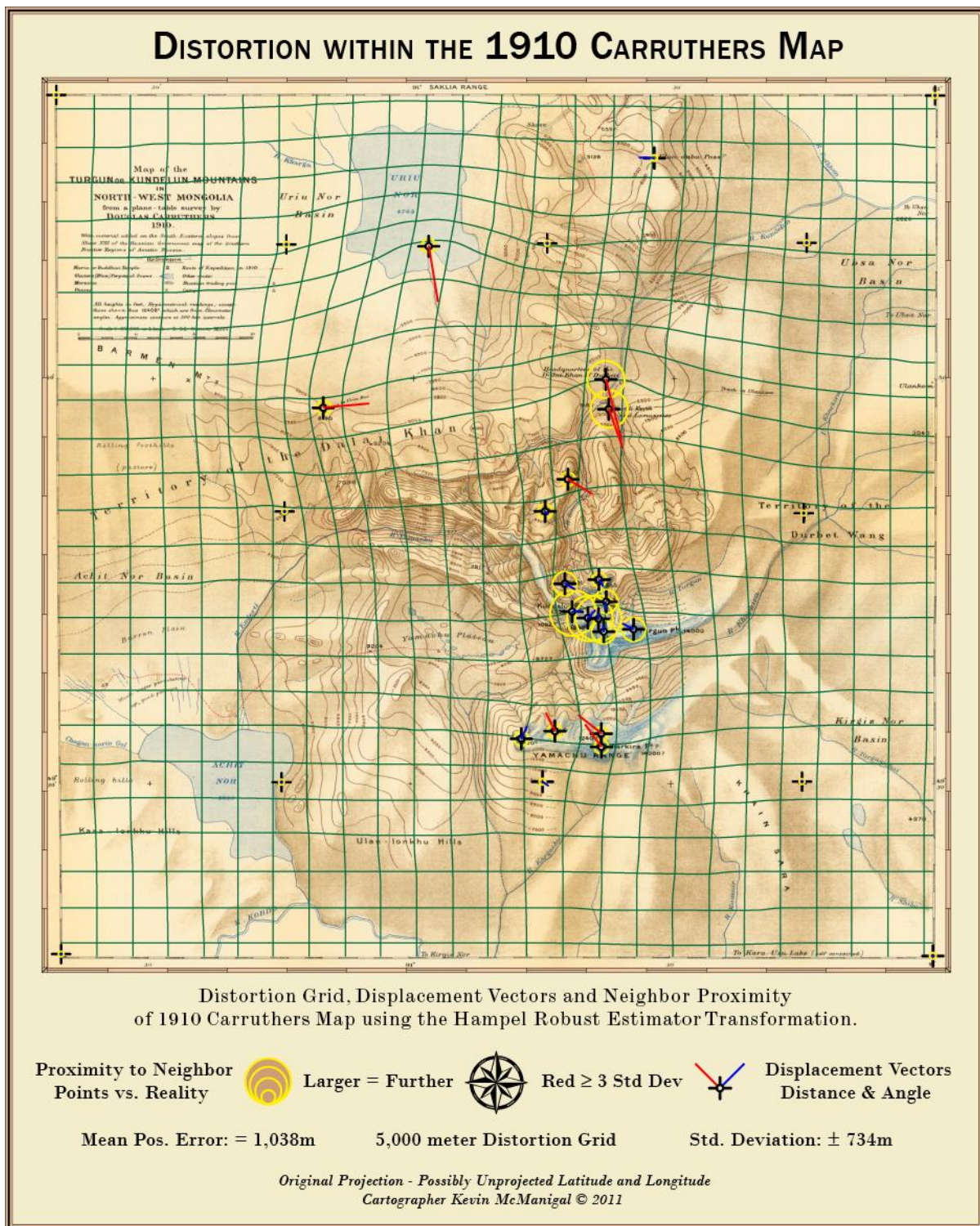


Figure 21. Distortion and displacement in the 1910 map by Carruthers.

summer of 2010. The ridge that borders the east side of the Turgen Valley is displaced northward by almost five kilometers at its head where the monastery is located. These seem to be simply errors in the Carruthers survey. An interesting trend of note is that most of the displacement vectors point inwards toward the core study area at the foot of Turgen Peak, indicating that Carruthers took more care with the surveying of the peak and its glaciers. Owing to the fact the Turgen Valley is a closed cul-de-sac, the expedition spent more time in the range, traversing the landscape twice. The neighbor proximity circles in the core confirm this as well, with the locations of matching points that were physically visited having less error than the surrounding peaks shot with an alidade and clinometer from the plane table.

Figure 22 shows the variation of scale within the georeferenced clip of the Carruthers map. Again the isoline interval is 5,000 units, with the average computed scale of 1:350,600 being only slightly higher than the original of 1:350,000. The core study area is again the most consistent near Turgen Peak and its northern glaciers; all falling between 1:350,000 and 1:355,000. The areas where the contours were inferred during digitizing, i.e. to the south of Kharkhiraa Peak, show the largest variance. An interesting low zone is present near the monastery, which mirrors the positional error found at this location in the unreferenced analysis.

The overall distortion of the georeferenced study area clip is shown in Figure 23. The 2,000 meter grid is less warped than the unreferenced map, but reflects it in several ways. There is northward distortion to the north of Turgen Peak and reverse to the south. Westward and eastward distortion is towards the peak. The area directly around the core study area shows some slight expansion. Again, displacement vectors tend to angle towards the peak except for a few points out on the Yamachu Plateau. The six red vectors that are $\geq 3\sigma$ from

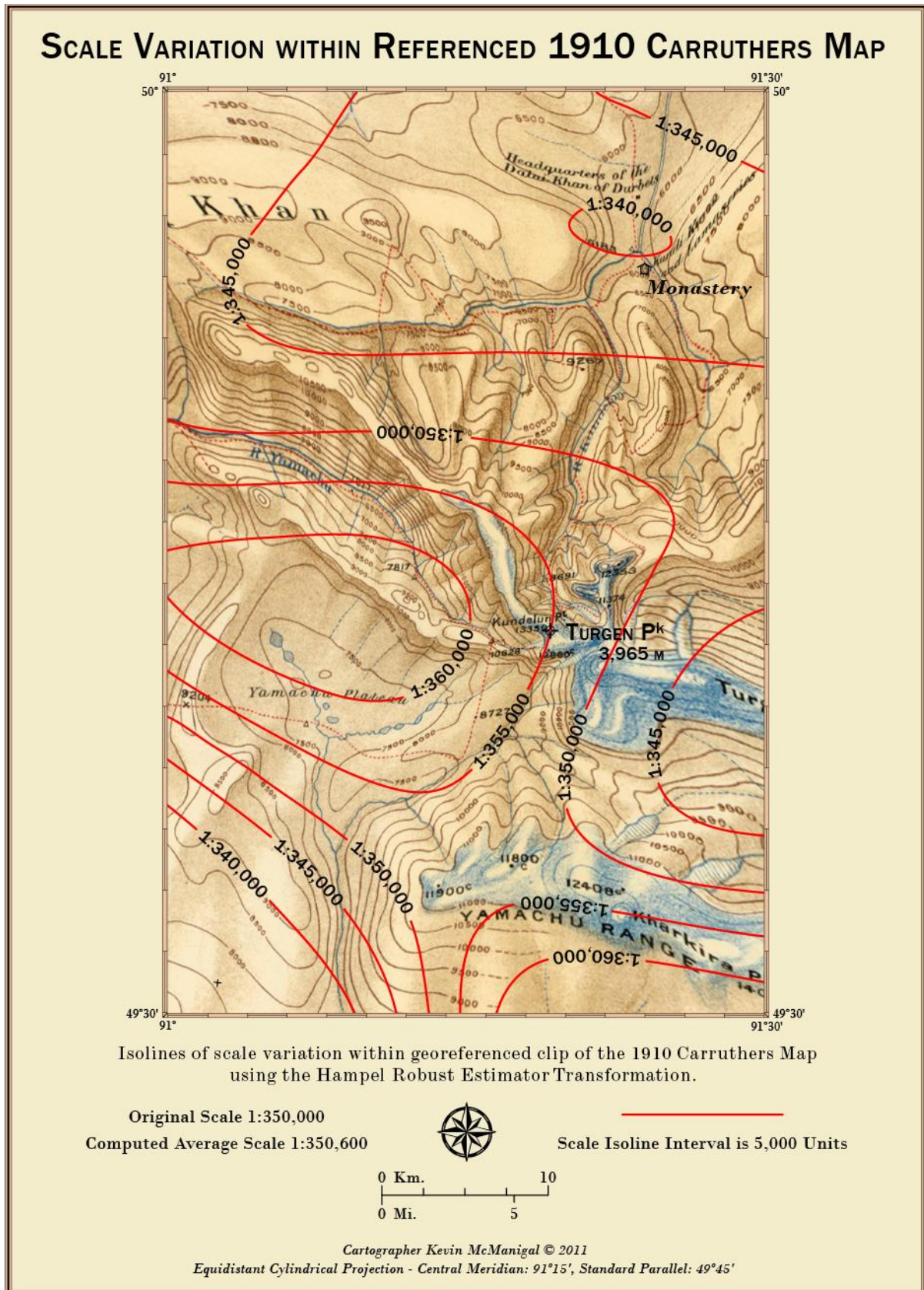


Figure 22. Scale variance in the georeferenced clip of 1910 map by Carruthers.

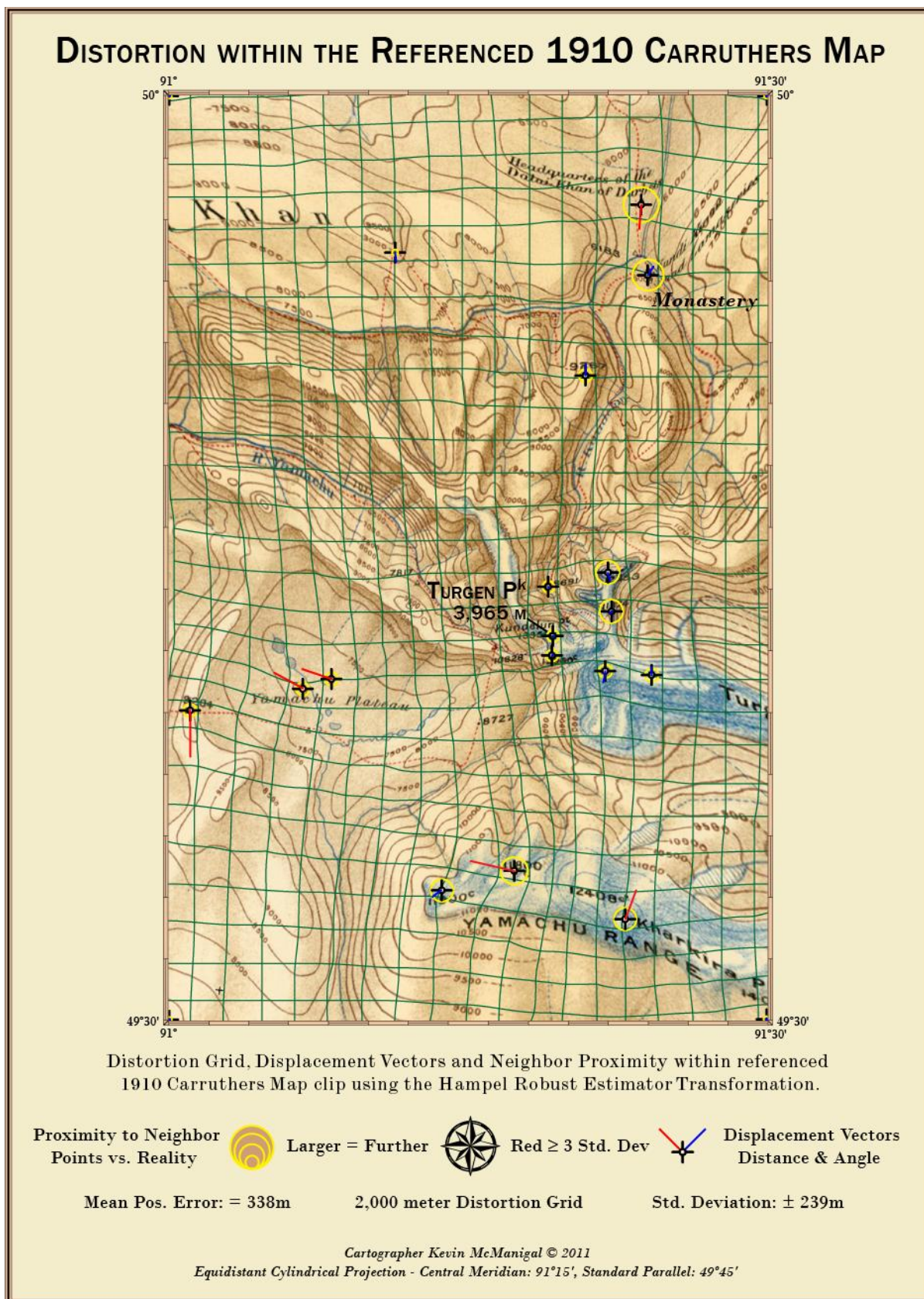


Figure 23. Distortion and displacement in the georeferenced clip of 1910 map by Carruthers.

the mean match many of the outliers from the unreferenced map. One exception is the monastery, which is now close to its proper location, and therefore contributed more weight in the analysis. The neighbor proximity circles are smaller than on the unreferenced map, displaying a generally good fit within the central Turgén Valley. The georeferenced clip of the Turgén map is more accurate than the original when compared to the Russian topographic maps, however, it is not a perfect match. This speaks to the many sources of error that may have crept in, including the work of Carruthers, the Russian cartographers, and the data manipulations done for this study. The mean positional error of ± 338 meters for the sampled points is likely smaller in the core study area and the standard deviation of ± 239 meters is roughly equal to the variation in scale at the head of the valley. Regardless, the statistics confirm that the accuracy of the Carruthers map is insufficient to evaluate the exact positions of the Turgén glaciers in 1910. However, when combined with evaluation of the repeat photography, a good estimate of the 1910 glacial landscape emerges.

SPECIALIZED CARTOGRAPHY

BACKGROUND

The iconic Swiss cartographer, Eduard Imhof felt that the base of almost all maps was the relief representation (Imhof 1982). He further remarked that the “proper rendering of relief is one of the primary tasks in cartography” (Imhof 1982, preface). In the past, this was accomplished by skilled artists that drew the landscape by hand, often from memory and sketches made in the field (Bagrow and Skelton 1964). With the advent of digital map making, the generation of relief from highly accurate digital elevation models has become prevalent, but the quality has suffered. The detail in modern relief can sometimes obscure the

most important features of a landscape, masking them in a blur of highlights and shadows. Tom Patterson (2010b), the master relief artist for the National Park Service believes “manual shaded relief often provides a clearer picture of major terrain features, especially at small scales”. Arthur Robinson, the grandfather of modern American cartography, speaks of the inherent challenge in mapping within a two dimensional environment, while trying to portray a three dimensional reality (Robinson 1952). The balance of this enigma is the threshold between cartography and art. Stock rendering of terrain is often the downfall of many maps. However digital relief does not have to be metallic and mechanical. With a little effort and some specialized techniques, digital relief can be customized beyond the ‘one button click’ defaults in the latest programs. Patterson (2010a, 13-14) calls for the pursuit of elegance in mapping, the aesthetic faculty to only include what is necessary for communication of the landscape. The goal here then is to present the map of the 2010 expedition in the style of the Carruthers’ map, using the best of the digital tools, and leaving the superfluous behind.

METHODS

DEM Processing:

The CGIAR DEM was mosaicked and clipped to the extent of the 1901 Carruthers map as previously mentioned. It was then output as an ASCII text file. The file was then imported into Terrain Sculptor, “a specialized application for the generalization of terrain models for relief shading” (Jenny and Leonowicz 2010). The Java-based software for custom cartography permits the user to remove some complexity from terrain and emphasize the most prominent features in the landscape. The GUI controls allow for a generalization in the

overall level of detail, and the exaggeration or reduction of mountains and valleys. In this way, the cartographer can reproduce the look of classic shaded relief within the modern digital workflow.

Once the terrain was generalized, it was exported from Terrain Sculptor as a DEM and re-imported back into ArcMap. There, a custom set of models were run to generate a Swiss Hillshade (ESRI 2008a). Through the use of focal statistics, the original hillshade is generalized and then combined with a highlighted version of the same calculation that deepens the shadows in the valleys and lightens the peaks (Figure 18). The process produces two distinct hillshade

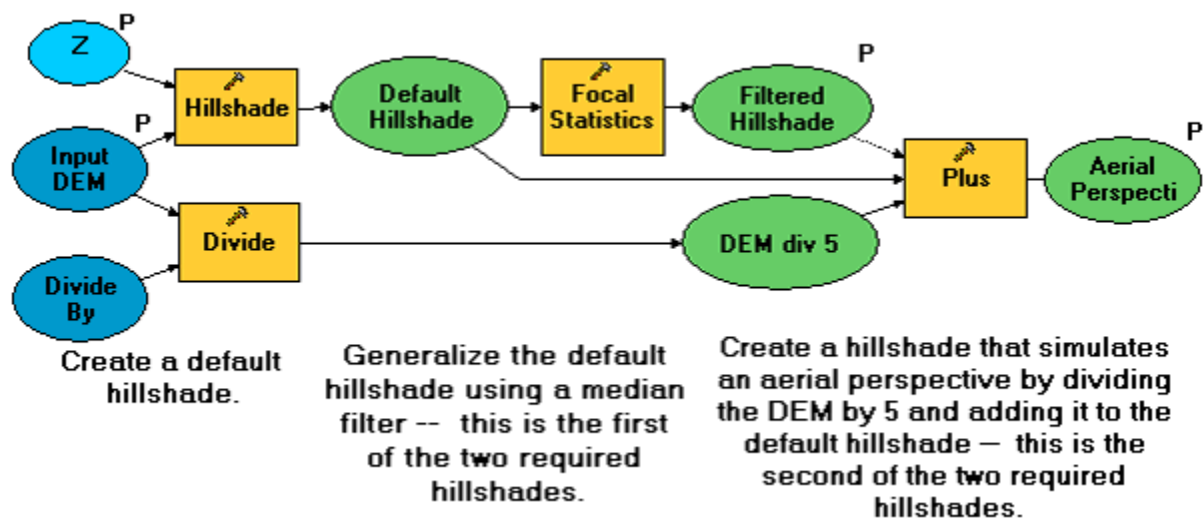


Figure 24. Swiss hillshade model (ESRI).

layers that are then overlain with the original sculpted DEM. All three layers were symbolized using a grey-scale color ramp and exported as 360 dpi tiffs to be blended in Photoshop.

Imagery Processing:

All seven bands of the L5TM_082910 Landsat scene were combined using the Composite Raster tool in Arc Catalog, and then imported into the working raster GDB as the 2010_L5TM layer. Each individual band was also imported into the GDB so that raster calculations and band ratios could be performed for analysis of the glaciers. The 2010_L5TM layer was symbolized in a true color combination of 3-2-1 and then pan-sharpened by a 7-4-2 band combination to aid in visually identifying the glacial extents against the classification calculations.

To construct a complete coverage of the entire 1910 map extent, the individual bands of the three L5TM Landsat scenes were mosaicked into Master Bands 1 through 7. The Mosaic tool parameters were set to use the Aug, 29th, 2010 scene as the first value, and fill subsequent values with the two September scenes. The tool was also set to match colormaps and ignore NoData values, removing the black collars around the images. The seven bands were then combined into a Master_2010_L5TM raster and clipped to the 1910 map extent.

Using the raster calculator, band 4 was divided by band 7 of the clean 2010_L5TM scene. The resulting calculation was then symbolized as two classes and the threshold adjusted until the split line matched the 2010 glacial extents. In this case, the breakpoint was 1.9. This technique, after Krumwiede (2010), differentiates very well between ice and the surrounding landscape. There can be a tendency to falsely misclassify debris-covered glaciers, but the Torgen ice is relatively debris free. The classification was also visually checked against the pan-sharpened 2010_L5TM, which displays the extent of the ice in surprising detail, even exposing moraine covered glacier at the margins (Figure 25). The final glacier classification was then converted to polygon feature classes and edited for a few small

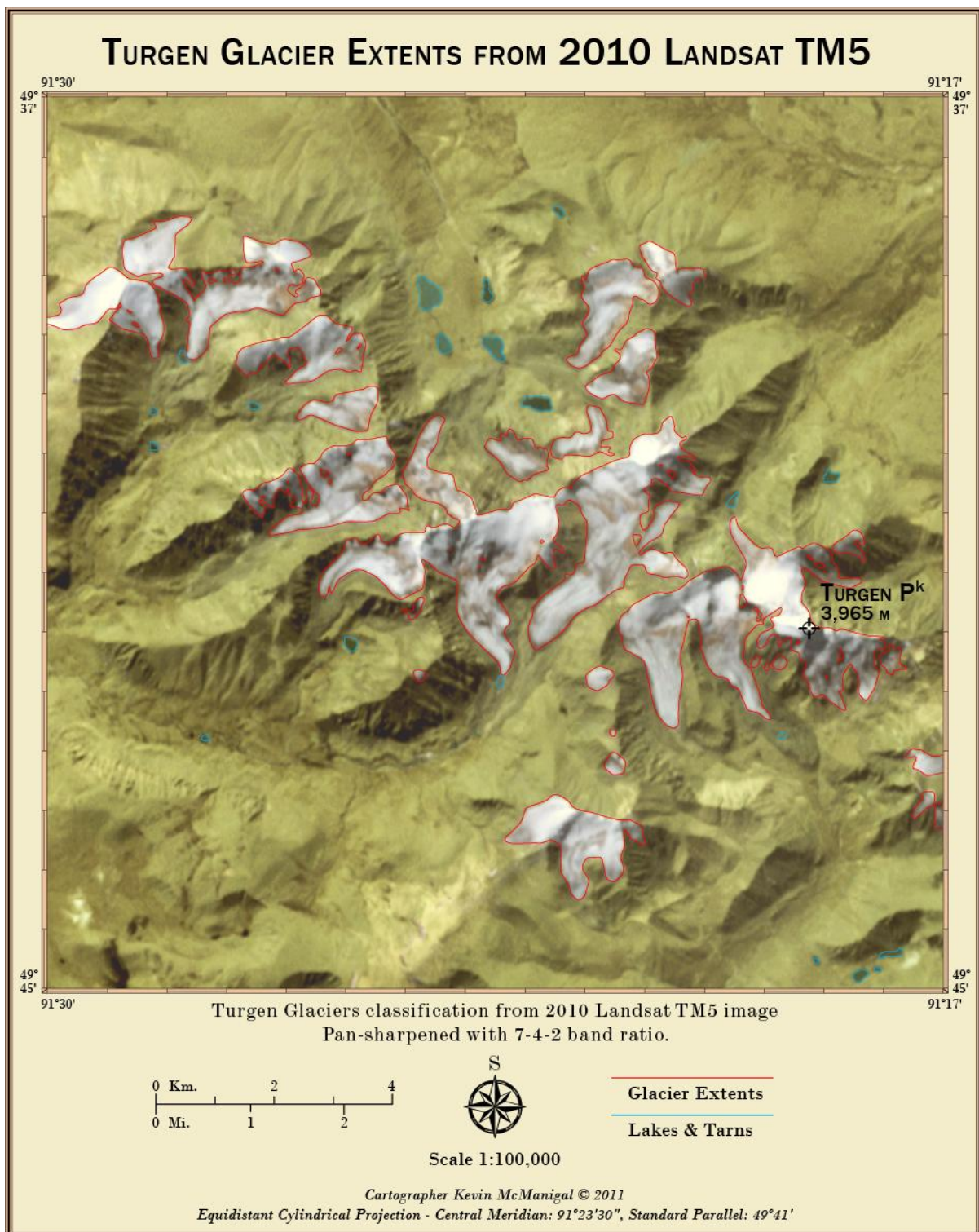


Figure 25. Identified Turgun glaciers in 2010 Landsat TM5.

proglacial lakes that had been mistakenly included. A copy of the glacier polygons were then simplified for cartographic representation, while the original was saved for area calculations at a later stage.

Next, a multivariate Maximum Likelihood Classification was performed to extract the boundaries of the small lakes in the scene. A sample point feature class of training signatures was constructed with nine classes consisting of at least ten samples each. Then, the Max-Like classification routine was run using all seven bands of the Master_2010_L5TM and the signatures from the training points. The calculated raster was then symbolized to show only the lakes, which were selected, converted to polygons, and edited. The final analysis collected roughly 90% of the small lakes within the 1910 map extent.

Graphic Design:

All vector layers, including roads, settlements, summits, contours, rivers, lakes, and the glacier features were exported from GIS into an Adobe Illustrator (AI) format at 720 dpi. ArcMap places the nodes of the vectors on a raster grid, so a high dpi is warranted to prevent vertices from being snapped to a coarse resolution and affecting accuracy (ESRI 2008b). The vector layers were then opened in AI and stripped of extra paths such as clipping masks. Excessive nodes were simplified and the layer structure constructed to organize visual hierarchy and facilitate placing the raster shaded relief.

The raster hillshade layers exported previously were processed in Photoshop (PS) using custom blending techniques developed by the researcher from experimentation with principles outlined by master relief artists (Patterson 2006). Using a combination of the layer modes, transparency, and the dodge/burn tools, the highlands of the relief were accented,

while the lowlands were subdued. The glacier outlines were imported as paths and custom-shaded with various brush tools to blend the aspects into the ambient lighting effects of the hillshades. Fine detail brushes were created and employed to produce the random detail of glacial moraines, placing each pixel with painstaking detail. Finally, the raster was placed into the Illustrator (AI) document as a linked file. This allowed updates to be instantly refreshed without slowing the processing speeds of the programs.

In AI, all vector artwork was carefully styled to emulate the feel and look of the 1910 map. The vector contour lines were labeled in AI, masked to knockout the line behind each label, then rasterized and blended into the landscape back in PS. This technique was developed to avoid the appearance of ‘floating contours.’ The route of the 2010 expedition was rendered from the GPS tracks and the photo stations labeled, along with the camps occupied during the trek.

Particular attention was placed on the font choices and type design. The title and legend block of the two maps is compared in Figure 26. Following best practices suggest by Robinson et al. (1995) and Dent (1985), a complimentary fontset of three families were chosen. The parent font of Franklin Gothic was used for main titles and important geographic point features. It is a heavy block sans serif typeface that closely resembles the Akzidenz Grotesk used on the original map. All Caps, Small Caps, and Super Script styles were employed to match the work of Carruthers. Monotype Modern was used for intermediate titles and large geographic features. Both the Extended and Wide formats were utilized. Finally, Bodoni Italics were used as a flowing serif script for rivers and blocks of text information.

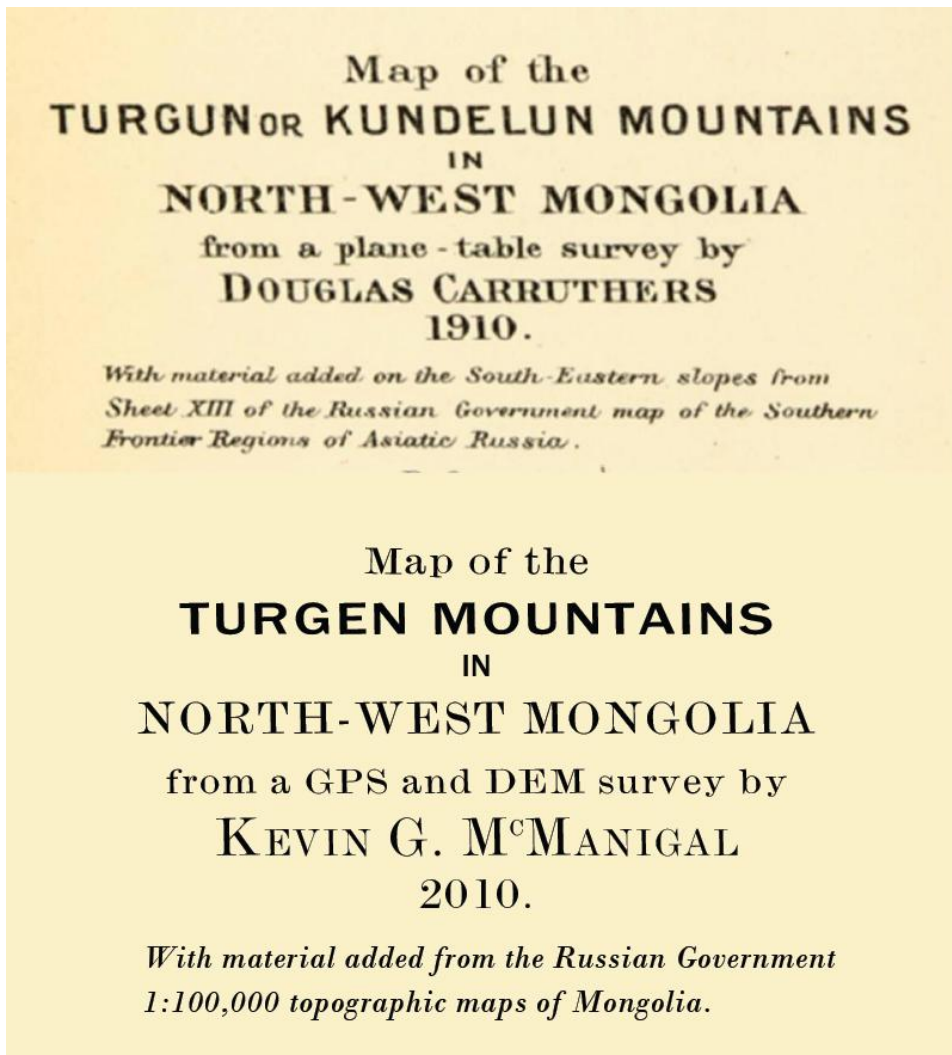


Figure 26. Comparison of typesets for 1910 and 2010 maps.

RESULTS

In extent and scale, the modern map exactly matches the 1910 Carruthers map. However, the depiction of locations and the lay of physical features are much more accurate. Some fine detail of the 90 meter CGIAR SRTM DEM was lost in generalization, but all tracks and GPS waypoints have a maximum error of 15 meters. The extent of the glaciers is also highly accurate, but that is addressed in the final chapter. In order to preserve the historic context of the original, the units of scale and contour intervals were duplicated in feet and

miles. The coordinate grid in the neatline remained in latitude and longitude. Once final styling was completed, the full size map, which measures 15” x 15” inches, was packaged for CMYK offset printing, and saved to RGB format for digital display.

DISCUSSION

Digital shaded relief may never be able to match the artistic flair of hand painted terrain. However, the process of trying to imitate those techniques leads to the invention of new methods that advance the science of modern cartography.

Research into the fonts and typesetting techniques at the turn of the 20th century revealed specific practices that were ubiquitous at the time (Casey 2005; Harley and Woodward 1987). All Caps sizes were regularly combined with Small Caps within the same word to produce visual hierarchy. Also, the use of Super Script styles that ascend above the Cap Height in the second and third letters of abbreviations added to the style. Unfortunately, modern type engines in graphic programs cannot reproduce all styles that were available on



Figure 27. Summit labels.

manual typeset printing presses. An example is the period directly below the Super Script ascender. This can be seen in the label of Turgun Peak (Figure 27).

The process of imitating the cartographic style of a previous era lead to a map of the modern expedition that appears at first glance to be from the Carruthers period. Working within a modern digital workflow, the task of trying to duplicate long forgotten techniques required the invention, or rediscovery, of methods lost to a new generation of cartographers. This work also inspired respect for the quality and craftsmanship of the Carruthers map, and fascination with the technologies used to produce it.

REPEAT PHOTOGRAPHY ANALYSIS

BACKGROUND

Historical Photography:

The science of repeat photography was invented and first applied to the study of glaciers in the Alps by Sebastian Finsterwalder in the late 19th century (Webb 2007). In general terms, the methods only require that previous locations of historical photographs be reoccupied for a new series of pictures which are then used for comparative interpretation of landscape transformation (Nüsser 2001). Rogers et al. (1984) compiled a comprehensive summary of reimaging techniques, which were then adopted by the United States Forest Service to monitor re-vegetation after wildfire and the expansion of urban zones (Hall 2001). Previous repeat photography studies in the mountains have concentrated on vegetation changes in relation to the cultural uses of the land by local peoples (Ives 1987; Nüsser 2000). However, recent research has reintroduced comparative photography to the monitoring of glaciers not only in the Alps, but in the ranges of Africa, and the Americas (Zängl and Hamberger 2004; Hastenrath 2008; Schmidt and Nüsser 2009). The glaciers of Asia have recently been included in rephotography studies, with Byers (2007) working in Nepal and Schmidt and Nüsser (2009) in Pakistan, but this study is the only one found applying the techniques in Mongolia.

Challenges arise in that many historic photo locations are not well documented, especially in mountain settings, and require extensive fieldwork to reacquire (Fagre 2010). This is the case with the Carruthers collection from 1910. While the route of his expedition was well recorded on his map of the region, the specific locations of photographs are not marked, nor are they noted in the field journals. Only by careful examination of photo

captions and the occasional non-specific remark in a field book, were the 1910 photo points narrowed in on. Through the use of virtual rephotography, the Carruthers route was traveled utilizing the 3D model within Google Earth and the probable photo stations estimated (Webb et al. 2010). Then, once in Mongolia, the 1910 route was followed by GPS paying careful attention to the landscape until a viewpoint could be matched with a printed historic photo.

The Carruthers expedition carried several cameras and a good supply of film for their two year journey. It is unclear whether the camera equipment was on loan from the Royal Geographical Society or owned by the expedition members. The following list comes from the personal diaries of Carruthers viewed at the RGS archives in the summer of 2010:

- Kodak A3 Postcard camera (Figure 28)
- New Newman & Guardia “Nydia” w/ changing box (Figure 29)
- Kodak Panorama camera (Figure 30)
- Pack Film Adapter
- 200 Plates @ 78 speed
- 72 Pack Films
- 72 Postcard Rolls
- 80 Panoramas

There was also a note about a supply of developer to make trials in the field and periodically develop prints to test the cameras.

There are no explanations of how the cameras were used either in the personal diaries or in the published accounts of the expedition. It appears that the cameras were utilized more as a tool for documentation of the journey, and not viewed as scientific instruments. Most of the pictures are of a cultural nature, consisting of portraits of the various ethnic groups



Figures 28 and 29. Kodak A3 postcard camera and a Newman & Guardia “Nydia” camera. encountered along the way. The scenes of landscape photography seem to have been chosen purely by the vistas which most inspired the expedition members. The majority of scientific investigation was concentrated on collection and preparation of geologic, botanical and taxidermy samples. The mapping of the landscape was also a priority.

The journals do not mention which camera was used for each photograph. This makes it difficult to determine the focal length for individual pictures and prevents the use of more advanced photogrammetric techniques in this study. There is also no credit given to the photographers responsible for specific images. Carruthers (1914a, 289) writes of Miller taking photographs in between hunting forays, while in another section noting that Price was occasionally with a camera in hand. At least one photograph shows both Price and Miller, implying that Carruthers was sometimes behind the lens. Considering the extended periods that Carruthers spent at the plane table and preparing skins, it is likely that most of the photographs were taken by Miller or Price. The exact credits, however, will never be known.



Figure 30. Kodak panorama camera from 1910.

In most cases, the photographs in the Carruthers collection are in focus and properly exposed. Some appear to be clearer than others, likely due to the camera model, with the one panoramic of the Turgan Range being the sharpest. They are all of sufficient quality for repeat photography purposes, which is amazing considering that the exposed film was carried for over twenty months, across 5000 miles, and under every conceivable condition.

DATA

1910 Photos:

In the archives of the Royal Geographical Society, dozens of photos from the Carruthers expedition were viewed in the summer of 2010. Of the eleven related to the Turgan Range, four matched the photographs that were published in *Unknown Mongolia* (Carruthers 1914a), however, many are unpublished or were taken from a slightly different vantage points. Several of the published photographs were not in the RGS collection, and

only exist in the Carruthers book. Unfortunately, the RGS archives are not in possession of original negatives, holding only prints that are almost a century old. There are two pages covering the Turgen portion of the expedition in a large format photo album that contains hundreds of images. The photos are mounted to the pages with glue and are in fair condition, showing some staining and yellowing. The average size of these nine images is 4 x 3 inches, with two in portrait format and the rest in a landscape orientation (Figures 31 and 32). In addition, there are two large prints loose in a folder. One is a landscape panorama of the Turgen Range measuring 3 ½ x 11 ¾ inches, while the last 9 x 12 inch shot is of the summit Turgen Peak (Figures 33 and 34). The RGS picture librarian arranged for the images to be scanned with a large format flatbed scanner at 96 dpi and uploaded to an ftp site. The scans were downloaded en-route to Mongolia and printed in Kathmandu for use in the field.

Upon returning from the field, the images were cropped from the larger pages, rotated to square, and filtered for contrast and brightness. Some images with extensive yellowing and stains were restored using black & white filters and content aware fills (Fitzgerald 2010). Care was taken not to alter any portions of the images that depicted mountains or glaciers, which was easily accomplished, as most of the damage was along the peripheral edges.

2010 Photos:

The repeat photographs captured in the summer of 2010 were all taken with a Nikon D90 digital camera. The body has a 12.3 megapixel sensor that writes RAW 4288 x 2848 pixel files at 240 dpi to SD digital media cards. All photographs were shot in both RAW NEF and jpg formats using a Nikon 18-105 mm f/3.5-5.6 lens. The pictures were bracketed in ± one third stop increments to ensure proper exposure in the variable lighting conditions of the mountains. However, with the use of RAW format images, the problems of incorrect

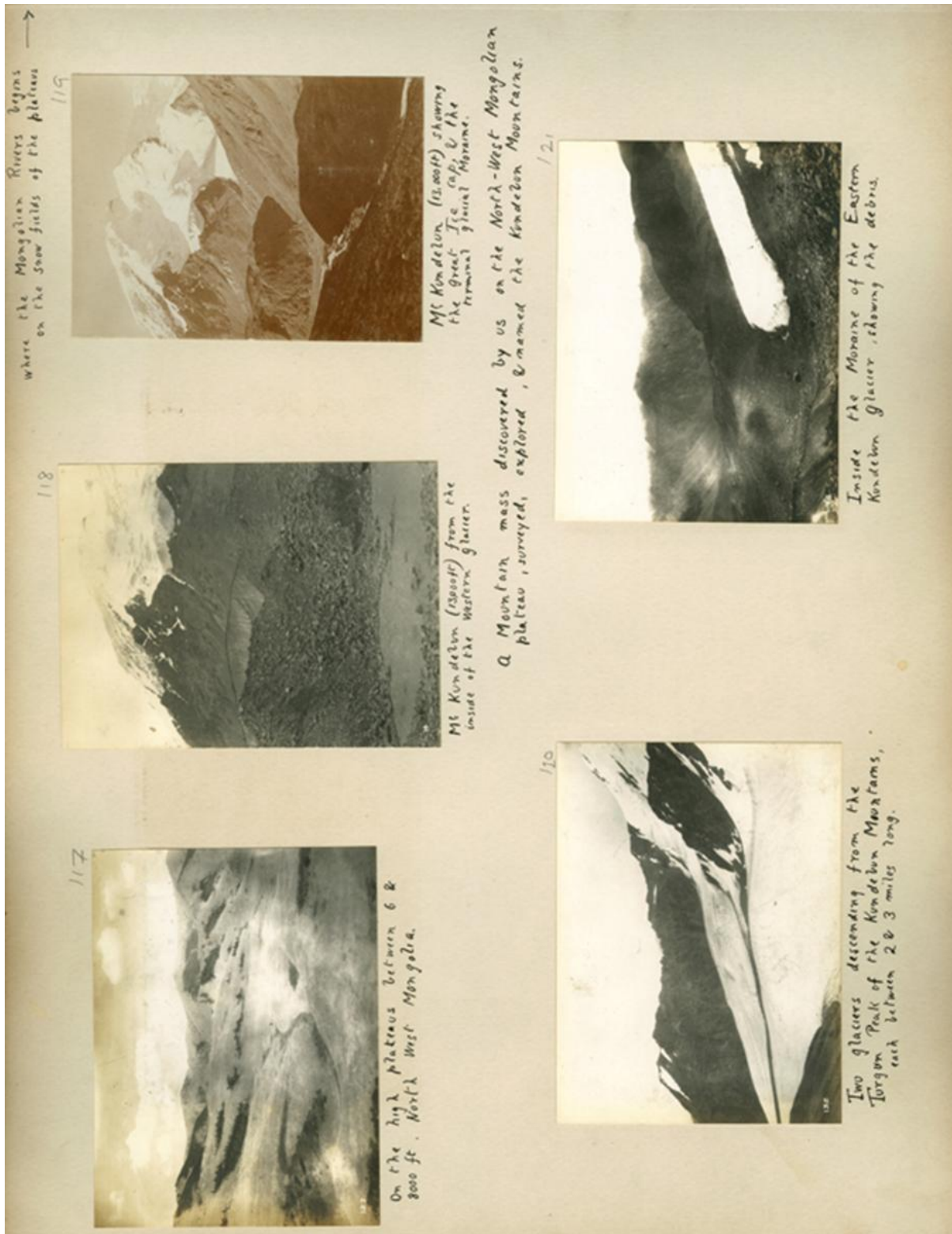


Figure 31. Original page of Carruthers photo album (RGS).

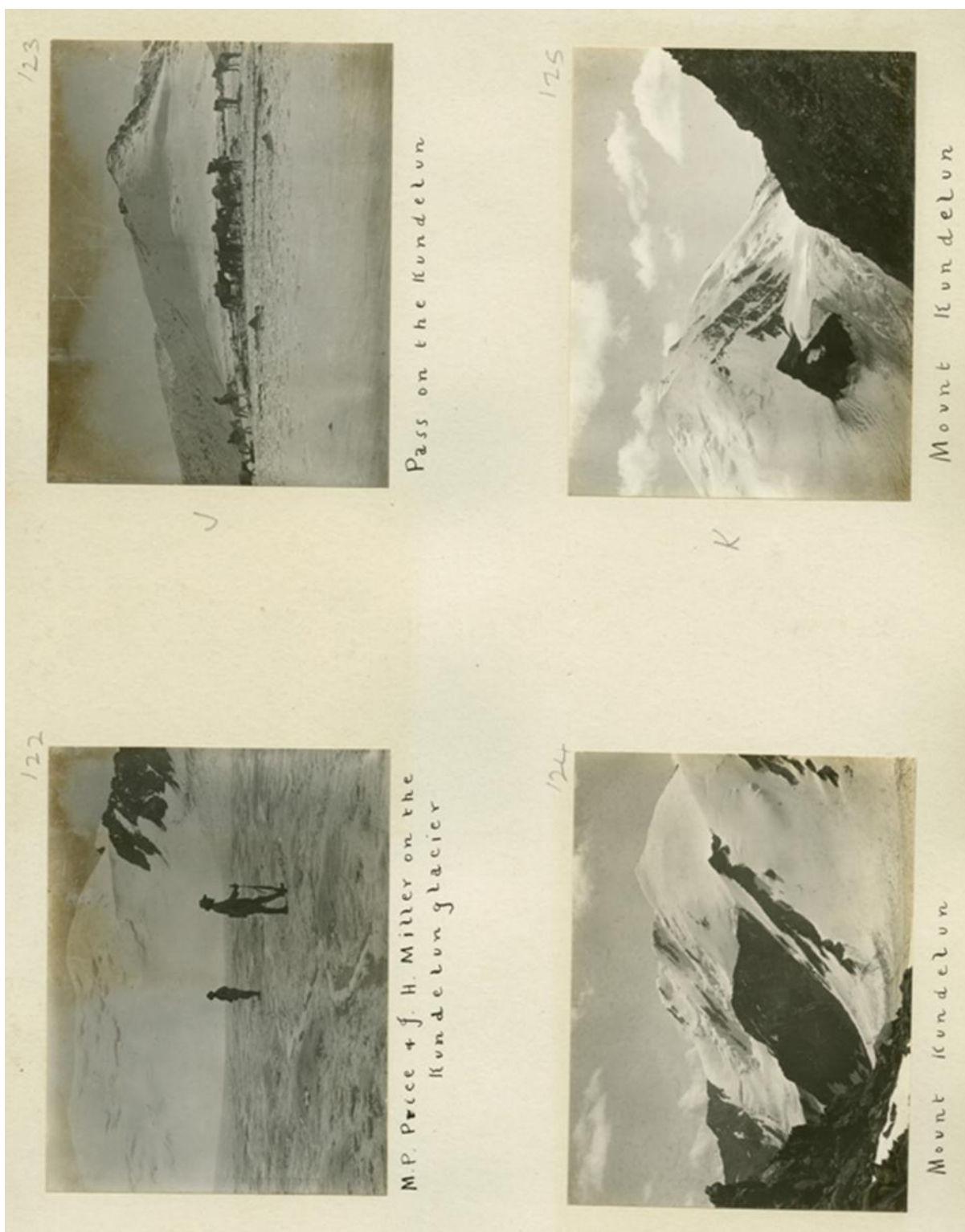


Figure 32. Original page of Carruthers photo album (RGS).



Figure 33. Original Carruthers large format photograph of Turgun Peak (RGS).

exposure are easily addressed in post processing as all data captured by the sensor is retained. In most cases, the camera was mounted on a Slik Sprint Mini tripod for stabilization during recapture. All images were transferred from SD cards to a laptop, and then backed up on a portable hard drive in the field. Initial processing of the RAW files was done in Adobe Lightroom 2, where all images were archived, sorted, and tonally adjusted based on a preset calibrated camera profile.

Of the eleven scanned photographs from the RGS, eight photo stations were able to be located in the field and recaptured. Two of the images not relocated were shots of subjects with non-definable landscape features in the background. These include a shot of Price and Miller on the Kundelun [Turgun] Glacier and one of the 1910 expedition horses on a snowy

pass. The third picture that was not repeated is of a grassy hillside with small stands of trees that were not distinct from any vistas within the Turgun landscape.



Figure 34. Original Carruthers large format panorama of Turgun Range (RGS).

Field Techniques:

From the preliminary work, GPS tracks and waypoints digitized from the 1910 Carruthers map were used to approximate the original photo stations. There were also clues in the original captions written in Carruthers' hand below many of the photographs. The locations were generally not easy to access, demanding ascents of a thousand meters or more, with field days above basecamp regularly lasting from sun-up to sun-down. Some sites required the use of specialized mountaineering gear and techniques to safely traverse moderately crevassed, steep glacial terrain. Utilizing a copy of the Carruthers map and a handheld Garmin 60CSx GPS, the general location of a station was approached on foot until views matching the original photo could be aligned by hand (Figure 35). At the assumed point, the location was further refined using parallax assessment of ridgeline intersections, perspective alignments, and location of foreground features (Hall 2001; Rogers 1984). Once the photo station was accepted, the tripod was set-up and re-imaging conducted. A GPS waypoint was taken and its name, positional accuracy, azimuth of shot, date and time were recorded in a notebook along with any comments concerning the physical setting of the



Figure 35. Aligning the historical photograph from 1910 to the modern landscape.

location. The map in Figure 36 displays the core study area at the head of the Turgun Valley and the locations of the photos stations, along with the route and camps of the 2010 expedition.

In most cases, a series of handheld overlapping shots were taken by rotating 360° on the station. This was done to document the area and facilitate the stitching of individual photos into panoramas of the entire landscape (Figure 37). As the days progressed, establishing one station often led directly to finding the next, settling into the footsteps of the historic expedition. Table 9 lists the photo stations of the repeat pairs and various information including their coordinates.

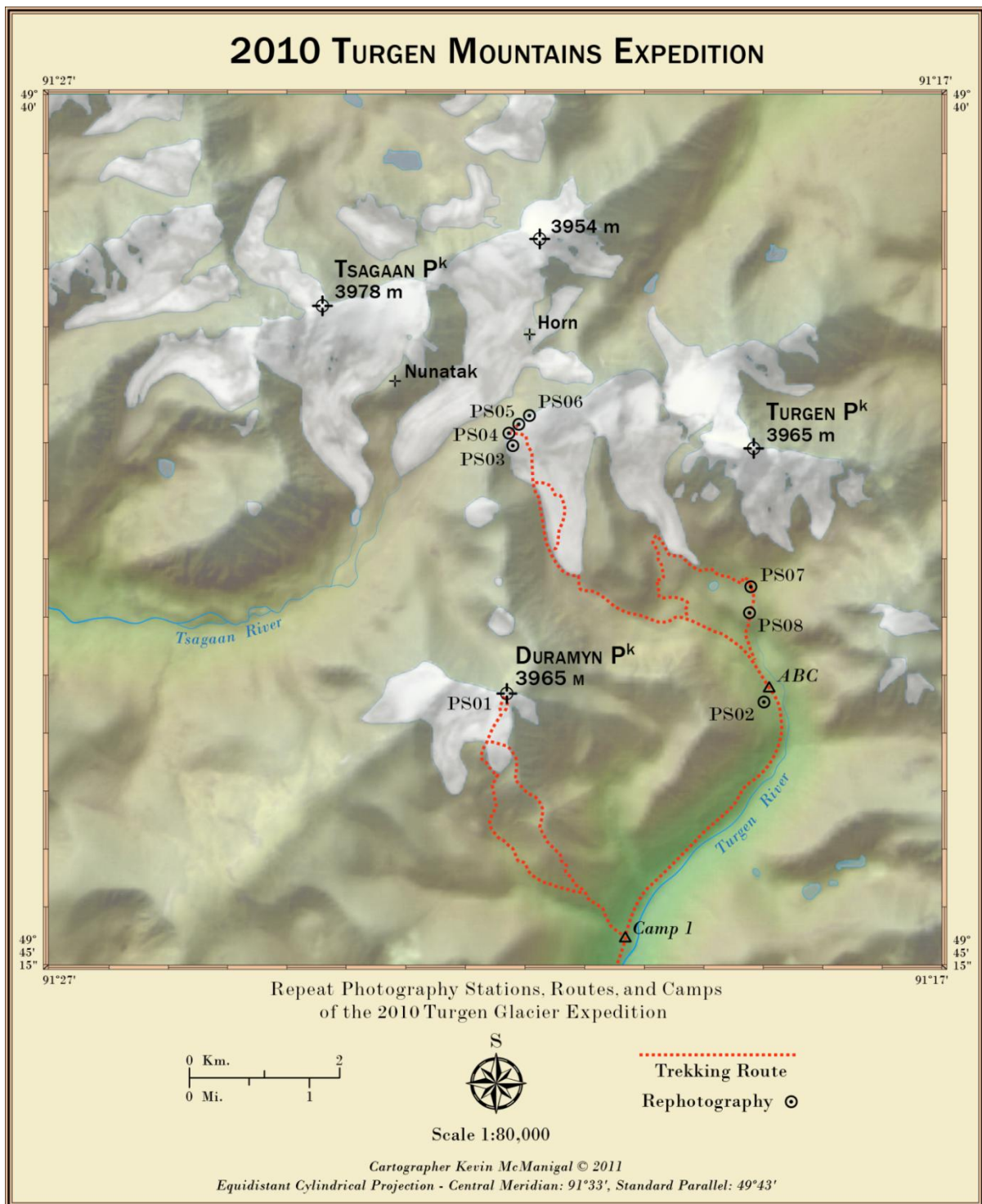


Figure 36. Map of the Turgun study area.

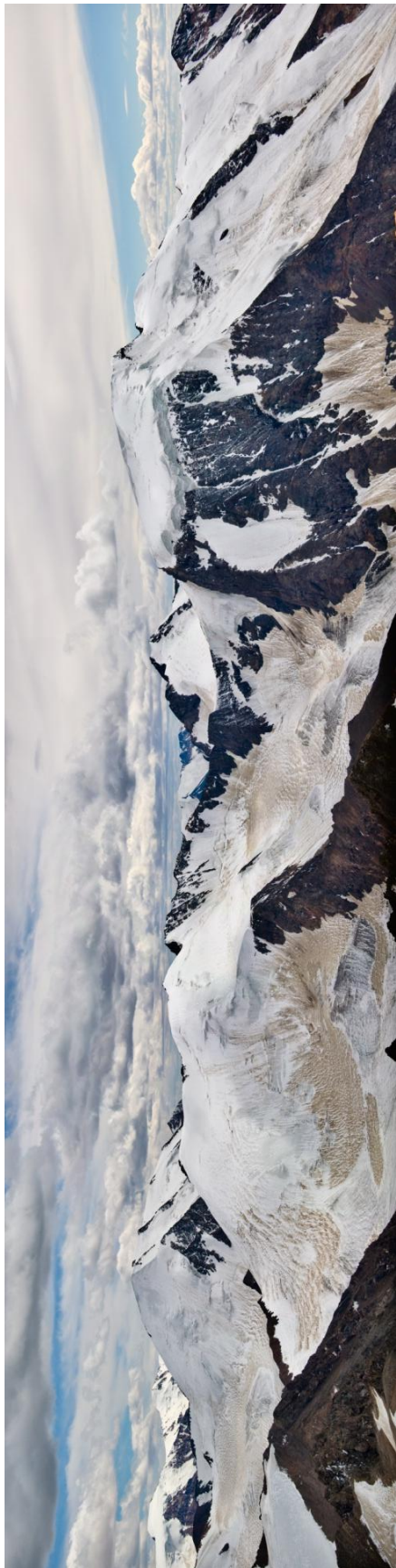


Figure 37. Panoramas ascending Duramyn Peak (top) and of the Turgun Range from the summit (bottom).

Photo Station #	Location	Elev. (m)	Azimuth	RGS Photo Call #	Original Caption	Original Date	Modern Date	Station Coordinates
PS01	Duramyn Peak	3750	212°	F039/0126	Panorama of the main peaks of the Kundelun [Turgen]	August 13 th to 19 th , 1910	July 13 th 2010, 15:32	49° 44' 17.97" N 91° 21' 52.06" E
PS02	Slope above Advanced Base Camp	2659	173°	F039/0119	Mt. Kundelun [Turgen] (13,000 ft) showing the Great Ice Cap and the terminal glacial moraine	August 13 th to 19 th , 1910	July 14 th 2010, 17:15	49° 44' 21.57" N 91° 19' 00.92" E
PS03	High slope on East Turgen Glacier	3482	273°	X0738/ 024743	Peak Kundelun [Turgen] in the Turgun Highlands	August 13 th to 19 th , 1910	July 15 th 2010, 14:05	49° 42' 26.14" N 91° 21' 51.72" E
PS04	Col above East Turgen Glacier	3479	79°	F039/0120	Two glaciers descending from the Turgen [Tsagaan] Peak [...], each between 2 & 3 miles long	August 13 th to 19 th , 1910	July 15 th 2010, 13:58	49° 42' 25.19" N 91° 21' 50.78" E
PS05	Col above East Turgen Glacier	3478	209°	F039/0125	Mount Kundelun [Unnamed Horn]	August 13 th to 19 th , 1910	July 15 th 2010, 14:18	49° 42' 23.75" N 91° 21' 50.82" E
PS06	Col above East Turgen Glacier	3501	92°	F039/0124	Mount Kundelun [Tsagaan]	August 13 th to 19 th , 1910	July 15 th 2010, 14:44	49° 42' 22.18" N 91° 21' 44.17" E
PS07	S. moraine of West Turgen Glacier	2808	96°	F039/0121	Inside moraine of the eastern [western] Kundelun [Turgen] glacier showing the debris	August 13 th to 19 th , 1910	July 16 th 2010, 14:08	49° 43' 32.13" N 91° 19' 09.68" E
PS08	In moraine of West Turgen Glacier	2755	172°	F039/0118	Mt. Kundelun [Turgen] (13,000 ft) from inside the western glacier	August 13 th to 19 th , 1910	July 16 th 2010, 14:31	49° 43' 43.27" N 91° 19' 10.50" E
* All 1910 photographs by D. A. Carruthers or M. P. Price [credit not specified], all 2010 photographs by K. G. McManigal								

Table 9. Repeat photography stations.

COMPARATIVE ANALYSIS

METHODS

The scans of the original Carruthers photographs from RGS were loaded into Photoshop CS5 (PS) and processed as previously mentioned. The individual scenes were resampled and saved as 300 dpi .tif files. Each 1910 scene was then compared to the bracket of repeat images taken in the summer of 2010. A match for each photo station was selected from the library in Lightroom, processed, and then saved as a 300 dpi .tif as well. Each set of paired repeats was then placed on a separate layer in PS, with the 2010 picture on top and set to 75% transparency. The 2010 image was then positioned and resized until the best fit was



achieved. The images were not distorted in any way, only resized and aligned after methods outlined by Webb (2010). As a visual check, a transparency mask was applied on another layer which allows the 2010 image and the 1910 image to fade into each other on any axis set in the mask. The results confirmed a high degree of alignment between the paired repeats (Figure 38). Three paired repeats were then labeled with letters corresponding to areas

Figure 38. 1910 – 2010 blend mask to check alignment.

of noticeable change between the images. Number labels were applied to features that exhibit little or virtually no change, similar to the techniques used in the Desert Laboratory Repeat Photography Collection (Webb 2007). This labeling for qualitative analysis was applied to images from photo stations PS01, PS05 and PS06. The remaining pairs were better suited for quantitative analysis.

RESULTS

PS01 – Photo station one is located on the summit of Duramyn Peak, which was called White Peak in 2010 field notes. The mountain was approached by way of the grassy slopes rising to the southeast above Camp 1. The final stages of the ascent required technical glacier climbing of the last 300 meters leading to the summit. The 2010 re-photography from this point does not exactly match the 1910 image taken from a similar vantage. It is likely that the original photo was taken from a point to the southwest and slightly lower, possibly along the ridge leading off the summit. On the day that the station was visited in 2010, time considerations and impending weather forced the team to abandon the summit back towards Camp 1, not exploring the southwest ridge. However, the paired images share enough similarities to facilitate comparative analysis. As depicted in Figure 39, the hanging glacier marked as ‘A’ has ablated considerably between 1910 and 2010. The bergschrund at ‘B’ has moved upslope and there is more rock exposed on the face. In the modern picture, there is a small rock rib protruding out of the glacier at ‘C,’ while the seracs at this spot in 1910 appear to have completely ablated. The main Torgen icecap, labeled ‘1’ shows almost no change; the large serac face appearing roughly the same as in 1910.



Figure 39. Repeat 1910 and 2010 photo pair of Turgen Range from PS01.

PS05 – Photo station five is located on the ridge above the East Turgen Glacier that forms the divide between the Turgen and Tsagaan watersheds. The repeat photo point was approached from the Turgen Valley by way of ascending the moraine to the glacial snout, and then climbing the 40° slope of the accumulation zone using roped glacier travel techniques. The photo pair looks southeast to a rock horn between two larger un-named peaks. There are glaciers flowing on either side of it. This 2010 repeat is an exact match of the 1910 counterpart as seen in Figure 40. The area of label ‘A’ shows a substantial ablation of ice behind the horn. The glacier has melted down to exposed moraine and appears to no longer flow around the south side of the horn. There is also a significant loss of ice on the slopes of the background peak labeled as ‘B’ and ‘C,’ with considerably more exposed rock in the 2010 photo. Label ‘1’ on the high slopes of the peak looks similar in both images,



Figure 40. Repeat 1910 and 2010 photo pair of rock horn from PS05.

however, the modern photo shows bare ice in this area indicating that the equilibrium line may have risen high onto the peak over the last century. The slope also looks to be steeper in the modern picture, indicating a loss of volume.

PS06 – The photos of station six were taken from a similar vantage point as PS05, only looking to the east. The repeat image could not be made to match the rocks on the left of the 1910 picture because the snow on the col has melted and lowered the position of the station an estimated five meters. Regardless, the nunatak in the distance and the surrounding slopes are coincident enough for analysis (Figure 41). The steep glacier in area ‘A’ has wasted severely in the preceding hundred years and no longer flows into the glacier below it. The snow and ice on the slopes in areas ‘B’ and ‘C’ has completely ablated exposing bare rock and moraines. Again, the area of label ‘1’ on the high slopes looks similar between the years, but the ice appears to be bare and steeper in the modern photo, indicating that the ice there has at least begun to recede.

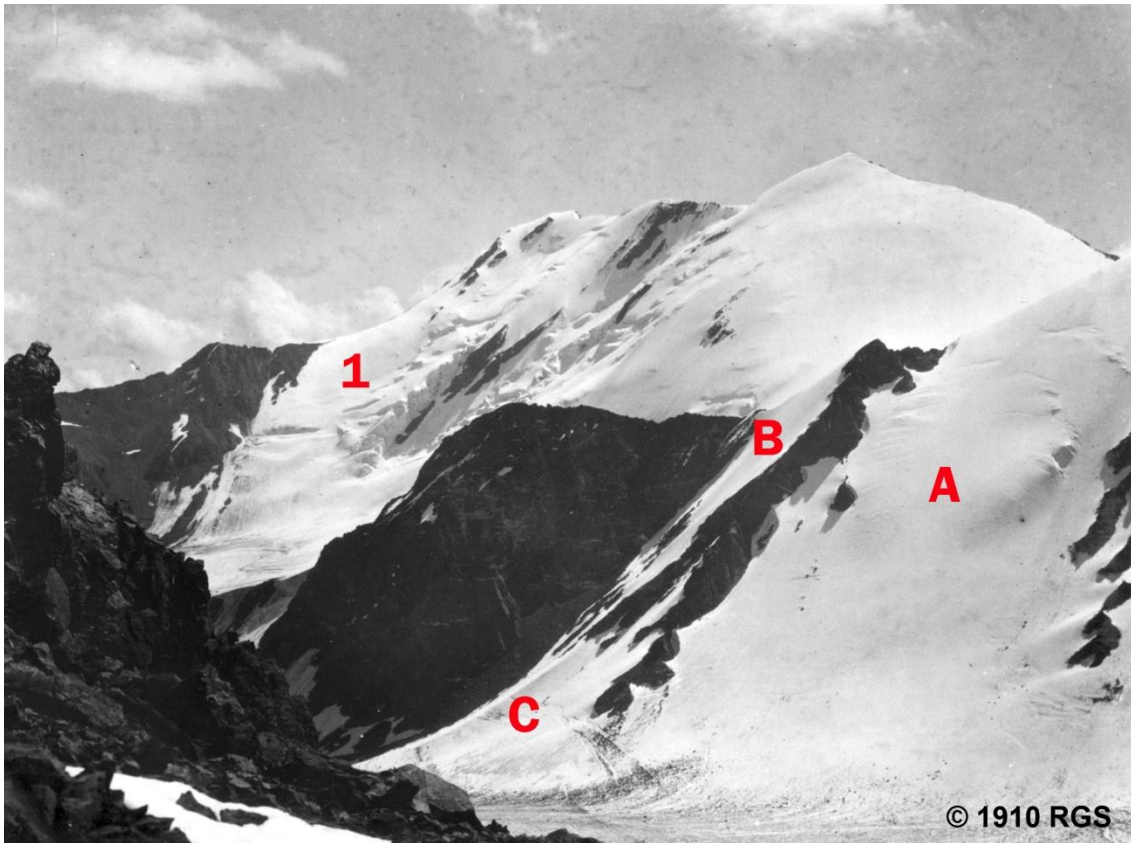


Figure 41. Repeat 1910 and 2010 photo pair of nunatak from PS06.

PIXEL ANALYSIS

METHODS

Previous studies have attempted various techniques to quantify change between pairs of oblique photographs. Roush et al. (2007) overlaid images with a grid in GIS to extract pixel values of each photo that were classified as vegetation types. Munroe (2003) used a random sample grid, but also digitized meadows in GIS to measure relative changes in size. More advanced methods by Aschenwald et al. (2001) georeferenced oblique photographs to DEMs for change analysis, but this required a network of installed ground control targets visible in the images. All these procedures produce quantitative results; however they were impractical here due to the nature of the photographic pairs.

To quantify relative change in glacial cover for this study, specialized image analysis software from the biological sector was adapted. The program Pixcavator (2007) is generally used to measure quantity, area and perimeter of features like bacteria in microscope images. The software determines contours, or outside edges, based on contrast, color and brightness. When paired temporal photographs are processed to have exactly matching resolutions and extents, it is possible to quantify differences in features based on pixel calculations. Tests were run on both the 1910 and matching 2010 images, but the differences between B & W, color, clarity and sharpness produced unsatisfactory results. The decision was made to digitize the exposed ice on each paired image with Adobe Illustrator to construct pure bi-tonal slides where white polygons represent ice, and black equals no ice (Figure 42). The ‘no ice’ polygons included all vegetation, moraines, rocks and sky. The pairs were then analyzed individually in Pixcavator, where the program delineated the contours of the white and black polygons.



Figure 42. Bi-tonal classification.

Paired images from stations PS02, PS03, and PS08 were processed in this way. The program output statistics on the percentage of light and dark pixels, along with the perimeter and total pixel count of the white ‘ice’ polygons (Figure 43). By comparing these measures for paired images, changes in relative ice cover were assessed. Since photographic pairs were all of the Turgén ice cap, but taken from differing viewpoints, the percent of relative change for the three image pairs was averaged to estimate the total change in ice cover on the Turgén summit.

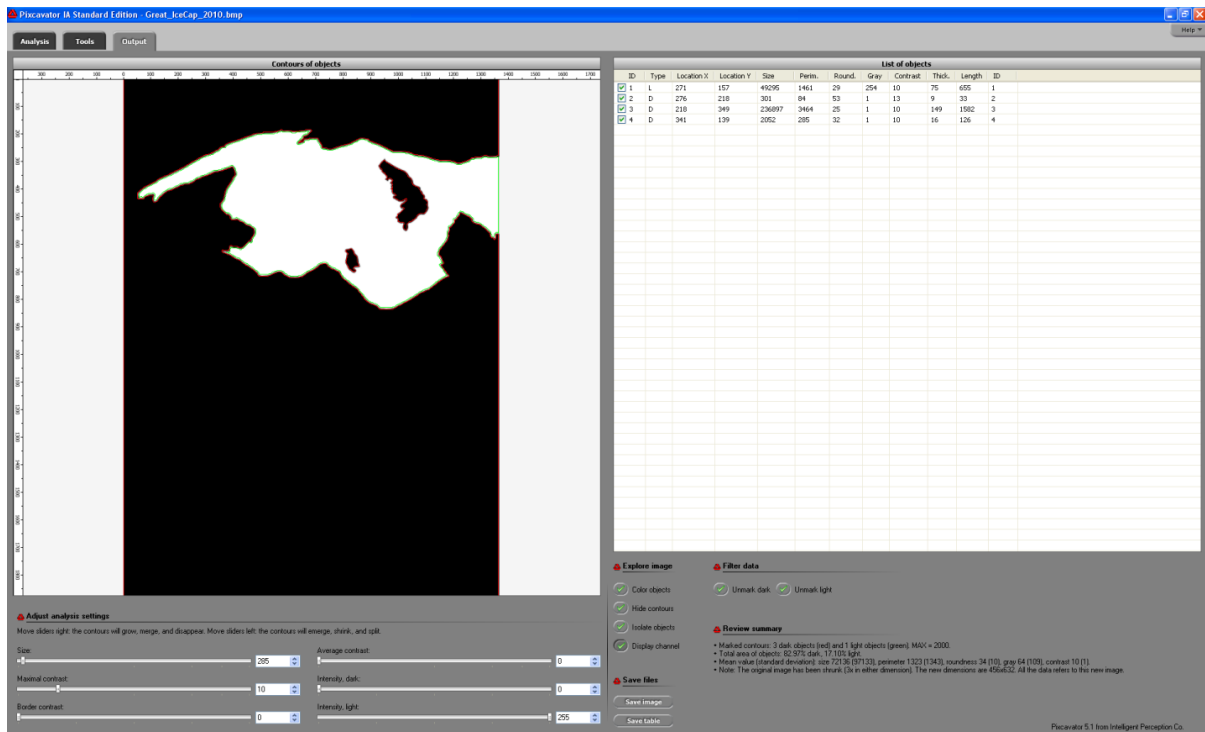


Figure 43. Pixcavator output screen.

RESULTS

PS02, PS03, PS08 – The photos in these pairs, all depicting the main Torgen Peak, are very well aligned. PS02 pairs were taken on the slope just east of Advanced Base Camp, looking southeast toward the mountain. The summit ice cap looks unchanged in the set, but the small glacier descending from the cirque on the right has retreated, along with a reduction of ice in the center frame seracs. The debris-covered ice in the center of the moraine has also completely ablated (Figure 44). The debris-covered glacier of 1910 was photographed close-up from PS08, along with a view of the summit from within the western moraine. Again, the debris-covered ice is completely absent from the moraine in 2010, but the summit appears almost identical (Figure 45). The photo pair taken from PS03 looks west toward the main summit of Torgen, and is located high on the slope of the East Torgen Glacier. There are large sections of slope in the foreground, but only the glacial cap was considered here, which again looks to be almost the same between the two years (Figure 46).

The results of the Pixcavator analysis on these photo pairs are shown in Table 10. The changes are almost undetectable by visual evaluation, but the pixel analysis results suggest a slight decrease in ice ranging from -0.29% to -2.36% with an average ice loss of -1.5% between the three pairs. The process also reveals the changes graphically when the traced ice polygons on one image pair from 1910 and 2010 are overlain (Figure 47).

Table 10. Results of Pixcavator analysis.

Photo Station	% Dark Pixels	% Light Pixels	Ice Area Pixels ²	Ice Perimeter Linear Pixels	% Difference 1910 to 2010
PS02 _1910	80.31%	18.97%	54,748	1,705	-1.87%
PS02 _2010	82.97%	17.10%	49,295	1,461	
PS03 _1910	87.15%	12.13%	35,417	1,306	-2.36%
PS03 _2010	89.94%	9.77%	28,487	1,136	
PS08 _1910	97.55%	2.45%	7,150	461	-0.29%
PS08 _2010	97.84%	2.16%	6,310	481	



Figure 44. Repeat 1910 and 2010 photo pair of Turgun Peak from PS02.

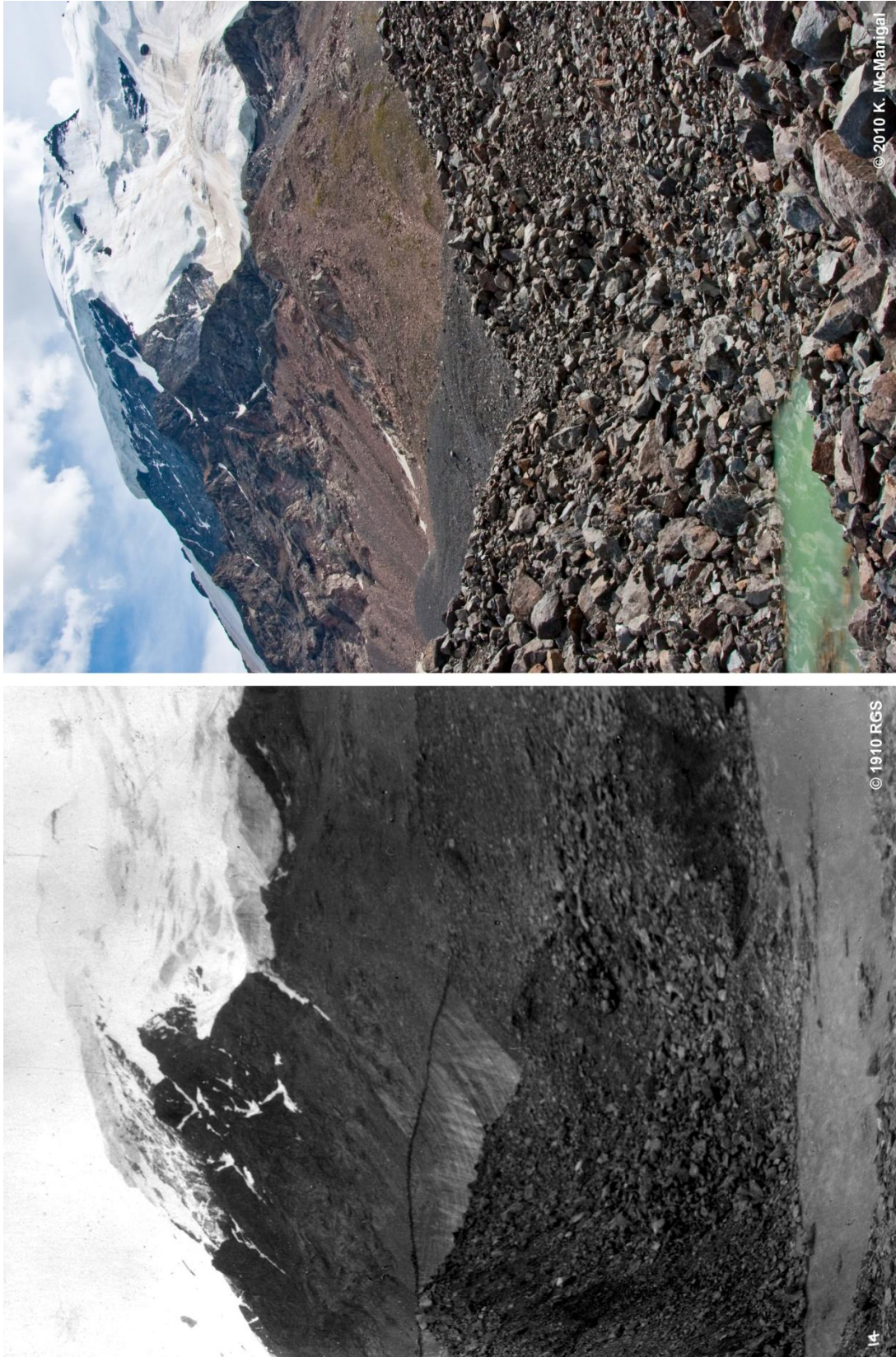


Figure 45. Repeat 1910 and 2010 photo pair of Turgun Peak from PS08.



Figure 46. Repeat 1910 and 2010 photo pair of Turgun Peak from PS03.



Figure 47. 1910 ice contour in red vs. 2010 ice contour in black from Pixcavator analysis.

MULTI-DATA INTEGRATIVE ANALYSIS

METHODS

The relationship between repeat oblique photography and topographic maps for glacial ablation studies has thus far been limited to locating the photo stations on the maps (Roush et al. 2007; Fagre 2010). The delineation of changes in glacial extent from multi-temporal series maps and satellite imagery is well established, however, inclusion of terrestrial photography in these measurements tends to be problematic since most scenes are wide panoramas taken from high vantage points (Byers 2007; Schmidt and Nüsser 2009). Most of the rephotography in this study falls into this category, but two pairs lend themselves to more accurate measurements.

PS04 – Photo station four is part of the group of stations located on the col above the East Turgen Glacier as previously described. The images were taken facing northeast and cover the same nunatak photographed from PS06. The photo pair captures two glaciers converging in a medial moraine around a nunatak to the east of the East Turgen Glacier. The nunatak was identified in the CGIAR DEM and measured using the ArcScene 3D program.

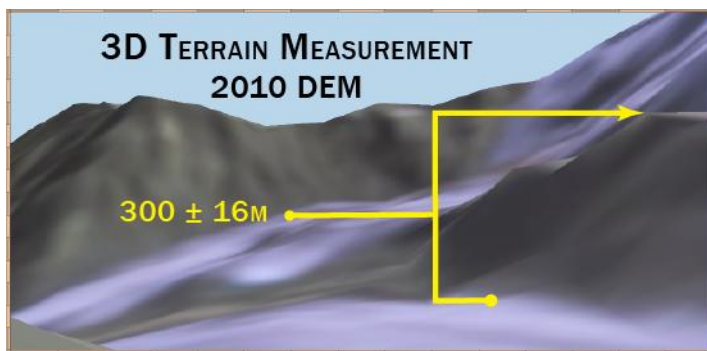


Figure 48. 3D model of nunatak in 2010.

The DEM was draped with the 2010 Landsat image and rotated on multiple axes to locate the top of the rock formation and the relatively flat surface of the glacier below it. Elevations for the

corresponding pixels were subtracted to determine that the height of the nunatak was 300 ± 16 meters above the glacier in 2010 (Figure 48). The paired photographs of matching

resolution were then loaded onto separate layers in Adobe Illustrator and baseline vectors drawn at the 1910 and 2010 glacier levels. Vertical lines were then drawn perpendicular to the glacier baselines up to the summit of the nunatak. The length of the lines is given by the program in pixels and was used in the simple ratio:

$$\frac{300\text{ m}}{262\text{ pix}} = \frac{X}{199\text{ pix}}$$

Where X equals the height of the nunatak in meters above the glacier in 1910. The ablation of the glacier over the last century at that location was derived from the elevation difference.

PS07 – Photo station seven is located on the high sloping western moraine of the West Torgen Glacier, with the images taken facing to the east. It is about a two hour hike from ABC over loose talus. The position is directly below the summit seracs of Torgen Peak and may be exposed to calving ice. The historic 1910 photograph from PS07 was taken perpendicular to the West Torgen Glacier terminus. The repeat photo station occupied in 2010 was matched almost exactly with the 1910 position using the parallax techniques outlined previously. A blended hybrid photograph of the 1910 and 2010 images was created so that the 1910 terminus could be seen simultaneously with prominent landscape features in the background of the 2010 image. Then a vector (line) was drawn from the known location of the photo station, across the historic 1910 terminus, and intersecting with a peak in the distance (Figure 49). The azimuth of this ‘terminus vector’ was then plotted between the GPS location for PS07 and the background peak visible in the Landsat image from 2010. By measuring the distance between the 1910 terminus vector and the 2010 glacier terminus in the GIS, a century of glacial recession was measured. Also, outlines of the West Torgen Glacier terminus were digitized from the 1970 Russian topographic map and the 1992

Landsat image. The glacial recession between these years was measured for comparison to the repeat photography results.

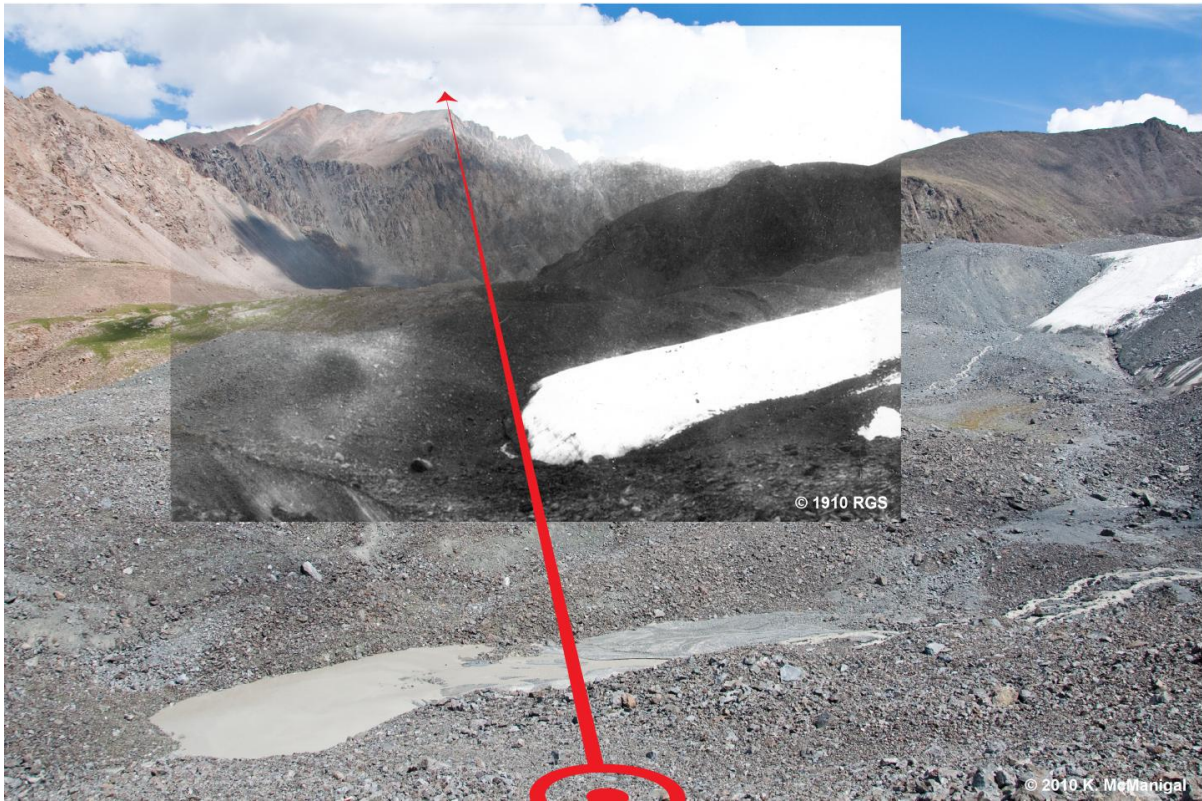


Figure 49. Rephotography blend with plotted terminus vector bisecting West Turgen Glacier.

RESULTS

PS04 – The two glaciers that converge below the rock face and flow north show considerable ablation over the one hundred year time span (Figure 50). The ice also seems to be thinning more rapidly downslope as evidenced by the trim lines and changing surface angles between the two images. From the ratio of pixels to nunatak height described in the methods, the exposed rock above the glacier in 1910 was measured at 228 ± 16 meters. Subtracted from the 300 ± 16 meters height in 2010, the glacier surface at the base of the nunatak has down wasted 72 ± 16 meters in the last century (Figure 51).



Figure 50. Repeat 1910 and 2010 photo pair of nunatak from PS04.

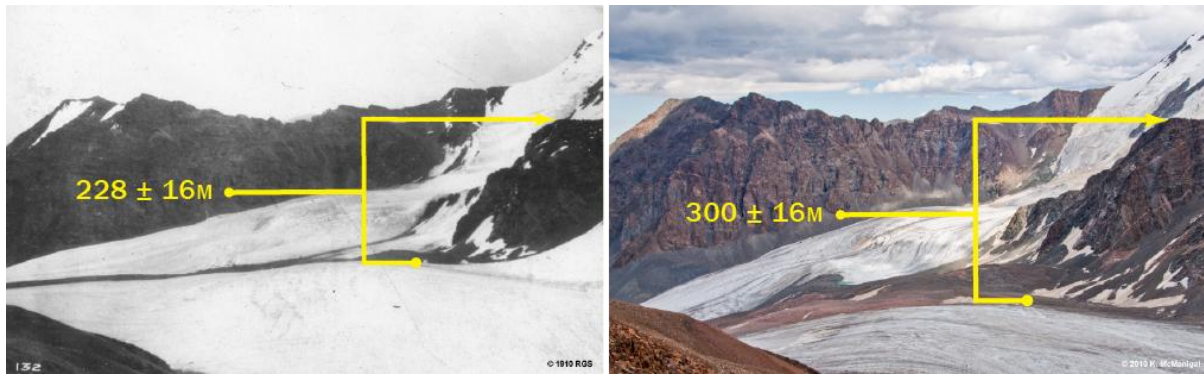


Figure 51. Photo pair from PS04 showing differences in height of nunatak above glacier.

PS07 – The paired photographs from this station match exactly and display the most extreme glacial recession of the study. Cropped to the 1910 extent, the tongue of the West Turgen Glacier is completely absent in the picture from 2010 (Figure 52). The debris-covered ice visible in the 1910 photo has also completely disappeared, changing the structure of the moraine noticeably. The azimuth of the capture angle plotted over the hybrid Landsat and DEM relief map in GIS reveals that the glacier has retreated 600 meters in the last century (Figure 53). Multi-temporal glacier termini locations are also plotted on the map from the 1970 Russian topographic sheets, as well as the Landsat images from 1992 and 2010. An estimated frontal lobe for the West Turgen Glacier in 1910 was extrapolated from the known terminus, the shape of the ice in the 1910 photo, and the curvature of the moraine. Table 11 shows the recession differences between the years and the changing rates of retreat. For the first sixty years of the study period, the West Turgen Glacier retreated 403 meters, averaging 6.7 meters per year. Then, the retreat rate appears to have slowed to 3.9 meters per year, receding 87 meters over the next two decades. In the last two decades, the retreat rate has increased to 6.1 meter per year, losing 110 meters of ice. The measurements from this photo pair are the only ones that demonstrate high accuracy quantitative glacial changes. Therefore, PS07 is the most important repeat station in the project.



Figure 52. Repeat 1910 and 2010 photo pair of West Turgun Glacier from PS07.

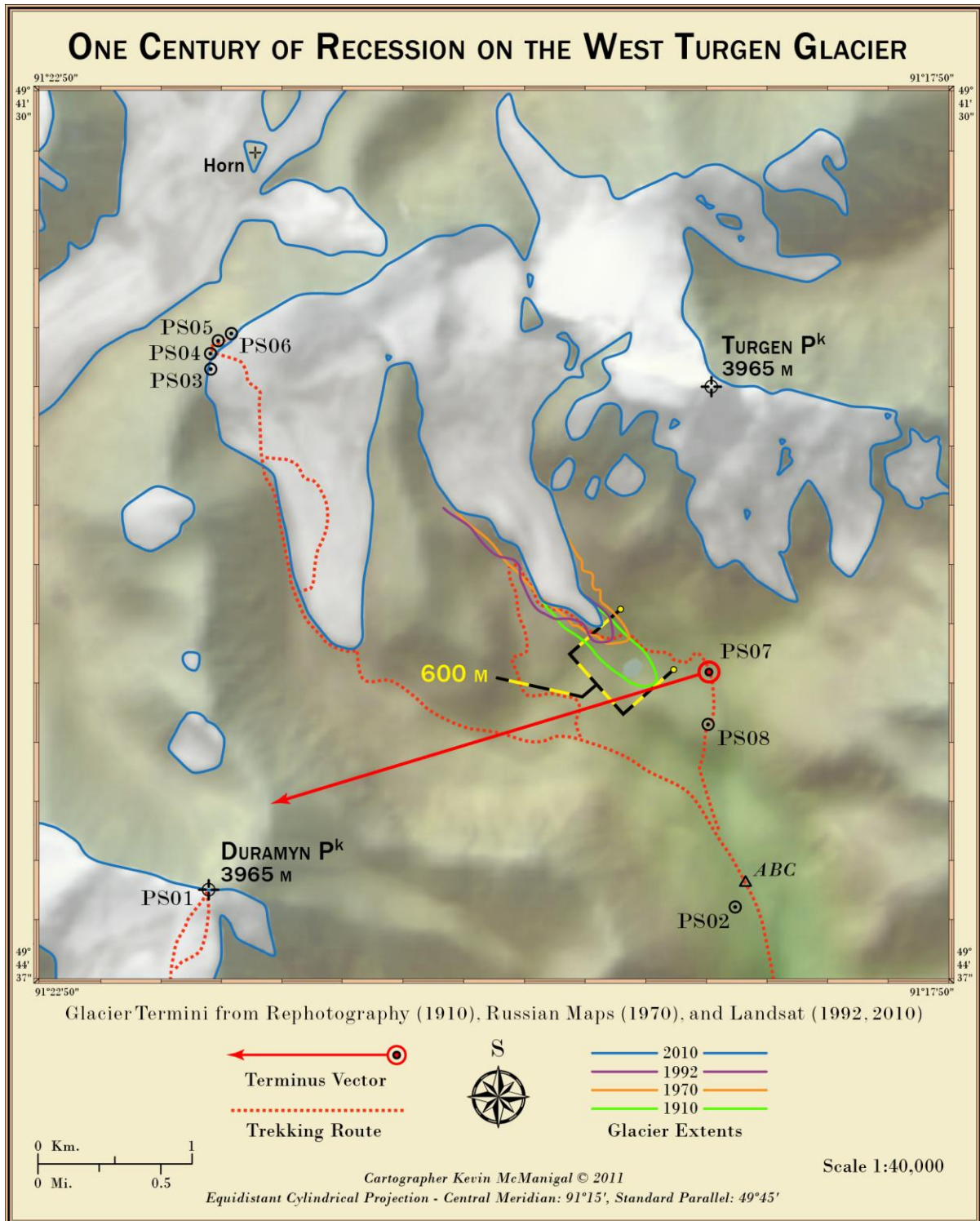


Figure 53. Map of West Turgén Glacier with glacier termini changes from 1910 to 2010.

Table 11. Results of multi-data integrative analysis.

Year	1910		1970		1992		2010
Years between images		60 yrs.		22 yrs.		18 yrs.	
Avg. m retreat per year		6.7 mpy		3.9 mpy		6.1 mpy	
Total avg. m per year	5.6 m						
Retreat between years		403 m		87 m		110 m	
Retreat 1910 – 1992	490 m						
Retreat 1910 – 2010	600 m						

REPEAT PHOTOGRAPHY DISCUSSION

Multiple analysis techniques were used to assess the repeat photography of the Turgan Range. Whereas comparative re-photography has generally been applied to qualitatively describe landscape change, as was demonstrated with several pictures here, advanced methods that produce more quantitative measurements were successfully implemented. While the comparison of pixels between temporal images can provide percentages of relative change in ice cover, the most robust calculations of glacial recession came from photographic measurements made in combination with remotely sensed data.

From the comparative analysis of the side-by-side temporal images, some general statements can be made about the state of the glaciers in the Turgan Range. The ice of the upper glaciated zones above 3500 meters appears to have changed very little in the last one hundred years. Conversely, the glacier cover and thickness at lower elevations has reduced noticeably. While it is not possible to make definitive statements expressing exact quantities of ice loss from visual assessments of photographic pairs, there is little doubt that the glaciers of the range have continued their retreat that was first documented by Carruthers (1914a; 1912) a century ago. However, there are clues present in the images that portend the current trends. Of interesting note is the thin layer of brown sand covering substantial areas of the glaciers in the 2010 images, likely blown in off the Gobi desert to the south. As mentioned

by Hewitt (2005), this layer of dust has the opposite effect of a thicker insulating layer of debris, actually enhancing ablation of the ice. The dust layer observed in the field in 2010 was only a few millimeters to a centimeter thick, coating the base of ablating sun cups. Unfortunately, no research was found that addresses the patterns and frequency of dust storms in the study area. Also, the presence of bare ice on high, steep slopes in the 2010 photographs may indicate that the accumulation zones of these peaks have moved above the physical elevation of some glaciers. When all snow from a previous winter is ablated before summer's end, the prospect for a rapidly wasting glacier is high (Knight 1999).

The extent of coverage and thickness of the ice on the Turgén icecap is almost identical between the photographs, but using pixel analysis, some small decreases were detected. The average ice loss from the three image pairs analyzed with Pixcavator is -1.5% . Although small, the differences in ice cover that are undetectable by eye were quantified by this technique. However, the pixel comparison does have several limitations. In the field, the camera locations, azimuth, angle and elevation must match perfectly. In the lab, the resolution and size of the paired images also have to be exactly coincident. Slight variations in any parameter will affect the percentages calculated by the software. There may also be error introduced by the manual digitization of the ice polygons, where visual interpretations have to be made. Changes in volume of ice that ablates directly away from the camera angle would be indiscernible as well. Also, ice or snow surfaces at varying focal lengths should not be analyzed together. For example, in the photo pair from PS03, a reduction of the snow along the ridgeline in the foreground would reveal more ice on the summit cap in the background, prejudicing the measurements. Regardless, the technique is a valuable confirmation of visual assessments that inferred slight reductions in the ice cap.

The measurement of down-wasting in the glaciers captured from PS04 is a hybrid of techniques, combining the use of DEMs after Surazakov and Aizen (2006), and the incorporation of oblique imagery referenced to the modeled landscape as demonstrated by Aschenwald et al. (2006). The limitations of the technique lie in the error inherent in the DEM and the same host of photographic considerations that were mentioned previously. Considering that the capture parameters of the re-photography appear to match very well, those errors are likely within the ± 16 meters of vertical inaccuracy in the DEM. There may be some locational inconsistencies with the surface measurements of the 1910 and 2010 glaciers, but the summit of the nunatak was easy to pinpoint in each photo. Therefore, the measurement of glacial ablation over the last century for this one location can be considered fairly accurate.

The glacial recession measurement derived from PS07 is another example of rephotography being integrated with remote sensing data to derive measurements that had previously only been possible with temporal satellite imagery or topographic map comparison (Schmidt and Nüsser 2009; Bishop et al. 2007). Again, the photo capture angle must be perpendicular to the glacier terminus and exactly matched to the historical location. If this is accomplished to a high degree of accuracy, as was the case here, the conversion of an oblique measurement to a planar distance on a satellite image can precisely locate the frontal margin of the historic terminus. Then, when evaluated against previous remote sensing research, not only can the total amount of recession be determined for a lengthened timespan, but also the variations in the rate of change over the entire study period. This technique can therefore be utilized to effectively extend the modern satellite archives, theoretically, to the earliest photographic records of glaciers.

CONCLUSION

This study employed multiple techniques to evaluate the historic records of the 1910 Carruthers expedition against modern sources of data for the same area. The aim was to assess the viability of incorporating classical geographic field studies within a modern program of glacier monitoring, largely conducted with remotely sensed imagery. Because the contemporary satellite records in most cases cover only fifty years, an inadequate span in geologic time, it is desirable to integrate older records of glacial positions. To this end, the cartographic work of Carruthers was scrutinized to determine both the planar and elevation accuracy. The photographs of the expedition were also repeated and analyzed for signs of glacial change. Finally, the notes and publications of Carruthers were researched for indications of the glacial positions in 1910.

Looking back to the original research questions, this study has clearly demonstrated that historical archives of mountain expeditions are a valid resource for extending the modern record of glacial change. While not all of the Carruthers records provided definitive measurements of glacial recession, the sum total of qualitative and quantitative analysis applied to multiple forms of data built a comprehensive overview of the Turgan glaciers in the last century. In the end, the cartography by Carruthers was not as valuable for glacier monitoring as the repeat photography. Nonetheless, all of the historical data did play an important role in constructing the complete assessment.

The Turgan map from 1910 is a beautiful piece of cartography that represents the historic landscape surprisingly well considering that it was largely hand-drawn in the field. The elevations are slightly low for the core study area, but this is only once some severe planar distortions are corrected by way of a 'rubber-sheet' transformation. The 1910 map at

its full extent has too many generalized or missing contours to even compare it to the modern DEMs. The ‘best fit’ cartometric calculation of 338 ± 239 meters means that while the center of the Carruthers map is probably within a margin of error for its scale, it is not sufficiently precise to locate the glaciers in 1910 with any certainty. In fact, the highest estimate of planar error, 577 meters, is very close to the 600 meters of recession measured for the West Tugen Glacier from the PS07 rephotography analysis. Also, the 1910 location of the West Tugen Glacier terminus on the georeferenced clip of the Carruthers map is roughly 620 meters misplaced from the derived 1910 position in the GIS. Consequently, the locational error of the Carruthers map is on par with the glacial recession being measured, rendering it unusable for change detection.

In all fairness, even Carruthers admitted the possibility of errors in his map stating that while he had constructed it with every detail, he could not “vouch for its correctness” (1913, 347). Instead, he acknowledged the “ample work awaiting [future] explorers” in the resurvey and correction of his work, which was attempted here (Carruthers 1913, 347). Even so, the Carruthers map was a valuable resource in the field and lab for pinpointing the photographic capture locations of the 1910 expedition.

The full gamut of rephotography techniques applied to the photo pairs, ranging from visual assessment to measurements derived from integrative methods, produced the most effective measurements of the Tugen glaciers. The standard repeat photography approach of side-by-side comparison detected recognizable reductions of both volume and area in the glaciers of the range. The visual evaluation of glacial change was supported further here with pixel analysis of the photo pairs, a new technique developed for this study. This method quantified a slight ice loss on the Tugen summit and confirmed the slight ablation inferred

by the photographic comparisons. Then, techniques for extrapolating DEM elevation from the oblique repeat photographs were refined here to estimate loss of volume at the glacial surface. This method for evaluating surface change using a ratio of DEM elevation to pixel counts is limited only by the accuracy of the data and thoroughness of the fieldwork. Finally, the total recession of the West Turgén Glacier between 1910 and 2010 was calculated with a newly developed hybrid technique. An azimuth angle was shot across the historic terminus photograph from the known photo station, and then plotted over the rephotography, intersecting with a physical feature visible in the background. When this ‘terminus vector’ was plotted over the satellite imagery in the GIS, a very accurate measurement of recession was made. In total, the various techniques applied in this study produced a clear assessment of the Turgén glacial conditions over the last century, verifying the utility of integrating historic records into the modern programs of glacial monitoring.

The second research question that the study answered addresses how the glacial system of the Turgén Range has changed over the last century. From the visual assessment of the repeat photography, the higher elevation ice appears more intact, while the lower altitude termini show a more pronounced recession and ablation. There is also some evidence of rising lines of equilibrium, as inferred by the existence of snow-free glaciers extending to the ridgelines of some slopes. The glacier on Turgén Peak shows a slight reduction of -1.5%, as measured by the pixel analysis. The twin glaciers on the east side of the range have a measured ice loss of 72 ± 16 meters below the nunatak, as calculated from the DEM and rephotography integration. The West Turgén Glacier has receded 600 meters in the last century, as demonstrated by the precise ‘terminus vector’ technique that combined the rephotography with the accuracy of the latest 2010 Landsat imagery.

These measurements can in turn be applied to related glaciers in proximity to the proxy with some confidence. For example, it seems reasonable to suggest that the recession of the East Turgén Glacier would have been comparable to the measured 600 meters of retreat for the West Turgén Glacier over the same period. This assertion is corroborated by the 1910 termini elevations given by Carruthers (1912: 1914a). His measurement of 2895 m (9500 ft) for the East Turgén Glacier frontal lobe is 50 meters lower than the DEM at a point 600 meters down moraine from the 2010 terminus. The Carruthers' measurement of 2974 m (9758 ft) for the West Turgén Glacier terminus has more error, being 200 meters below the DEM elevation at the derived 1910 terminus, but both errors are $< 1 \sigma$ of the mean error computed from the Carruthers map.

The 490 meters of recession between 1910 and 1992 for the West Turgén Glacier found in this study is comparable to the 200-500 meters of retreat estimated by Lehmkuhl (1998) between 1948 to 1991, although the periods do not match exactly. Interestingly, Kadota and Gombo (2004; 2007) found that the Turgén glaciers had lost 19% of their surface area between 1970 and 1990, but remained stagnant thereafter. This is the exact opposite of the trends found here for the West Turgén Glacier where the recession rate decreased from 1970 to 1992, and then increased to the present. As mentioned previously, these inconsistencies probably stem from the differing methodologies and data sources. Rectifying these differences would require careful examination and recreation of the previous studies, which was not attempted here. The surface measurements below the nunatak could likewise be used to develop ablation estimates for local glacial surfaces at similar altitudes, however estimating total volume loss for entire ice bodies would require advanced modeling beyond the scope of this study.

Finally, by way of making recommendations for future research of this scope, a possible methodology for integrating historical and modern data is presented here. The records of expeditions may have many diverging data types, collected in numerous ways and with varying precision. Therefore, it is important to locate historical records that have a mixture of data that will allow for a multitude of analytical techniques. A diverse dataset will also insure against the problems of insufficient resolution that can impede valid results, as was the case with the historical cartography here.

Any future research of this nature would necessarily start with a review of the archival data. Concerning historical cartography, the method of production and scale are important considerations for glacial studies. Smaller scales should have more accurate glacial margins, however, only the most careful fieldwork can render the precision required. Plane table methods may produce satisfactory results, but it depends on the generalization decisions made by the cartographer. Maps produced from aerial photography can generally be considered accurate to within the limitations of scale, but they should be assessed as well. Therefore, the best practice would be to start with a cartometric evaluation of the maps planar accuracy as outlined in this work. If this is found to be acceptable, then a historic DEM can be generated as described here, and compared to modern sources of elevation data. When combined with multi-temporal glacial extents, map analysis can produce robust estimates of changes to both glacial area and volume.

The next step would be to evaluate the quality, format, and orientation of the original photographs to determine the kinds of rephotography analysis possible. The comprehensive work done here suggests that for glacial change monitoring, the location and capture angle of photographs plays a large role in the kind of measurements that can be derived. In general,

panoramic photographs of summits and glacial landscapes without a clearly discernable ice margin are only useful for qualitative visual analysis. Conversely, photographs taken perpendicular to the termini or encompassing large stable features which can be located within a DEM are prime candidates for quantitative measurements that yield very strong estimates of former glacial phases. Even without additional fieldwork, the refinement of the integrative techniques herein could be implemented to analyze existing scientific repeat photography studies with photographs taken perpendicular to the glaciers.

Once in the field, the repeat photo stations must be matched as closely as possible. This may require visiting sites at different times during the day, and under different weather conditions, as subtle changes in lighting conditions can greatly influence decisions when attempting to match photographs to the landscape. It is advisable to take photographs from many different locations surrounding the estimated recapture location, and carefully document all the photo parameters in a field book. Each shot should also be bracketed to cover a range of exposures. By over documenting each site, there is some measure of insurance that at least one image will be properly matched to the historic photograph. The use of a laser range finder in the field could also be employed to increase the accuracy of landscape feature measurements that will be compared to DEM data. It may be helpful to document distance measurements and the bearings of capture angles directly onto topographic map sheets. It is also advisable to keep a GPS unit actively logging a track as the team moves through the landscape. This way all of the images taken during the research can be geotagged by syncing the timestamps. This is also a backup of the individual waypoints taken at the photo stations.

Upon returning to the spatial analysis laboratory, it is important to immediately start to organize the data while the particulars of the expedition are still fresh in the mind. All spatial data should be entered into a well-designed geodatabase, with the proper coordinate system and projection assigned. The photography should be processed as outlined here and geotagged. It is also prudent to edit and clarify the field notes while fine details can still be recalled. Once all of the data is arranged, the analysis can commence.

In closing, retracing portions of the 1910 Royal Geographical Society Expedition to the Tugen Mountains has clearly demonstrated the value of historical expedition material to the modern science of glacier monitoring. By combining thorough fieldwork with multi-methods lab analysis, it was possible to compare the Carruthers material with remotely sensed data. At the time of this writing, no other study could be found that so thoroughly integrates historic records with modern remote sensing data for the purpose of glacial studies. Through the use of a breadth of techniques, some newly developed here, it is possible to extend the records of glacial change and peer back to a time when the ‘truth on the ground’ was the only reliable mode of measurement.

REFERENCES

- Adobe. Online help and user manuals for Adobe products. http://help.adobe.com/en_US/photoshop/cs/using/Photomerge. [Accessed on September 11th, 2010].
- Andrews, D. 1974. A robust method for multiple linear regression. *Technometrics* 16:523-531.
- Aschenwald, J., K. Leichter, E. Tasser, and U. Tappeiner. 2001. Spatio-temporal landscape analysis in mountainous terrain by means of small format photography: a methodological approach. *IEEE transactions on geoscience and remote sensing* 39 (4).
- Bagrow, L., and R. A. Skelton. 1964. *History of cartography*. London,: C.A. Watts.
- Bamber, J., and A. Rivera. 2007. A Review of Remote Sensing methods for Glacier Mass Balance Deterination. *Global and Planetary Change* 59:138-148.
- Bartkowski, T. 1974. *Zastosowania geografii fizycznej* Warsaw: PWN.
- Batima, P., N. Batnasan, and B. Lehner. 2004. *The Freshwater Systems of Western Mongolia's Great Lakes Basin: Opportunities and Challenges in the Face of Climate Change*. Ulan Bator, WWF Mongolia Programme Office: 59.
- Batima, P., L. Natsagdorj, P. Gombluudev, and B. Erdenetsetseg. 2005. *Observed climate change in Mongolia*. AIACC Working Papers. Nairobi 13:26.
- Batima, P. 2006. *Climate Change Vulnerability and Adaptation in the Livestock Sector of Mongolia*. Assessments of Impacts and Adaptations to Climate Change (AIACC) Project Office. Washington D.C.: 84.
- Bishop, M. P., J. Shroder, U. Haritashya, H. Bulley, G. Tartari, and E. Baudo. 2007. Remote sensing and GIS for alpine glacier change detection in the Himalaya. *Developments in Earth Surface Processes* 25.
- Böhner, J. 2006. General climatic controls and topoclimatic variations in Central and High Asia. *Boreas* 35:279–295.
- Bolch, T., and U. Kamp. 2006. Glacier Mapping in High Mountains Using DEMs, Landsat and ASTER Data. *Grazer Schriften der Geographie und Raumforschung*. Band 41:37-48.
- Brown, D. G., D. P. Lusch, and K. A. Duda. 1998. Supervised classification of glaciated landscapes using digital elevation data. *Geomorphology* 21:233–250.

- Burnett, D. Graham. 2000. *Masters of all they surveyed : exploration, geography, and a British El Dorado*. Chicago: University of Chicago Press.
- Bury, J., B. Mark, J. McKenzie, A. French, M. Baraer, K. In Huh, M. Alfonso, Z. Luyo, and R. Gómez López. 2010. Glacier Recession and Human Vulnerability in the Yanamarey Watershed of the Cordillera Blanca, Peru. *Climate Change* 105(1-2):179-206.
- Byers, A. C. 2007. An assessment of contemporary glacier fluctuations in Nepal's Khumbu Himal using repeat photography. *Himalayan Journal of Sciences* 4 (6):21-26.
- Chaplot, V., F. Darboux, H. Bourennane, S. Leguédais, N. Silvera, and K. Phachomphon. 2006. Accuracy of interpolation techniques for the derivation of digital elevation models in relation to landform types and data density. *Geomorphology* 77 (1-2):126-141.
- Cheetham, G., ed. 1905. *Textbook of topographical surveying*. Ministry of Defence, Great Britain. London: H.M. Stationery Office.
- Carruthers, Douglas. 1912. Exploration in North-West Mongolia and Dzungaria. *The Geographical Journal* 39 (6):521-551.
- Carruthers, Douglas. 1913. Notes on the Maps Illustrating the Exploration in Mongolia and Dzungaria. *The Geographical Journal* 41 (4):346-349.
- Carruthers, Douglas. 1914a. *Unknown Mongolia: A Record of Travel and Exploration in North-West Mongolia and Dzungaria: With three chapters on sport by J.H. Miller*. 2 vols. Vol. 1. London: Hutchinson & Co.
- Carruthers, Douglas. 1914b. Further Information on the Turgun or Kundelun Mountains in North-Western Mongolia, and Notes on a New Map of This Region. *The Geographical Journal* 44 (4):382-385.
- Casey, E. S. 2005. *Earth-mapping : artists reshaping landscape*. Minneapolis: University of Minnesota Press.
- Dent, B.D. 1985. *Principles of Thematic Map Design*. 5th ed. Massachusetts: Addison-Wesley Publishing Company Inc.
- Enebish, N. 2004. *Renewable Energy Application in Mongolia*. (PREGA) Second Regional Training and Planning Workshop. Manila, Philippines.
- Easson, G., and H. Robison. 2001. Assembling DEM Files for Watershed Analysis. *Arc User Magazine*. <http://www.esri.com/news/arcuser/0701/moredem.html>. [Accessed February 14th, 2011].

- ESRI. 2007. "Setting the Z Factor Parameter Correctly," Mapping Center Blog, Posted June 12th. <http://blogs.esri.com/Support/blogs/mappingcenter/archive/2007/06/12/setting-the-z-factor-parameter-correctly.aspx>. [Accessed November 23rd, 2010].
- ESRI. 2008a. "Updated Hillshade Toolbox," Mapping Center Blog, Posted October 7th. <http://blogs.esri.com/Support/blogs/mappingcenter/archive/2008/10/07/updated-hillshade-toolbox.aspx>. [Accessed March 20th, 2011].
- ESRI. 2008b. "Output resolution of vector data from ArcMap," Mapping Center. Ask a Cartographer, Posted November 10th. <http://mappingcenter.esri.com/index.cfm?fa=ask.answers&q=493>. [Accessed September 17th, 2010].
- ESRI. 2009. "Georeferencing a Raster Dataset," Online Help, Posted November 9th. http://webhelp.esri.com/arcgisdesktop/9.3/index.cfm?TopicName=Georeferencing_a_raster_dataset. [Accessed November 24th, 2010].
- Fagre, D., 2010. "USGS Repeat Photography Project Documents Retreating Glaciers in Glacier National Park." National Park Service. <http://nrm.usgs.gov/repeatphoto/htm> [Accessed May 4, 2010].
- Fitzgerald, M. 2010. *Photoshop CS5 Restoration and Retouching For Digital Photographers Only*. Hoboken, NJ: John Wiley & Sons.
- Forstner, G., and M. Oehrli. 1998. Graphic representations of the analysis of old maps and the development of distortion grids. *Cartographica Helvetica* 17:35-43.
- Gilbert, Pamela K. 2004. Mapping the Victorian social body. In *SUNY series, studies in the long nineteenth century*. Albany: State University of New York Press.
- Gillespie, W. M. 1855. *A treatise on land surveying comprising the theory developed from five elementary principles; and the practice with the chain alone, the compass, the transit, the theodolite, and the plane table*. New York, London: D. Appleton & Co.
- Hall, F. C. 2001. Ground-based photographic monitoring. In *General technical report PNW*. Portland, OR: U.S. Dept. of Agriculture, Forest Service, Pacific Northwest Research Station.
- Hardy, R. L. 1971. Multiquadric Equations of Topography and Other Irregular Surfaces. *Journal of Geophysical Research* 76 (8):1905-1915.
- Harley, J. B., and D. Woodward. 1987. *The History of cartography*. Chicago: University of Chicago Press.
- Harvard University. 2011. Department of the History of Science. Online catalog of artifacts. <http://dssmhi1.fas.harvard.edu/emuseumdev>. [Accessed March 23rd, 2011].

- Hastenrath, S. 2008. *Recession of equatorial glaciers: a photo documentation*. Madison, WI: Sundog Publishing.
- Herget, J. 2005. *Reconstruction of Pleistocene ice-dammed lake outburst floods in the Altai Mountains, Siberia*: Geological Society of America.
- Hewitt, K. 2005. The Karakoram Anomaly? Glacier Expansion and the 'Elevation Effect, Karakoram Himalaya. *Mountain Research and Development* 25 (4):332-340.
- Hill, L.L. 2006. *Georeferencing: the geographic associations of information*: MIT Press.
- Hubbard, B., and N. Glasser. 2005. *Field Techniques in Glaciology and Glacial Geomorphology*. John Wiley & Sons. West Sussex: England.
- Hutchinson, M. F. 1988. *Calculation of Hydrologically Sound Digital Elevation Models. Third International Symposium on Spatial Data Handling*. Sydney, Australia.
- Hutchinson, M. F. 1989. A New Procedure for Gridding Elevation and Stream Line Data with Automatic Removal of Spurious Pits. *Journal of Hydrology* 106: 211-232.
- Hutchinson, M. F. 1993. "Development of a continent-wide DEM with applications to terrain and climate analysis," In *Environmental Modeling with GIS*, ed. M. F. Goodchild et al., 392–399. New York: Oxford University Press.
- Imhof, E. 1982. *Cartographic Relief Presentation*. New York and Berlin: Walter de Gruyter.
- Ives, J. D. 1987. Repeat Photography of Debris Flows and Agricultural Terraces in the Middle Mountains, Nepal. *Mountain Research and Development* 7 (1):82-86.
- Jacoby, G., R. D'Arrigo, N. Pederson, B. Buckley, C. Dugarjav, and R. Mijidorj. 1999. Temperature and precipitation in Mongolia based on dendroclimatic investigations. *IWA Journal* 20:339–350.
- Jansen, A., 2010. Modeling of Climate Parameters for Characterizing Glaciers in the Turgon-Kharkhiraa Massif (Mongolia). Unpublished Ph.D. Thesis, Technical University of Aachen, 143 p. + Appendix. (In German).
- Jenny, B. 2005. "MapAnalyst - The Map Historian's Tool for the Analysis of Old Maps." Online user manual. <http://mapanalyst.cartography.ch>. [Accessed December 10th, 2010].
- Jenny, Bernhard. 2006. MapAnalyst - A digital tool for the analysis of the planimetric accuracy of historical maps. *e-Perimetron* (3), http://www.e-perimetron.org/Vol_1_3/Vol1_3.htm.

- Jenny, B., A. Weber, and L. Hurni. 2007. Visualizing the Planimetric Accuracy of Historical Maps with MapAnalyst. *Cartographica* 42 (1):89-94.
- Jenny, B. and A. Leonowicz. 2010. "Terrain Sculptor." Specialized application for the generalization of terrain models. <http://terrainscartography.com/terrainsculptor>. [Accessed January 18th, 2011].
- Jenny, B., and L. Hurni. 2011. Studying cartographic heritage: Analysis and visualization of geometric distortions. *Computers & Graphics* 35 (2):402-411.
- Kadota, T., and D. Gombo. 2004. *Recent Glacier Variations in Mongolia*. Proceedings of the 3rd International Workshop on Terrestrial Change in Mongolia. Tsukuba, Japan: 20-22.
- Kadota, T., and D. Gombo. 2007. Recent Glacier Variations in Mongolia. *Annals of Glaciology* 46:185-188.
- Kamp, U., T. Bolch, and J. Olsenholler. 2003. *DEM Generation from ASTER Satellite Data for Geomorphometric Analysis of Cerro Sillajhuay, Chile/Bolivia*. ASPRS, Annual Conference Proceedings, Anchorage, Alaska.
- Khrutsky, V. S., and E. I. Golubeva. 2008. Dynamics of the Glaciers of the Turgent-Kharkhiraa Mountain Range (Western Mongolia). *Geography and Natural Resources* 29:278-287.
- Knight, P.G. 1999. *Glaciers*. Cheltenham: Stanley Thornes.
- Knight, Peter G. (Ed.). 2009. *Glacier Science and Environmental Change*. West Sussex: Wiley-Blackwell.
- Krumwiede, B. 2010. Mapping Glacier Variations from 1990 to 2006 in the Central Mongolian Altai. Master's thesis, The University of Montana.
- Lattimore, O. 1978. Douglas Carruthers and Geographical Contrasts in Central Asia, The First Douglas Carruthers Memorial Lecture. *The Geographical Journal* 144 (2):208-217.
- Lawniczak, R. 2008. Use of Cartographic Analysis for Determining the Morphometric Features of Selected Groups of Glacial Configuration Forms. *Cartographic Journal* 45 (4):286-295.
- Lehmkuhl, F. 1998. Quaternary Glaciation in Central and Western Mongolia. *Quaternary Proceedings* 6:153-167.
- Low, J. W. 1952. *Plane table mapping*. New York: Harper.

- Mather, K. F., and B. Washburn. 1938. *The telescopic alidade and the plane table as used in topographic and geologic surveys*. Granville, OR.
- McCarthy, J. J., O. F. Canziani, N. A. Leary, D. J. Dokken, and K. S. White (Ed.). 2001. Contribution of working group II to the third assessment report of the intergovernmental panel on climate change (IPCC) UK7 Cambridge University Press: 1000.
- Mool, P. K., D. Wangda, S. R. Bajrachary, K. Kunzang, D. R. Gurung, and S. P. Joshi. 2001. *Inventory of Glaciers, Glacial Lakes and Glacial Lake Outburst Floods, Bhutan. International Centre for Integrated Mountain Development*. Kathmandu, Nepal: 227.
- Morinaga, Y., S. Tian and M. Shinoda. 2003. Winter snow anomaly and atmospheric circulation in Mongolia. *International Journal of Climatology* 23:1627–1636.
- Munroe, J. S. 2003. Estimates of Little Ice Age Climate Inferred through Historical Rephotography, Northern Uinta Mountains, U.S.A. *Arctic, Antarctic, and Alpine Research* 35 (4):489-498.
- Nüsser, M. 2000. Change and Persistence: Contemporary Landscape Transformation in the Nanga Parbat Region, Northern Pakistan. *Mountain Research and Development* 20 (4):348-355.
- Nüsser, M. 2001. Understanding cultural landscape transformation: a re-photographic survey in Chitral, eastern Hindukush, Pakistan. *Landscape and Urban Planning* 57 (3-4):241-255.
- Oerlemans, J. 1994. Quantifying Global Warming from the Retreat of Glaciers. *Science* 264: 243-245.
- Patterson, T. 2006. “Shaded Relief.” Online resource of shaded relief techniques. <http://www.shadedrelief.com>. [Accessed October 31st, 2011].
- Patterson, T. 2010a. Outside the Bubble: Real-world Mapmaking Advice for Students. *Cartographic Perspectives* 65 (Winter):7-15.
- Patterson, T. 2010b. “Shaded Relief Archive.” Online depository of hand rendered shaded relief. <http://www.shadedreliefarchive.com>. [Accessed March 17th, 2011].
- Pearson, A.W., M. Schaefer, and B. Jenny. 2009. A Cartometric Analysis of the Terrain Models of Joachim Eugen Müller (1752–1833) Using Non-contact 3D Digitizing and Visualization Techniques. *Cartographica* 44 (2):111-120.
- Pellikka, P. K. E., and Gareth Rees. 2010. *Remote sensing of glaciers: techniques for topographic, spatial and thematic mapping of glaciers*. Boca Raton FL, London: CRC Press.

- Pixcavator. 2007. Intelligent Perception Inc. Pixel analysis software for the biological sciences. http://inperc.com/wiki/index.php?title=Math._Images._Software. [Accessed April 18th, 2011].
- Price, M. P.. 1968. A Journey in the Upper Yenesei Basin, Outer Mongolia and Chinese Turkestan in 1910. *The Geographical Journal* 134 (2):181-193.
- Pugh, J.C. 1975. *Surveying for field scientists*: University of Pittsburgh Press.
- Racoviteanu, A. E., W. Manley, Y. Arnaud, and M. W. Williams. 2007. Evaluating digital elevation models for glaciologic applications: An example from Nevado Coropuna, Peruvian Andes. *Global and Planetary Change* 59 (1-4):110-125.
- Raup, B., G. Scharfen, S. Khalsa, and A. Kaab. 2001. *The Design of the GLIMS (Global Land Ice Measurements from Space) Glacier Database*. EOS Transactions Supplement. American Geophysical Society 82(47).
- Raup, B., A. Kääb, J. Kargel, M. Bishop, G. Hamilton, E. Lee, F. Paul, F. Rau, D. Soltesz, S. J. S. Khalsa, M. Beedle, C. Helm. 2007. Remote Sensing and GIS Technology in the Global Land Ice Measurements from Space (GLIMS) Project. *Computers & Geosciences* 33 (1):104-125.
- Rentsch, H., W. Welsch, C. Heipke, M. Miller. 1990. Digital Terrain Models as a Tool for Glacier Studies. *Journal of Glaciology* 36(124), 273-278.
- Robinson, A., J. Morrison, P. Muehrke, A. Kimmerling & S. Gupitill. 1995. *Elements of Cartography*. 6th ed. New York: Wiley.
- Robinson, A. H. 1952. *The look of maps; an examination of cartographic design*. Madison: University of Wisconsin Press.
- Rogers, G. F., H. E. Malde, R. M. Turner. 1984. *Bibliography of repeat photography for evaluating landscape change*. Salt Lake City: University of Utah Press.
- Roush, W., J. S. Munroe, and D. B. Fagre. 2007. Development of a Spatial Analysis Method Using Ground-Based Repeat Photography to Detect Changes in the Alpine Treeline Ecotone, Glacier National Park, Montana, U.S.A. *Arctic, Antarctic, and Alpine Research* 39 (2):297-308.
- RGS Picture Library. 2005. Royal Geographical Society. Online catalog of images and artifacts. <http://images.rgs.org/img=14394>. [Accessed March 24th, 2011].
- RGS Bibliography. 2008. Royal Geographical Society. Online catalog of explorers and their archives. <http://www.aim25.ac.uk/cats/10/6397.htm>. [Accessed May 4th, 2010].

- RGS Archives. 2010. Royal Geographical Society. In-house documents containing journals, diaries, photographs, notes, telegrams, letters and newspaper articles by or about Carruthers. [Accessed in person June 2nd – 4th, 2010].
- Rumsey, D. and M. Williams. 2002. *Historical maps in GIS. Past time, past place. GIS for History*. La Vergne, TN: ESRI Press.
- Schmidt, S., and M. Nusser. 2009. Fluctuations of Raikot Glacier during the past 70 years: a case study from the Nanga Parbat massif, northern Pakistan. *Journal of Glaciology* 55 (194):949-959.
- Strebe, D. 2011. Owner of Mapthematics, Designer of GeoCart Projection Software. Interview by Author. Seattle, WA. April 14.
- Schmidt, S., and M. Nusser. 2009. Fluctuations of Raikot Glacier during the past 70 years: a case study from the Nanga Parbat massif, northern Pakistan. *Journal of Glaciology* 55 (194):949-959.
- Shinoda, M., H. Utsugi, and W. Morishima. 2001. Spring snow-disappearance timing and its possible influence on temperature fields over central Eurasia. *Journal of the Meteorological Society of Japan* 79:37–59.
- Surazakov, A. B., and V.B. Aizen. 2006. Estimating Volume Change of Mountain Glaciers Using SRTM and Map-Based Topographic Data. *IEEE Transactions on Geoscience and Remote Sensing* 44 (10):2991-2995.
- Tobler, W. R. 1966. Medieval distortions:the projections of ancient maps. *Annals of the Association of American Geographers* 56.
- Webb, R. H., D. E. Boyer, and R. M. Turner. 2010. *Repeat photography : methods and applications in the natural sciences*. Washington, DC: Island Press.
- Webb, R. H. 2007. The Desert Laboratory Repeat Photography Collection: an invaluable archive documenting landscape change. In *Fact sheet 2007-3046*. Reston: VA: U.S. Dept. of the Interior, U.S. Geological Survey. <http://pubs.usgs.gov/fs/2007/3046/>. <http://purl.access.gpo.gov/GPO/LPS97494>. [Accessed March 22nd, 2011].
- Wood, D. 1992. *The Power of Maps*. New York: Guilford Press.
- Zängl, W. and S. Hamberger. 2004. *Gletscher im Treibhaus: eine fotografische Zeitreise in die alpine Eiszeit*. Steinfurt, Tecklenborg.
- Zeiler, M. 1999. *Modeling our world :the ESRI guide to geodatabase design*. Redlands CA: ESRI Press.

DATA

CGIAR. Online portal for processed and filled SRTM data. <http://srtm.csi.cgiar.org>. [Accessed April 1st, 2011].

Earth Explorer. Portal for DEM and satellite data, NASA. <http://edcsns17.cr.usgs.gov/NewEarthExplorer/>. [Accessed January 8th, 2011].

Geo Community. Online portal for global GIS data. <http://www.geocomm.com>. [Accessed February 12th, 2011].

Global Land Cover Facility (GLCF). Online satellite imagery and land classification data from the University of Michigan. <http://www.glcg.umd.edu/index.shtml>. [Accessed March 23rd, 2011].

Mapstor. Online Russian and Foreign maps. <http://mapstor.com/>. [Accessed February 3rd, 2011].

WIST. Online portal for ASTER data. <https://wist.echo.nasa.gov>. [Accessed November 24th, 2010].

.